Sedimentology of the Grønfjorden Bed and associated sedimentary deposits: Grønfjorden, Svalbard

Tor Kristian Berg

Thesis for the degree of Master of Science
in Petroleum Geology/Sedimentology

Department of Earth Science

University of Bergen

January 2018

ABSTRACT

The Grønfjorden Bed represents the earliest Paleogene sedimentary deposits in the Central Tertiary Basin on Spitsbergen. It has a patchy distribution, and consists of conglomerates and sandstones of fluvial origin that rest unconformably upon Lower Cretaceous strata. The Grønfjorden Bed is a sub-unit of the coal-bearing Todalen Member of the Firkanten Formation, and has received limited emphasis due to the attention received by the productive coal seams higher up in the stratigraphy. This study has investigated the Grønfjorden Bed and associated sedimentary deposits in detail through the use of conventional sedimentary logging and remote photography and photogrammetric modelling. The photogrammetric models have provided virtual outcrops on which detailed sedimentological analysis has been performed.

On the basis of detailed facies analysis, three facies associations were recognized: deposits of gravel-bed fluvial channel environment, deposits of sand-bed fluvial channel environment and deposits of a floodplain environment. The study supports previous interpretations of a fluvial depositional environment that was gradually flooded by an elevation in the groundwater table as a response to the initial Paleogene transgression.

The study presents evidence of a northwest towards the southeast paleocurrent direction for the fluvial conglomerates and sandstones. This ties well together with previous studies from nearby exposures, and suggests the presence of a wide fluvial valley in the Grønfjorden area at the time of deposition. The paleocurrent direction of the fluvial valley further coincides with the provenance of the conglomeratic clasts suggesting a source to the west and northwest.

The study suggests that the initial fluvial environment contributed as a tributary valley to a much larger fluvial valley system evident by the presence of the Grønfjorden Bed and also swell and depression topography of the unconformity.

The study as a whole improves the general understanding of the Grønfjorden Bed depositional environment in the study area, and adds to the further understanding of the regional context of the Grønfjorden Bed.

ACKNOWLEDGEMENTS

This thesis was written as a part of a master's degree in geoscience at the Department of Earth Science at the University of Bergen and the Department of Arctic Geology at the University Centre in Svalbard.

First and foremost I would like to give my sincere thanks to my main supervisor Assoc. Prof. Maria Jensen at UNIS, whom has provided excellent guidance in the process of writing my master thesis. Thank you for great feedback and motivating words, and for always taking time to discuss, whether it is only for a few minutes or a few hours. Your way of imparting constructive criticism has really been a boost to my work and my self-esteem during periods of heavy workloads. Thanks to my co-supervisor PhD Malte Jochmann at UNIS for intellectual conversations and helpful discussions and to my co-supervisor Prof. William Helland-Hansen at UoB for providing helpful resources for fieldwork and writing.

A special thanks to Graham Gilbert for great discussion and constructive feedback, your words are greatly appreciated. Thanks to my other good friends at UNIS, Holt and Sara and my office mates Mari and Nina for always being supportive, putting up with my many office visits and keeping me busy in my spare time. Many thanks to my best friend Joar Skien Grannes for providing field assistance during my first field season in summer 2016, and to the rest of LB for being supportive friends.

Special gratitude goes to my father, both for contributing to my second field season in September 2017 as a field assistant, and also for excellent discussion during my thesis work. To my whole family: Thank you all for being incredibly supportive during my two years as a master's student. You are eternally appreciated.

Thank you to my co-workers in the department of Arctic Geology at UNIS for great discussions and help in understanding difficult aspects of my work. I would also like to express my gratitude to UNIS logistics department for providing equipment for fieldwork, and especially Sebastian Sikora for providing and piloting his personal drone during the first field season.

Last but not least, my sincere thanks to Ole-Marius, Eirik, Håvard, Tone and all my other friends at UiB for these last five years. It has been a fantastic journey!

Tor Kristian Berg

Bergen, 15.01.2018

Table of contents

1 INTRODUCTION

1.1 Aim of study

The lower Paleogene Grønfjorden Bed marks the onset of sedimentary deposition in The Central Tertiary Basin on Spitsbergen after a prolonged period of non-deposition and erosion. The superior unit of the Todalen Member has for a long time been the objective for research, due to its economically produced coal seams, whereas Grønfjorden Bed has commonly received little emphasis.

The exposure of the Grønfjorden Bed in northwestern Grønfjorden, Svalbard is the most laterally extensive high-quality exposure of the basal conglomerates and sandstones found on Spitsbergen. It is situated at elevations rendering it inaccessible with use of conventional methods. By the use of modern methods of remote photography and photogrammetry, the outcrop can be used to get an exceptional insight of the earliest Paleogene deposits in the Central Tertiary Basin on Spitsbergen, Svalbard.

Through this study it is intended to create a detailed sedimentological analysis of a previously inaccessible study area. This includes a detailed facies analysis, depositional environmental interpretation and paleocurrent studies of the depositional agent of the sedimentary rocks.

1.2 Previous works

The Paleocene Firkanten Formation has been of interest for a long time due to the economic importance of the coal-bearing Todalen Member. A. E. Nordenskïold and his expedition were the first researchers to carry out studies on the Cenozoic succession in Svalbard in the 19th century. A.G. Nathorst's expedition in 1898 made several discoveries on Svalbard. Based on these and several other expeditions in the 19th and early 20th century, Nathorst published a synthesis containing the first lithological subdivision of the Paleogene succession in 1910, dividing it into six units (Harland et al., 1997). This six-fold division of the strata was adopted by scientists in years to come. Ravn (1922) studied marine molluscs of the succession, and from these studies could determine a Paleogene, probably Paleocene age of the strata that had formerly been interpreted as Eocene or Miocene of age. Systematic surveying of coal reserves started with the implementation of the Svalbard Treaty in 1925 (Harland et al., 1997). Orvin (1940) clarified the six-fold division of the Cenozoic strata that

Nathorst had implemented in 1910. It was modified in the years to come by several researchers (Harland, 1969; Livsic, 1965, 1974; Major and Nagy, 1964, 1972; Vonderbank, 1970), to form the further lithostratigraphic definitions and terms used today. W.B. Harland was one of the main, early researchers of the tectonic activity of the Cenozoic, with his works in 1965, 1966 and 1969. He later assembled a comprehensive synthesis of the geology of Svalbard (Harland et al., 1997).

Studies on the tectonic framework of the Central Basin have been reported by e.g. Kellogg (1975), Steel et al. (1981), Steel and Worsley (1984), Müller and Spielhagen (1990) and Bruhn and Steel (2003) among others. They have worked on connecting the Cenozoic sedimentation to the tectonic controls of the stratigraphy.

Recent studies of Svalbard's Paleogene strata and related tectonics have been performed by Piepjohn et al. (2016) and Petersen et al. (2016). Piepjohn et al. (2016) made a regional study of the tectonic deformation of the arctic areas. The tectonic history of Svalbard was covered in this work. Petersen et al. (2016) made a provenance study on the Firkanten Formation, focusing on the dating of zircon minerals from the lower Paleocene unit.

The name "Grønfjorden Bed" was first used in Dallmann (1999). Before this, the unit was usually referred to as "the basal conglomerate" (Kalgraff, 1978; Major and Nagy, 1972; Ohta et al., 1992; Ytreland, 1980). The type locality of Grønfjorden Bed is located in Grønfjorden (Dallmann, 1999) within the study area for this study. It was first described in Ohta et al. (1992), from which the type log of the stratigraphy was derived (Fig. 1.1). The Grønfjorden Bed has been mentioned in several studies in the last decades, but only a few researchers have gone in detail and described its facies (Kalgraff, 1978; Kostro, 2005; Lüthje, 2008; Steel et al., 1981; Ytreland, 1980).

Major and Nagy (1972) discussed the Grønfjorden Bed as the "basal conglomerate", as it did not have a formal name at the time. They describe that it is well developed in the eastern part of their outcrop area while in the western part it is mostly absent. The outcrop area is in Adventdalen (Fig. 1.2). Their research reflects the irregular lateral character of the bed throughout the basin. They also mentioned that where Grønfjorden Bed is not present, it is often hard to distinguish Firkanten Formation from the underlying Carolinefjellet Formation.

Kalgraff (1978) and Ytreland (1980) both worked with the Firkanten Formation and did a short facies description of "the basal conglomerate", Grønfjorden Bed. Their synthesis of the bed is from Heerstupet, Kolfjellet (Van Mijenfjorden) and

Bassen (Adventdalen), (Fig. 1.2). They divided the basal conglomerates into clast-supported conglomerate and matrix-supported conglomerate.

Kostro (2005) studied the basal unconformity of the Paleocene succession on Svalbard, and also included a synthesis of the Grønfjorden Bed. The study documents a relief of up to 50 metres in the paleotopography of the unconformity surface on which Grønfjorden Bed is deposited. With the use of 3D mapping of the basal unconformity, it was clear that there is a slight dip towards west-southwest. He also noted east to west and east-northeast to west-southwest elongated depressions, separated by low highs are present. Kostro described the facies of Grønfjorden Bed with use of core data from Svea and Ispallen area, both from Van Mijenfjorden (Fig. 1.2). Four different facies were determined in his work.

Nagy (2005) described Grønfjorden Bed in a regional setting based on work from two outcrop localities in western Spitsbergen. It is interpreted as fluvial in origin connected to the lowstand systems tract of the Firkanten Formation sequence.

Lüthje (2008) analysed the Grønfjorden Bed at a few localities and through previous work by Kostro (2005) as part of a regional paleogeographic study of the Todalen Member. Marshall (2013) also analysed the Grønfjorden Bed for paleogeographic purposes. He studied the Grønfjorden Bed and its affiliation with the paleotopography of the unconformity surface. He generated maps of distribution of the bed and also a reconstruction of the paleotopography of the Grønfjorden valley system of southern Nordenskiöld Land (Fig. 1.2).
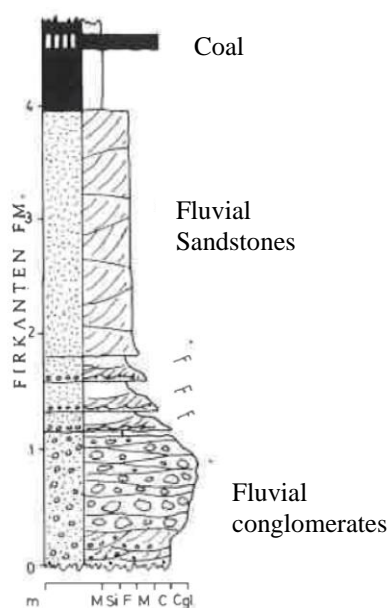

Figure 1.1: Type section of the Grønfjorden Bed from Grønfjorden. Ohta et al. (1992).

1.3 Study area
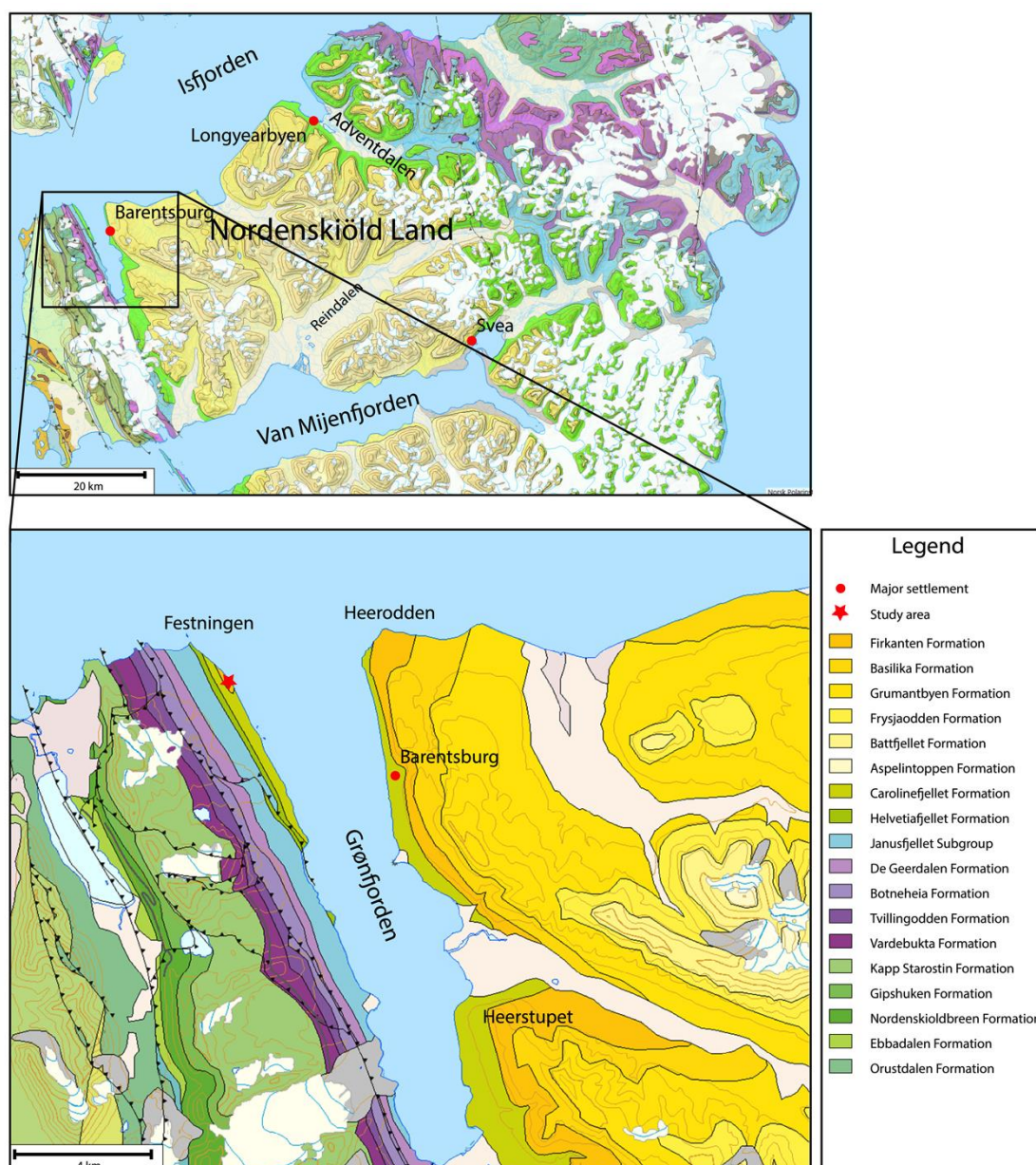
Figure 1.2: Geological map of Nordenskiöld Land, Grønfjorden and the study area. Paleogene strata are represented by yellow colours. From NPI (http://svalbardkartet.npolar.no/html5/index.html?viewer=svalbardkartet.html5).

The focus of this study is the Grønfjorden Bed in the northwestern part of Grønfjorden, Spitsbergen, located at the western margin of the Central Tertiary Basin. Thus it holds some of the westernmost outcrops of Paleogene sedimentary rocks deposited in the basin (Fig. 1.2, 2.1). The area is known as Festningen, from the very well known landmark of the 90 degrees tilted of Lower Cretaceous Festningen sandstone located at Festningsodden (Fig. 1.2), north of the outcrop area. From Festningen there is a 6 to 7 kilometres west-southwest long stretch along the coast

through vertically – sub-vertically outcropping strata ranging from Paleocene age to Carboniferous age as well as metamorphic basement rocks (Fig. 1.2, 2.2). The area has been exposed to significant deformation as a result of the tectonic forces that built the West Spitsbergen Fold and Thrust Belt (Braathen et al., 1995).

Pit mining of coal has been conducted in the area of the Todalen Member coals. In August 2004, mining inspector Per Zakken Brekke with the Norwegian Bergvesenet inspected a 900x200 metres area. The area was exploited for its mining resources first in 1899 by skipper Søren Zakariassen. During the years the area got known by the name "Cape Coal". The Norwegian state bought the area in 1933 and coal production was abandoned (Brekke and Kjærnet, 2005).

The lower Paleocene depositional rocks are outcropping in three localities within the study area. The main locality is roughly 350 metres long and situated in a vertical northwest to southeast trending cliff-face along the waterfront at elevations between 0 – 30 metres. This locality is difficult to reach, such that there has been no previous thorough sedimentological investigation of the strata.

The two other localities are situated 200 and 400 metres north of the northernmost point of the main locality (Fig. 5.1) and are accessible for first-hand observations. Both of these are restricted to less than ten metres in lateral extent and are tilted vertically to sub-vertically, leading to limited lateral exposure (see Fig. 1.4B and 5.8A). In winter the whole area is covered in snow and ice, including much of the steep cliffs, so fieldwork can only be performed in the arctic summer months.

2 GEOLOGICAL FRAMEWORK

2.1 Introduction

Svalbard is an archipelago that comprises all islands between 74 to 81 degrees north, and 10 to 35 degrees east, and is an exposed part in the northwestern corner of the Barents shelf (Kellogg, 1975). It makes up a land area of 62.000 km^2, of which approximately 60 per cent is covered by glaciers and inland ice. Steep glacier-carved valleys and fjords make for exceptionally good exposures of rock from Precambrian age to the Middle to Late Palaeogene (Steel and Worsley, 1984).

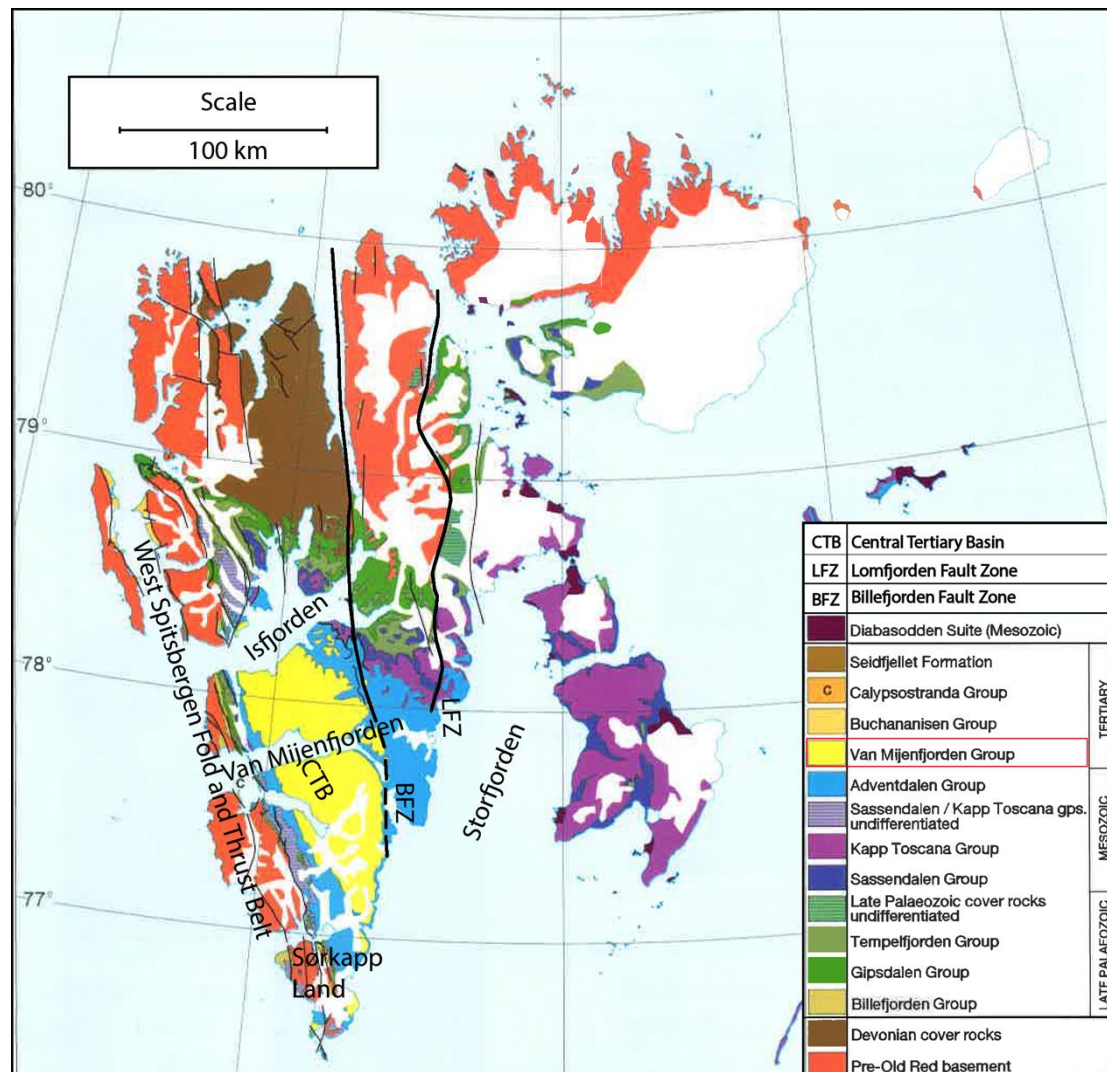
Figure 2.1: Geological map of the Svalbard archipelago. The Central Tertiary Basin deposits are centred more or less in between Isfjorden and Sørkapp Land and are indicated by yellow colour. It is bounded to the west by the West Spitsbergen Fold and Thrust Belt and the east by Billefjorden and Lomfjorden Fault Zones. Slightly modified from Serigstad (2011). Originally from Dallmann (1999).

2.2 Tectonostratigraphic framework

Introduction

The lower Paleocene strata of Firkanten Formation unconformably overlie Lower Cretaceous strata in the Central Tertiary Basin. These rocks belong to the Adventdalen Group and are of Middle Jurassic to Early Cretaceous age. They are mainly exposed along the margins of the Central Tertiary Basin, but also at some isolated locations around Svalbard.

The Cretaceous strata of the Adventdalen Group in Svalbard comprise Rurikfjellet, Helvetiafjellet and Carolinefjellet formations. Carolinefjellet Formation is of Aptian to Albian age and is up to 1200 metres thick (Dallmann, 1999). It is truncated by the basal unconformity of the Paleocene, which was formed by regional uplift and erosion preferentially in the northern part of Svalbard. This uplift is interpreted as a result of doming related to the development of the Arctic Basin further north (Maher, 2001; Steel and Worsley, 1984). Due to this tilting, Paleogene rocks deposited in the north of the Central Tertiary Basin overlie older strata than those in the south.

In southwestern Spitsbergen, the youngest recorded Cretaceous rocks are of late middle Albian age, approximately 105 Myr (Hurum et al., 2016). Further north Paleogene rocks overlie early Albian rocks, aged approximately 112 Ma (Grundvåg and Olaussen, 2017). U-Pb zircon dates from tephra layers close to the basal unconformity has yielded a mean $^{206}Pb/^{238}U$ age of 61,596 ± 0,028 Ma (Jones et al., 2017). This demonstrates the duration of the Cretaceous - Paleogene hiatus on central Spitsbergen to be between 43 and 50 Myr.

Paleogene tectonic setting

During the Paleogene, Svalbard was situated at approximately 75 – 80 degrees north (Dallmann, 2015). At the onset of the Paleogene, the separation of Eurasia and Greenland was still in the starting phase. Thus there was no major warm North Atlantic Current circulating north to the arctic areas, and the area probably had a continental-like climate, with cool winters and warm summers. Even though the climate was much cooler than in the Cretaceous, it was still considered as greenhouse conditions and much warmer than present day (Steel et al., 1985). During the Paleogene, in contrary to the relatively tectonically quiet Cretaceous period, Svalbard

experienced considerable tectonic activity (Steel and Worsley, 1984). This activity is presumably closely related to the evolution of the De Geer Zone (Fig. 2.5). The De Geer Zone is a complex transfer zone that during the Late Cretaceous and Paleocene times connected the spreading axes in the Norwegian-Greenland Sea, the Arctic Ocean and Baffin Bay (Bruhn and Steel, 2003).

Overall dextral transpression between the Eurasian plate and the Greenland plate during the Paleogene caused the formation of the West Spitsbergen Fold and Thrust Belt (Braathen et al., 1999). The West Spitsbergen Fold and Thrust Belt is up to 200 kilometres wide and 500 kilometres long. It strikes approximately north-northwest to south-southeast along the eastern side of the De Geer Zone in western Spitsbergen and the adjacent continental shelf in the northwestern Barents Sea (Bergh et al., 1997; Leever et al., 2011). Shortening in the West Spitsbergen Fold and Thrust Belt has been estimated to be between 20 and 40 kilometres, comprising mostly thin-skinned deformation (Bergh et al., 1997). The Central Tertiary Basin was also a result of movement along the De Geer Zone in the same period and has recorded important information about the tectonic events that took place (Steel et al., 1981). Several models have been suggested for the evolution of the Central Tertiary Basin in association with the plate tectonic setting of the Paleogene (Bruhn and Steel, 2003; Braathen et al., 1999; Helland-Hansen, 1990; Steel et al., 1981).

The Central Basin of Spitsbergen is a term used to define a large north-northwest to south-southeast trending structural syncline formed due to tectonic events in the Paleogene. It comprises most of the Carboniferous to Paleogene strata found on Svalbard. Paleogene rocks were deposited in what has been named the Central Tertiary Basin (Fig. 2.1) (Tertiary because the term was still in use when the basin was named), a depositional basin covering a large part central Spitsbergen (Harland et al., 1997).

The Central Tertiary Basin comprises today an area of approximately 200 kilometres north-northwest to south-southeast and 60 kilometres west-southwest to east-northeast and contains up to 2,3 kilometres of clastic deposits of the Van Mijenfjorden Group (Harland, 1969). Early vitrinite reflectance studies suggested that a minimum of 1,7 kilometres of clastic rocks has been eroded (Manum and Throndsen, 1978). More recent studies suggest that this overburden was much thinner, about 1,0 kilometre (Marshall et al., 2015).

The western limit of the Central Tertiary Basin is tectonically complex. The West Spitsbergen Fold and Thrust Belt forms a boundary that postdates most of the sedimentary rocks (Harland et al., 1997). The eastern limit of the basin is unclear. However, the Billefjorden and Lomfjorden Fault Zones (Fig. 2.1) have provisionally been proposed as the boundary (Harland et al., 1997; Nøttvedt et al., 1993).

Different models of basin configuration

Steel et al. (1981; 1985) suggested a two-stage evolution for the Central Tertiary Basin, in which the early Paleocene sedimentary succession slowly evolved from a series of smaller basins into a larger partly open marine basin. This basin configuration was driven by an extensional/transtensional tectonic regime situated east of the De Geer Line. During the Late Paleocene to Eocene, basin development changed characteristics to a compressional/transpressional regime. What is now represented by the West Spitsbergen Orogen was uplifted and provided the main sediment source in this period. The drainage reversal model demonstrates support for this basin development. Transgressive deltaic sequences were initially sourced from the east during the early Paleocene. As a response to the onset of compression and development of the West Spitsbergen Fold and Thrust Belt, the drainage system reversed causing sequences prograding from west to east during the late Paleocene to Eocene (Helland-Hansen, 1990).

Bruhn and Steel (2003) proposed a foreland basin model for the Central Basin development. This foreland basin model is based on the Central Basin originating as a flexural basin formed by thickening and thus loading in the west due to the buildup of the West Spitsbergen Fold and Thrust Belt. During the early Paleocene, the sediments were sourced from the eastern peripheral bulge. As the West Spitsbergen Fold and Thrust Belt developed, the provenance changed to a western source. Loading due to the development of the thrust sheet caused narrowing and deepening of the Central Tertiary Basin. This model is consistent with regional seafloor spreading models and tectonic models covering the West Spitsbergen Orogen (Bergh et al., 1997; Braathen et al., 1999).

In 2008, Lüthje proposed a different model compared to that of Bruhn and Steel (2003). Lüthje argued for compressional folding associated with a steep fault between the Central Basin and the West Spitsbergen Fold and Thrust Belt. With this model, Lüthje also argued for a westerly to northerly sediment source for the whole

Paleocene to Eocene succession. Shallow marine facies of Grumantbyen Formation extended across the whole basin, and Lüthje (2008) argued that erosion of the forebulge could not account for the volume required to make this happen. Recent work by Petersen et al. (2016) indicates an easterly source area for the sediments deposited in the early stages of the development of the Central Tertiary Basin. Their data and research cannot firmly differentiate between the different models of basin configuration, but the forebulge hypothesis of Bruhn and Steel (2003) is favored in their work.

Marshall (2013) built on former studies (Eiken, 1985; Harland et al., 1997; Livsic, 1974; Nøttvedt et al., 1988; Sokolov et al., 1968) to define a paleogeographic model for the initial deposition in the Central Tertiary Basin. He argued for a northern and eastern provenance area for the Todalen Member of Firkanten Formation. The unconformity surface contains northwest to southeast trending swells and depressions in which the Grønfjorden Bed was deposited, and is named the Grønfjorden Bed valley system. These swells and depressions were structurally controlled by underlying structures, which were present in response to the tectonic activity from which the West Spitsbergen Orogen originates.
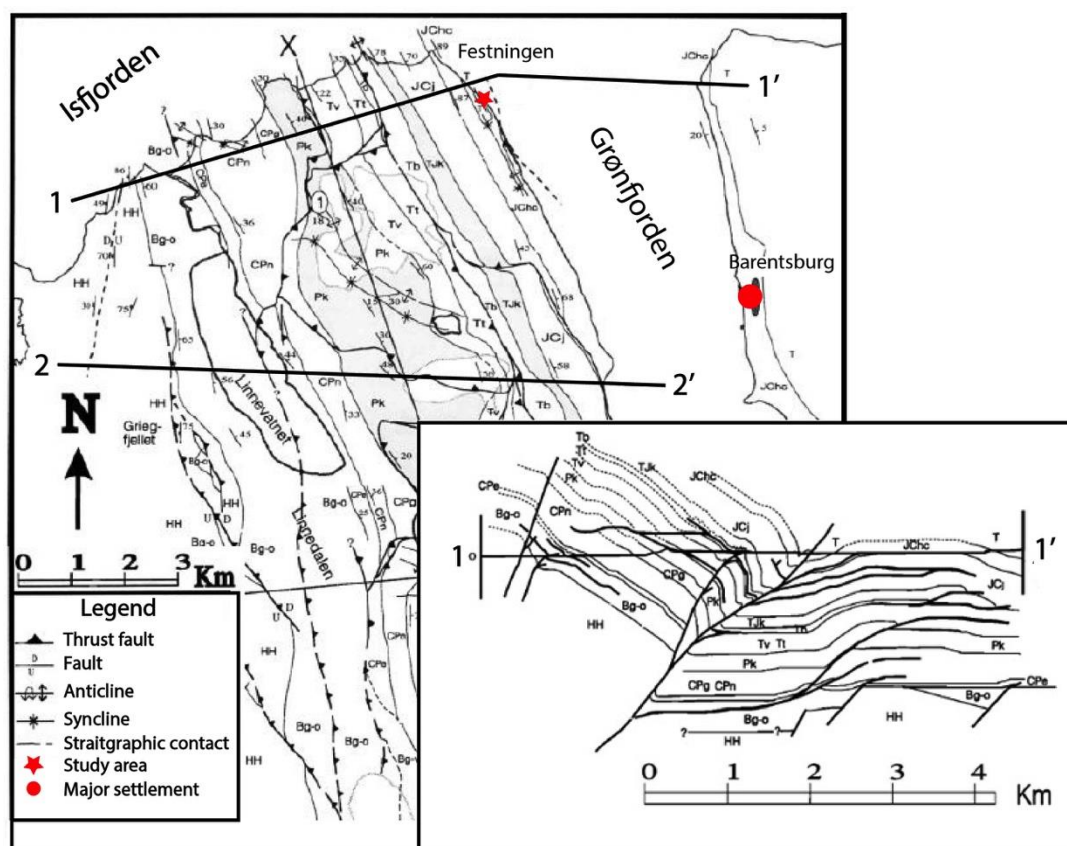
Structural elements of the study area

Figure 2.2: A) Structural map of western Nordenskiöld Land, from Grønfjorden and westwards. The different stratigraphic units and structural elements like faults and folds have been measured and mapped. **B)** Cross-section showing the large-scale structural elements and stratigraphic units of the Festningen area. A-A" was chosen as it is the most representative for the study area of this thesis. Slightly modified from Braathen et al. 1995.

There are several structural and tectonic elements affecting the exposures of the Grønfjorden Bed in the study area. Figure 2.2 A shows a structural map of the area, and figure 2.2 B shows the large-scale structural cross-section A-A" from figure 2.2 A, which is most representative of the study area. The northernmost exposures of the Paleogene rocks at Festningen are vertical. These are intensively deformed into east-verging folds (Braathen et al., 1995). Other associated tectonic elements are present such as crosscutting reverse and normal faulting in the Paleogene rocks (Fig. 2.3A) and folding (Fig. 2.3B) and duplex faulting (Fig. 2.3C) in the underlying Lower Cretaceous Carolinefjellet Formation. These structures are all associated with a major thrust fault that exists at depth along the northwestern shore of Grønfjorden (Braathen et al., 1995). In addition, the main outcrop is tilted approximately 20 degrees towards the east.
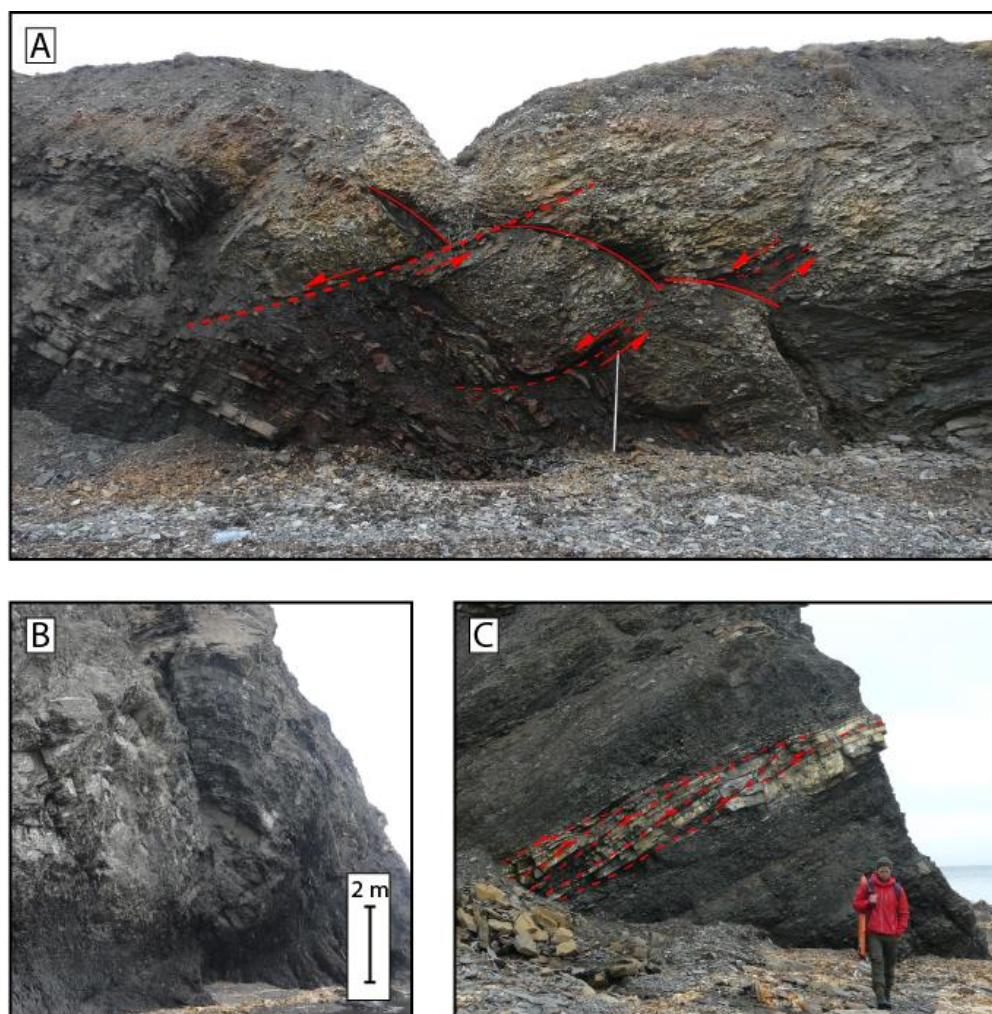
Figure 2.3: Structural elements caused by the tectonic activity that affects the outcropping Paleogene rocks in the study area. **A)** Faulting in the Grønfjorden Bed and the Cretaceous Carolinefjellet Formation. **B)** Folding in the shale of the Cretaceous Carolinefjellet Formation. **C)** Duplex faulting in a sandstone lens in the Lower Cretaceous Carolinefjellet Formation.

2.3 Van Mijenfjorden Group

Introduction

The Paleogene sedimentary rocks deposited in the Central Tertiary Basin of Spitsbergen are referred to as the Van Mijenfjorden Group (Harland, 1969), named after Van Mijenfjorden situated south of Isfjorden (Fig. 2.1). The group is subdivided into the Firkanten, Basilika, Grumantbyen, Frysjaodden, Hollendardalen, Battfjellet and Aspelintoppen formations. They reach a preserved thickness of more than 2 kilometres (Bruhn and Steel, 2003; Helland-Hansen, 2010; Petersen et al., 2016; Steel et al., 1985) (Fig. 2.4). The lower part of the Van Mijenfjorden Group (Firkanten, Basilika and Grumantbyen formations) is of early to middle Paleocene age, and the upper part (Hollendardalen, Frysjaodden, Battfjellet and Aspelintoppen formations) is

of late Paleocene to Eocene age (Steel et al., 1985). Identification of the Paleocene-Eocene Thermal Maximum (PETM) in the Gilsonryggen Member of Fysjaodden Formation, agrees with the proposition that the lower succession of the group is of Paleocene age (Dypvik et al., 2011; Harding et al., 2011; Nagy et al., 2013).
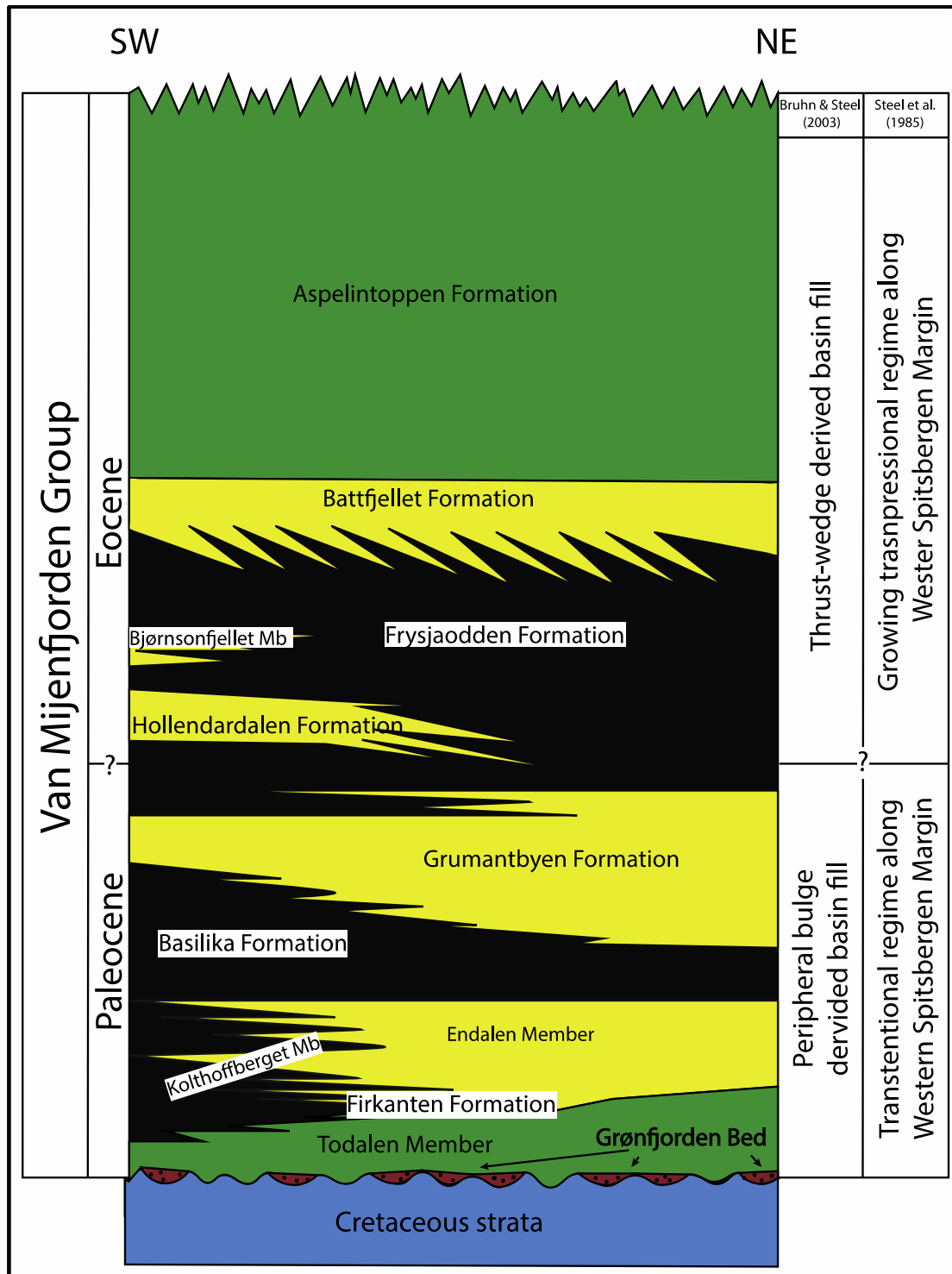

Figure 2.4: Stratigraphy of the Van Mijenfjorden Group. Slightly modified from Steel et al. (1985).

Early to middle Paleocene succession

The early to middle Paleocene succession of Van Mijenfjorden Group is up to 700 metres thick, thickening westwards and showing the deepest paleowater conditions in the west and SW of the Central Tertiary Basin, close to the present thrust front (Bruhn and Steel, 2003; Steel et al., 1985). The succession is built up of several small-scale sequences that stack to form two intermediate-scale transgressive-regressive cycles, one represented by the Firkanten Formation and the other represented by the Basilika and Grumantbyen formations (Bruhn and Steel, 2003). There has been debate whether the Paleocene succession in the Central Tertiary Basin was derived from the west or east-northeast.
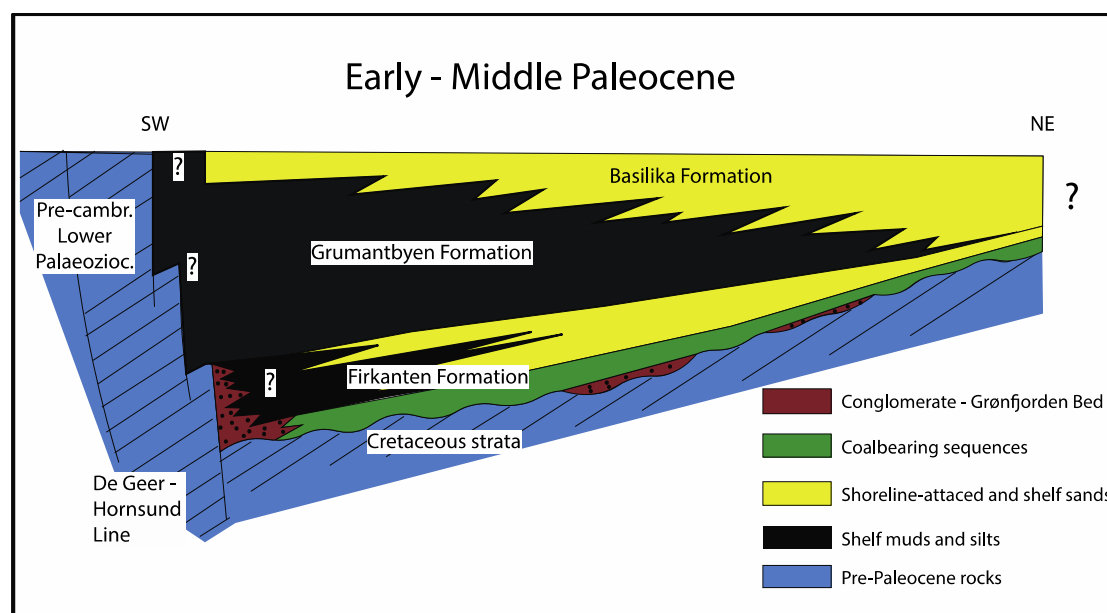

Figure 2.5: Early to middle Paleocene Succession of the Central Tertiary Basin. Slightly modified after Steel et al. (1985).

Firkanten Formation

The Firkanten Formation is the basal formation of the Van Mijenfjorden Group and is subdivided into Todalen, Endalen and Kolthoffberget members. In some western parts of the Central Tertiary Basin, it is up to 200 metres thick and thins eastwards to less than 100 metres (Bruhn and Steel, 2003; Kalgraff, 1978; Steel et al., 1981) (Fig. 2.5). Although it has an overall transgressive character, it consists internally of up to ten regressive parasequences (Nøttvedt et al., 1993; Steel et al., 1981). These parasequences normally have a coarsening upward trend and, are capped by either coal or clay ironstone (Steel et al., 1981).

The basal conglomeratic Grønfjorden Bed is part of the Todalen Member and defines the base of the Firkanten Formation in many places (Dallmann, 1999; Marshall, 2013; Nagy, 2005; Nagy et al., 2016). The overlying part of the Todalen Member largely consists of fine-grained, coal-bearing delta plain deposits with occurrences of delta-front sandstones (Aspøy, 2011; Nagy et al., 2001; Orheim et al., 2007). The overlying Endalen Member consists of shoreface/delta front deposits. The Kolthoffberget Member consists of prodelta and shelf mudstones located in the west and SW of the basin and interfingers with the Endalen Member to form its deeper-water equivalent (Bruhn and Steel, 2003; Jones et al., 2016; Steel et al., 1981).

- **Grønfjorden Bed**

The Grønfjorden Bed is a unit of Todalen Member and defines the base of the Paleogene deposits many places in the Central Tertiary Basin (Dallmann, 2015). It usually consists of clast-supported conglomerate but is also built up of matrix-supported conglomerates and sandstone (Dallmann, 1999; Kostro, 2005; Lüthje, 2008). The Grønfjorden Bed is principally regarded as incised valley fill deposited on an erosional unconformity during maximum regression (Kostro, 2005; Marshall, 2013; Nagy, 2005; Serigstad, 2011).

- **Todalen Member**

According to Dallmann (1999), the Todalen Member of the Firkanten Formation consists of 3-5 parasequences of shale-siltstone-sandstone-coal in the northeastern part of the basin and is usually less than 60 metres thick. Each of these parasequences represents progradation and retrogradation of northeastern and eastern-sourced deltaic systems (Dallmann, 1999; Steel et al., 1981). It is the most studied and well-known unit of the Paleogene deposits due to the long history of coal exploration along the northeastern and northwestern parts of the Central Tertiary Basin (Steel et al., 1981). All the commercially produced coal seams worked in Longyearbyen, Barentsburg and Sveagruva (Fig. 1.2) are of the Todalen Member (Dallmann, 2015). Steel and Worsley (1984) proposed that, at the time of deposition, there was a high-standing fault block south of the basin. This acted as a barrier that protected the deltas of the Todalen Member, which made it possible for the deltas to build out from the north and northeast without being greatly affected by wave action. This barrier was later

submerged, changing the coastal configuration and the more open coastal setup got more prone to wave influence (Steel and Worsley, 1984).

- **Endalen Member**

The Endalen Member consists of 4-5 coarsening upwards sandstone intervals (Dallmann, 1999). These sandstones are usually fine-grained and well sorted, often intermediate to heavily bioturbated, interbedded with some conglomeratic layers, clay ironstones and thin shales (Dallmann, 1999; Lüthje, 2008). The member is commonly between 40-100 metres thick and represents barrier bar-delta front deposits in a wave-dominated coastline (Steel et al., 1981). The unit thickens towards the west and southwest and interfingers with the time-equivalent deeper water deposits of Kolthoffberget Member (Dallmann, 1999; Jones et al., 2016). As mentioned in the Todalen Member section, the high-standing fault block barrier was submerged, and wave-energy was of larger influence when the Endalen Member was deposited. This resulted in a wave-dominated depositional unit where the development of extensive coals no longer was favoured due to the lack of extensive delta plains (Steel and Worsley, 1984).

- **Kolthoffberget Member**

The Kolthoffberget Member is the deeper-water equivalent of Endalen Member and only occurs in the western and southern reaches of the Central Tertiary Basin (Nagy et al., 2001; Steel et al., 1981). According to Dallmann (1999), it reaches up to 120 metres in thickness on Kolthoffberget, which is located in central northern Van Keulenfjorden, south of Van Mijenfjorden (Fig. 2.1). Koltohffberget Member consists of coarsening-upward sequences normally 10 metres or less, of dark, silty shales at the base to poorly sorted, organic-rich very fine sandstones in the top. The sequences are commonly highly bioturbated with a lack of visible primary sedimentary structures (Steel et al., 1981).

3 METHODOLOGY

3.1 Introduction

This study is based on data acquired during two field seasons in the Festningen area on Svalbard (Fig. 1.2). Traditional sedimentological field techniques were combined with virtual outcrop analysis to obtain results.

3.2 Data acquisition

Fieldwork

The first field season was in July 2016 and the second in September 2017. Snow cover in the study area combined with the dark season in the Arctic winter means that summer is the only time to perform efficient fieldwork. Due to late snow cover in summer 2017, planned fieldwork was postponed until September 2017. The fieldwork was performed together with a field assistant each season. A dog and a trip wire system around the tent camp were necessary safety measures due to the threat that polar bears pose all across the archipelago of Svalbard. The outcrops were reached by hiking 5 – 15 minutes from camp.

Sedimentological logging

Sedimentological logging was performed in a total of four localities. These are the only localities within reach as the other parts of the exposed Paleogene strata are situated in vertical cliffs high above the ground (Fig. 3.1). Logging was performed in 1:20 and 1:10 scales with focus on lithology, fabric, colour, sedimentary structures, bed boundaries and grain sizes. Special emphasis was on the conglomerate beds, in which fabric, texture, grain size and shape were analysed.

In-field observations are of higher resolution than those on virtual outcrops and yields information in greater detail.

Images taken by the use of drone

Due to the inaccessibility of the outcrop, images taken by use of a drone were initially supposed to be the main form of data acquisition. If used correctly, the drone images could give good results as it can fly quite close to the outcrop and provide proper images.

In the first field season, it was scheduled to bring a drone owned by UNIS to the field area to capture images of the outcrop for use in further analysis. Due to technical maintenance of the UNIS owned drones, a privately owned drone provided by UNIS staff was used during fieldwork in July 2016. The drone is a DJI Phantom 4.

The battery life and the camera quality on the private drone were insufficient to capture the required quality images. Wind conditions also resulted in poor flying conditions, which meant that the drone could not fly close to the outcrop. The result was approximately 120 photos from one run north to south along the outcrop with varying image quality. These images proved to be good for large-scale outcrop features (Fig. 5.1). However, detailed analysis could not be performed with the images captured by the drone.

Images taken by use of camera mounted on telescope pole

In the second field season, a telescope pole mounted camera was used (Fig. 3.1). The camera is a Sony ILCE-QX1 with 20,1 megapixels resolution. The telescope pole is made out of carbon fibre, making it relatively light, and can extend up to 20 metres. Additionally, Playmemories Mobile, an application for mobile phones and tablets controls the camera remotely through Wi-Fi.

The method is convenient because the camera provides images of high quality and it is easy to get close to the rock exposure. However, when extended beyond five metres the carbon fibre pole is greatly affected by even low winds. This causes the pole to swing and the camera to lose focus resulting in poorer image quality on the highest locations. The process of taking photos at one locality and moving on to the next is time-consuming. Nevertheless, a large number of high-quality photos were attained with this method.
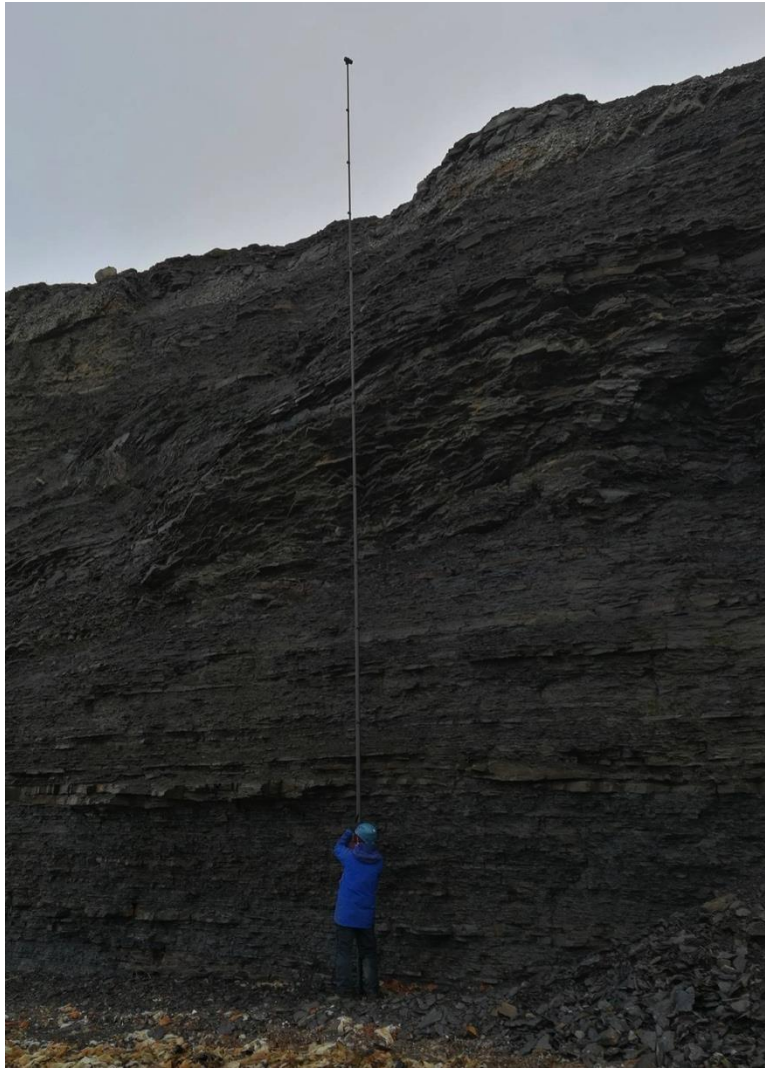
Figure 3.1: Field assistant holding the almost fully extended telescope pole with a camera mounted on top, used for taking pictures of the outcrop. Target outcrop is the lighter unit at the very top of the cliff, approximately 20 vertical metres off the beach.

3.3 Data processing and analysis

Digitizing of sedimentary logs and figures

For digitising of logs, the software Adobe Illustrator CC was used. The logs were digitised in the same scale as they were logged. These are from now on referred to as "logged sections". Other figures were also created and edited in the same software.

Creating virtual outcrops

Creating virtual outcrops has been necessary due to the limited access to the outcrops. It was performed using Agisoft PhotoScan, an image-based 3D modelling software that creates high-quality 3D models from still images.

The workflow used to create models in Agisoft PhotoScan is:

- Load photos

To start the process, photos must be loaded into the software

- Align photos

In this step, the software searches for common points on photographs and matches them. Also, it calculates the camera positions for all the pictures.

- Build dense cloud

Based on the camera positions from the previous step, Agisoft PhotoScan calculates depth information for each camera so that they can be combined into a single dense cloud.

- Build mesh

In this step, the software reconstructs a 3D polygonal mesh (or the geometry of the object) based on the dense cloud.

- Build texture

Agisoft PhotoScan imprints real texture on the geometrical (mesh) model

- Build tiled model

The tiled model uses parametres from the previous steps, and imprints tiles from photographs on to the geometric model. This is the step that makes the model high-resolution, and usable for grain-size inspection of the conglomerates.

Several models were made using this method. These have been used further for detailed sedimentological analysis. The models are of varying resolution and quality due to factors such as overlap and quality of photographs.

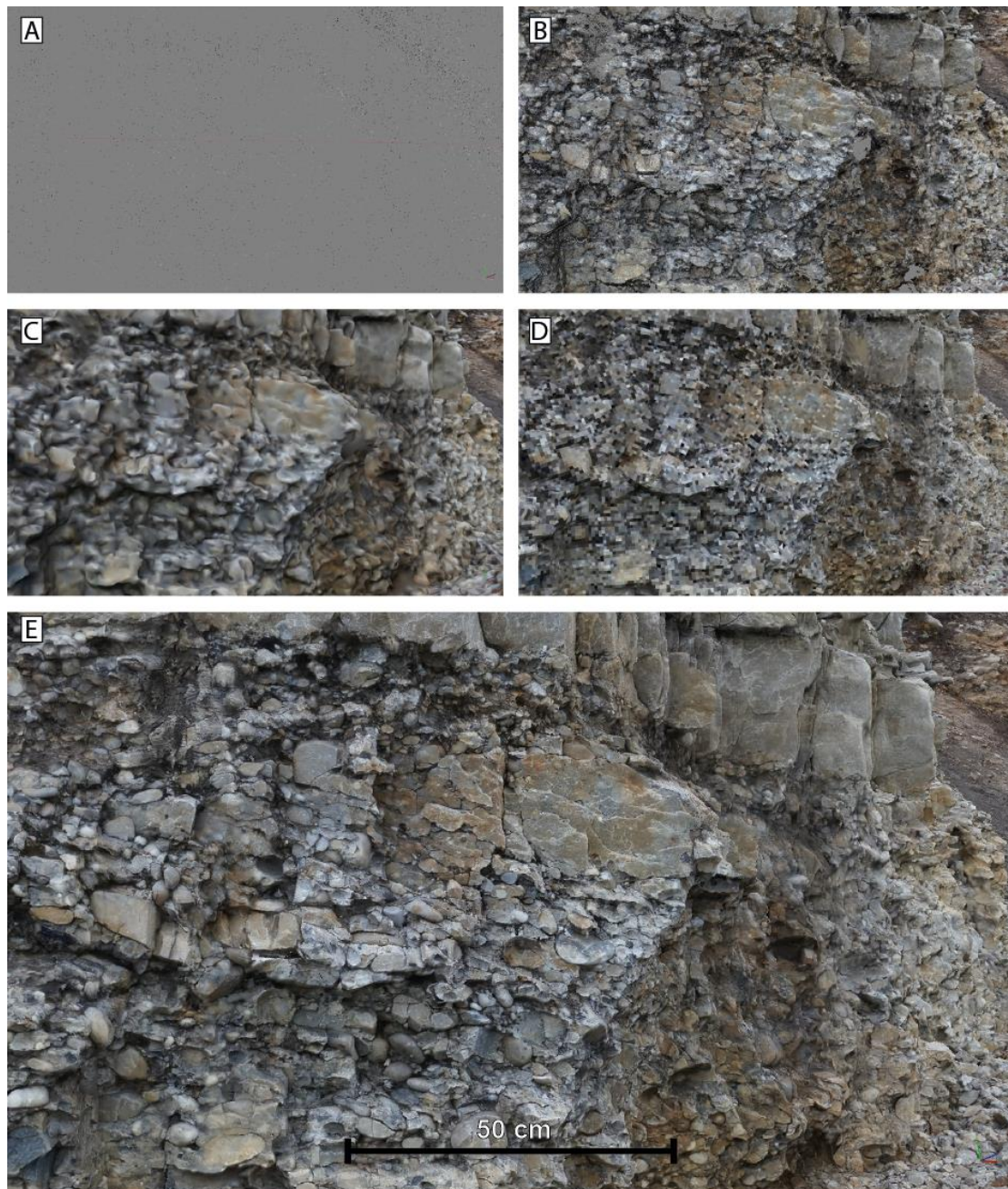These are from now on referred to as "virtual outcrops".

Figure 3.2: Screen captures from Agisoft PhotoScan showing the different stages of the workflow when making a 3D model. **A)** Align photos, sparse point clouds. **B)** Dense point cloud. **C)** Build mesh. **D)** Build texture. **E)** Tiled model. The software imprints the photos onto the texture, which gives it excellent resolution in some parts.

Analysis performed on the virtual outcrops

To perform sedimentological analysis on the virtual outcrop, the highest quality models, tiled models, were required. These are not possible to export to another software, so interpretation was made in Agisoft PhotoScan. The method of producing and using virtual outcrops provides a unique opportunity for inspection and analysis in otherwise inaccessible rock exposures.

The sedimentary strata are intensely fractured, fracture planes cutting directly across conglomerate pebbles, not discriminating between matrix and clasts (also noted by Lüthje (2008) and Petersen et al. (2016)). Several fracture planes are running parallel to the exposure, evident from 3D views and also from slickensides on the outcropping conglomerate. This causes poor view in some places and also obscures the 3D view of conglomerate clasts, as less than a percentage of clasts protrude from the outcrop.

Measuring of clast sizes and bed thickness has been made possible by georeferencing of the pictures from which the virtual outcrops were created. However, due to the accuracy of the georeferencing and the 3D nature of the virtual outcrops, there is an error to the measurements ranging from zero to five per cent. The error is greater at smaller scales as for when measuring clast sizes. Nevertheless, the error is not seen as a great obstacle as long as precautions are taken.

The studies of the basal unconformity characteristics is mostly based on virtual models, from which both local (centimetre to metre scale) and outcrop-scale scouring has been observed. Outcrop-scale scouring is the identification of angle between the strata below the unconformity and the unconformity itself. Local scouring has also been studied first-hand.

Paleocurrent studies are based solely on measurements from the virtual outcrops. The dip direction of sedimentary structures and inclined clasts are therefore based on values observed in 2D planes. This leads to only generalised directions of dip such as towards the southeast or northwest along the cliff face on which they are exposed.

Facies analysis

The term "facies" was introduced in 1669 by Danish natural scientist Nicholaus Steno to describe the whole aspect of parts of the earth's surface during a particular interval of geological time. However, the definition of the term has gone through many changes during the last centuries. The definition commonly used today is; Sedimentary facies are the basic types of sedimentary deposits, and are distinguished in descriptive terms as the elementary building blocks of a sedimentary succession (Harms et al., 1975; Harms et al., 1982; Reading and Levell, 1996). This means that a facies represents a type of sedimentary deposit directly connected with a sedimentary process. Ultimately the facies will be connected to a depositional environment.

However, this does not mean that one facies can only be connected to one depositional environment. Facies are grouped to form facies associations that then each represent a general depositional environment.

The facies analysis of this study is based on the logged sections, photos and the virtual outcrops. Resolution of the virtual outcrops and photographs is not good enough to distinguish grain sizes finer than fine pebbles. Hence all grain sizes from granules and finer are based on the observed grain sizes from the logged sections. However, the correlation between the logged sections to the virtual outcrops suggests that the grain sizes are closely related.

Sedimentary facies are described based on different lithological and sedimentary features such as grain size, sedimentary structures, colour and thickness. For the sandstone facies, different sedimentary structures give implications for flow regime of the depositional agent (Fig 3.3). Furthermore, conglomerate is the main facies type of this study, and emphasis has been given to these deposits. Certain parametres should always be considered when studying rudites and gravels. Harms et al. (1975) listed four very important parametres to these types of alluvium: Sorting and size distribution, fabric, stratification and grading. In addition to these, grain shape and texture are important parametres to evaluate (Collinson et al., 2006) (Fig. 3.4).
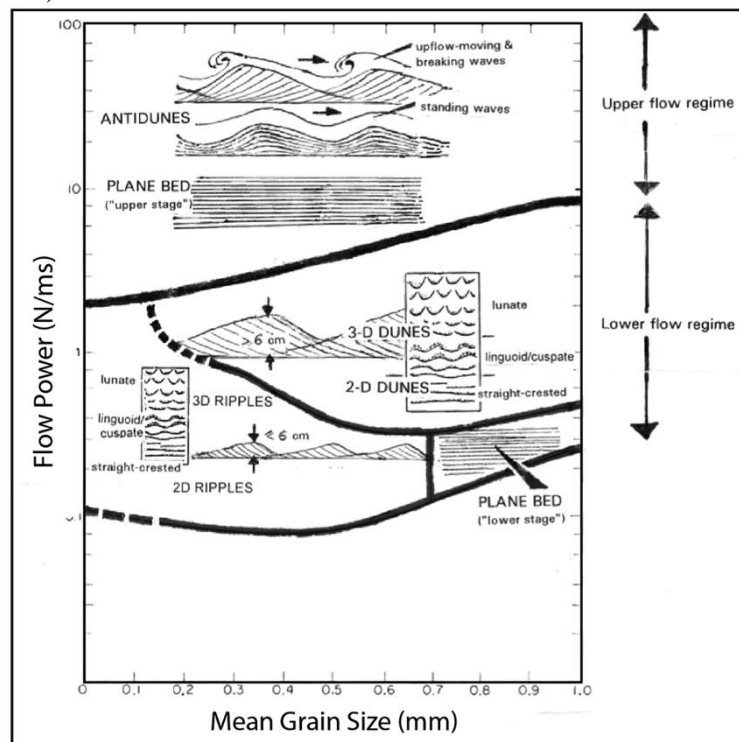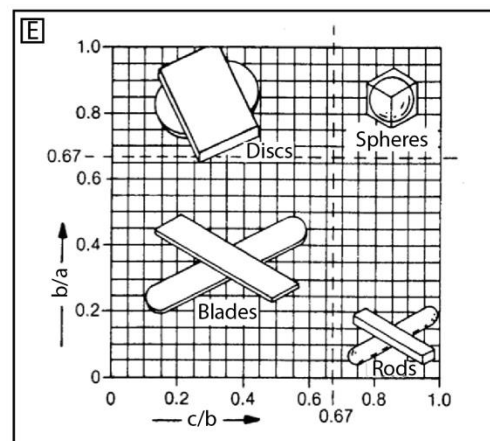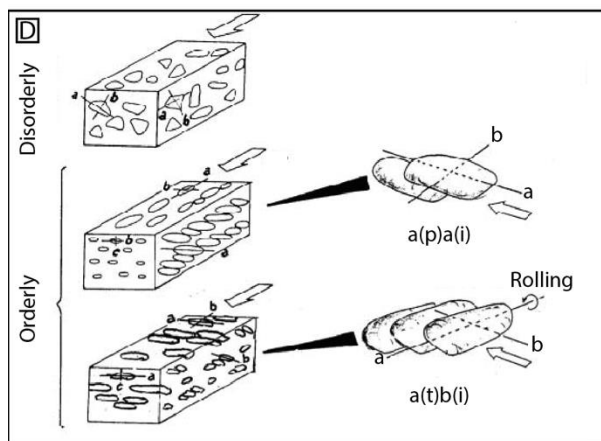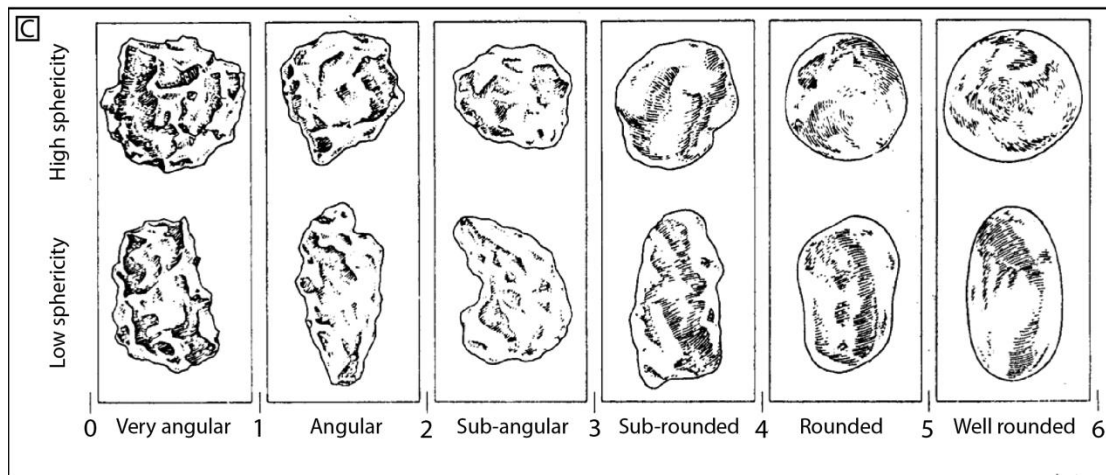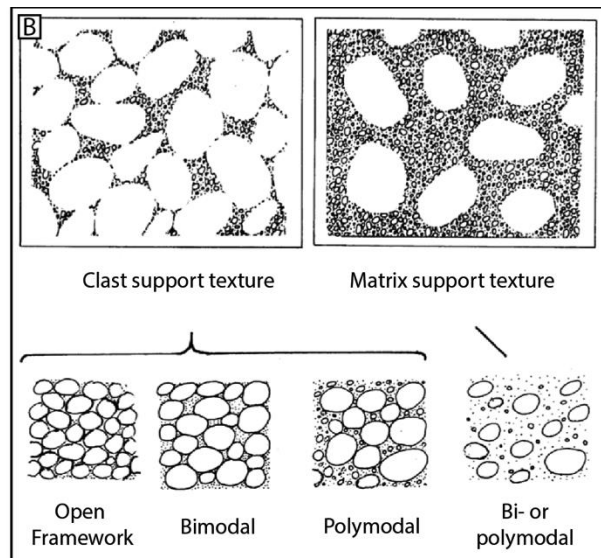

Figure 3.3: Flow regimes in sand and sandstone deposits according to bedforms created by unidirectional currents. Slightly modified from Allen (1982).
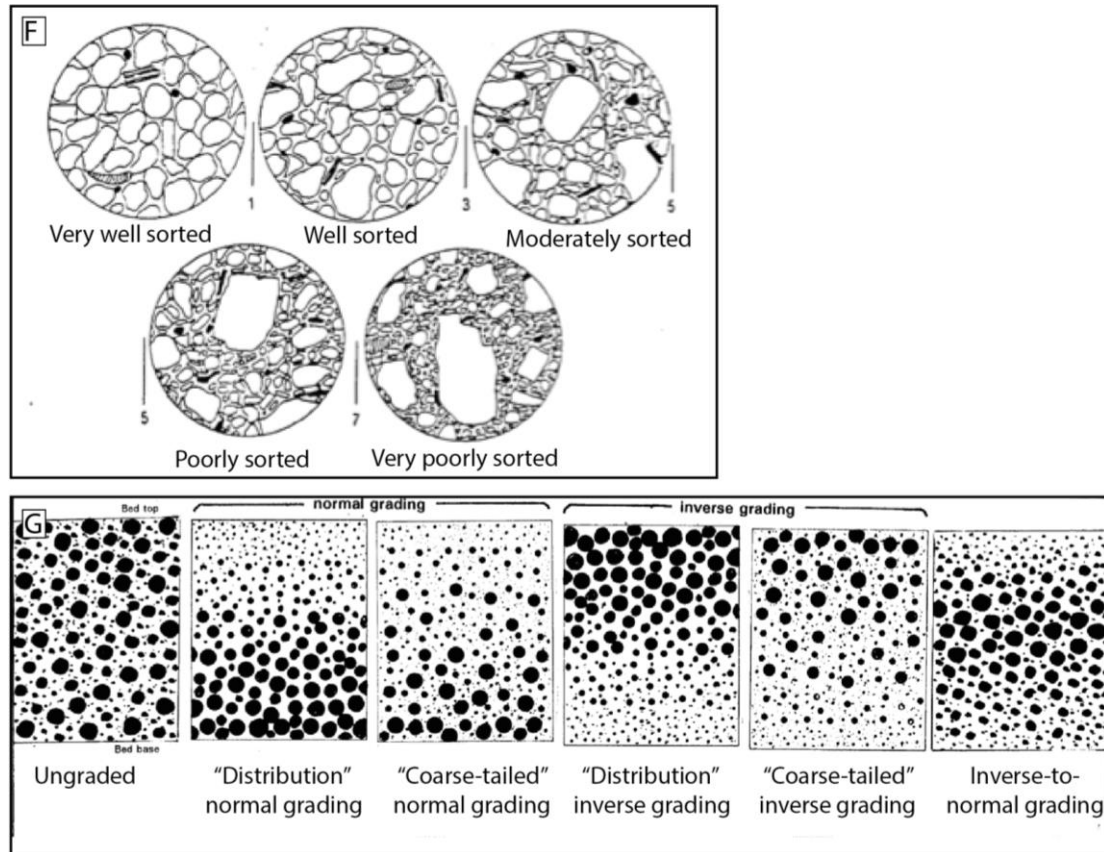
Figure 3.4: Tables and figures used to help classify sediments and sedimentary rocks and in particular gravels and conglomerates: **A)** Grain size classification scheme. Wentworth grain size classes are quantitative and useful in classifying grain size. Slightly modified from Blatt et al. (1980). **B)** An informative chart showing differences in texture of gravels. Slightly modified from Collinson et al. (2006). **C)** Rounding and sphericity chart. Slightly modified from Powers (1953). **D)** Clast fabric classification chart. The a-axis is the longest and the b axis is intermediate. Thus a(p)a(i) means that the longest axis is both parallel to flow direction and imbricated. a(t)b(i), however, means that the longest axis is transverse to flow direction and the intermediate axis is imbricated. Slightly modified from Harms et al. (1975). **E)** Zingg diagram. Slightly modified from Krumbein & Sloss (1951). **F)** Grain sorting chart from Compton (1985). Representing sandstone as seen with a hand lens. The same sorting parametres apply to conglomerates. **G)** Chart of different types of grading. Modified from Walker (1975).

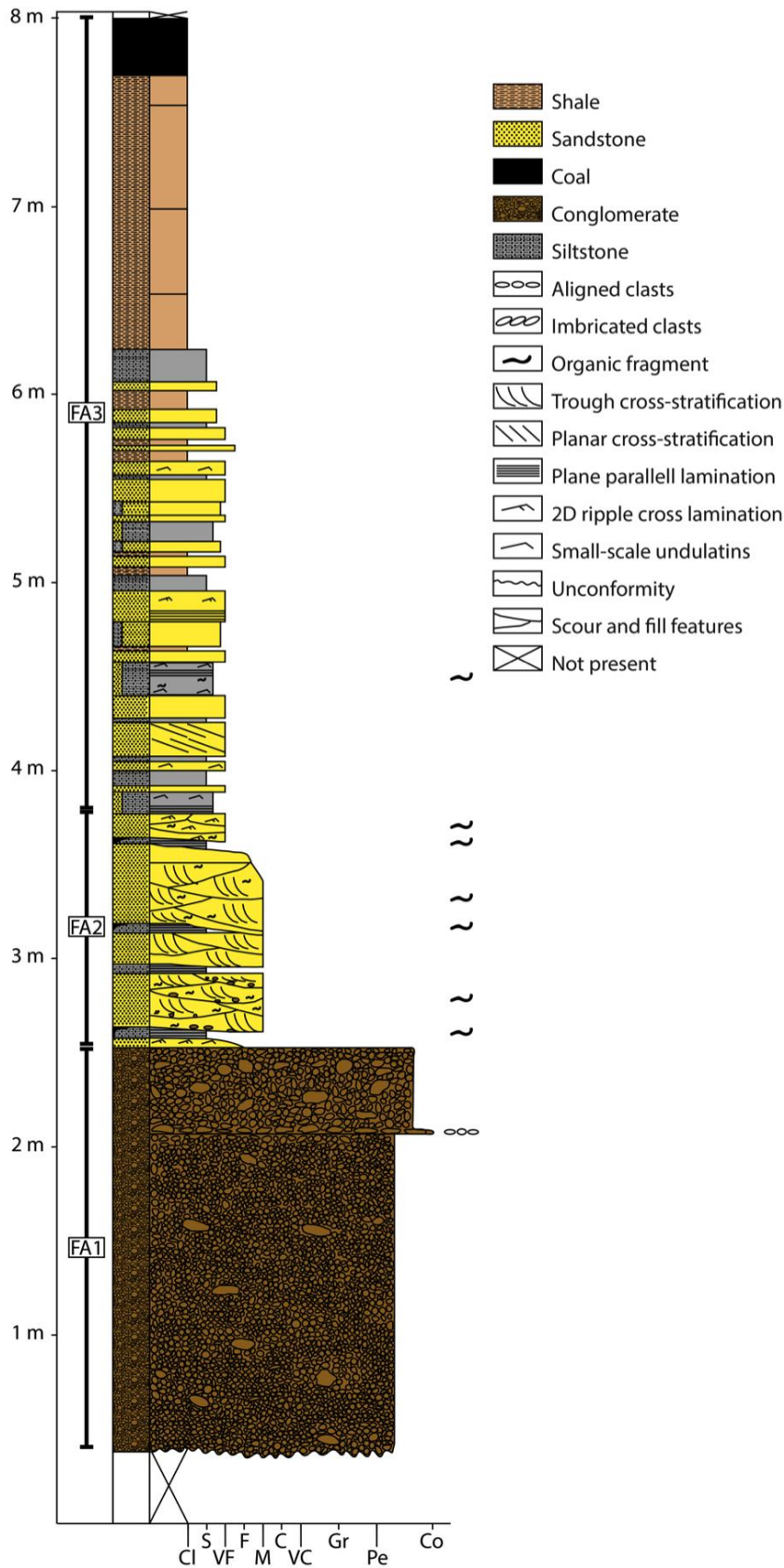# 4 FACIES ANALYSIS

4.1 Introduction

Figure 4.1: Log from logging locality 2, 200 metres northwest of the main outcrop area represented by figure 5.1. It represents the main logged section of Grønfjorden bed and the associated sedimentary deposits. This log includes many of the sedimentary facies that have been observed and described in the study area. The basal conglomerates represent the same facies with different clast sizes. The legend of this log also applies to figure 5.7.

As mentioned in section 3.3, the facies analysis is based on observations and interpretations both from logged sections and virtual outcrops. Figure 4.1 is the main logged section from the study area. It contains many of the sedimentary facies that have been recorded and represents a typical fining upwards succession of the earliest Paleogene deposition.

4.2 Sedimentary facies

Conglomerate facies

Introduction:

The conglomerate facies are the main facies type in this study and distinguishes the Grønfjorden Bed from other lithological units in Todalen member. These have been divided into facies based on the different attributes discussed in chapter 3.3 and figure 3.4.

The conglomerate facies area all polymict, and consist of quartzite, metaquartzite, vein quartz and granule to fine pebble fragments of black chert. Lüthje (2008) performed a provenance analysis in which she determined with some certainty the provenance of the Grønfjorden Bed clasts. She interpreted a western source for the conglomeratic clasts, arguing that the most suitable source rocks were of Paleozoic age. These include the highly silicified Carboniferous and Permian limestones of Gipsdalen and Tempelfjorden groups. There is also occurence of black chert in some of these strata. Furthermore, the basement rocks of the Hekla Hoek Group contain a variety of lithologies such as metamorphic quartzites, posing as potential source rocks for the clasts of the Grønfjorden Bed (Lüthje, 2008).

The mentioned lithologies are outcropping west, north and northeast of the Central Tertiary Basin, with the western outcrops being more proximal to the study area (Fig. 2.1). These observations imply that these rocks were undergoing erosion at the time of deposition of the Grønfjorden Bed (Dallmann, 1999; Lüthje, 2008).

Table 1: Description of various characteristics of the conglomerate facies with focus on clast sizes, texture, sorting rounding and fabric (Fig. 3.4). MPS (maximum particle size) is calculated as the average of the ten coarsest clasts in the single coarsest bed of each facies.

Facies	Average clast size (Wentworth)	MPS (cm)	Coarsest clast (cm)	Texture	Sorting	Rounding	Imbrication
CGL$_{CS}$	Coarse pebble	16	22.5	Clast-supported	Moderately to well sorted	Sub-rounded to well-rounded	Scattered
CGL$_{L}$	Medium pebble	12	18.6	Clast-supported	Moderately to well sorted	Sub-rounded to well-rounded	Scattered
CGL$_{M}$	Fine pebble	3	4	Matrix-supported	Poorly sorted	Rounded to well-rounded	No
CGL$_{GL}$	Fine pebble	2	3	Matrix-supported	Well sorted	Rounded to well-rounded	No
CGL$_{D}$	Medium pebble	15.7	24	Clast- to matrix-supported	Very poorly sorted to poorly sorted	Sub-rounded to well-rounded	Scattered
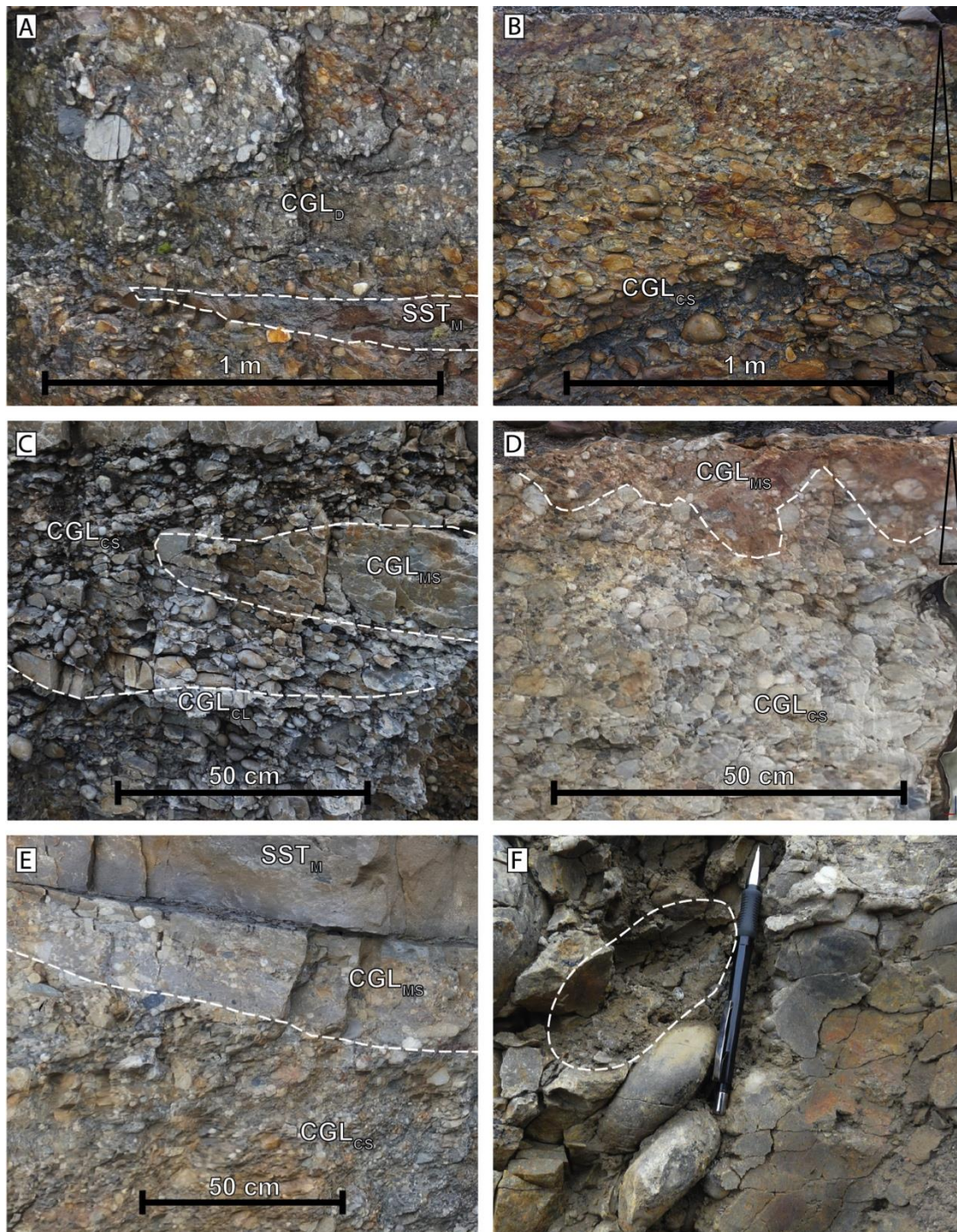
Figure 4.2: Different appearances of the conglomerate facies. **A)** CGL$_D$ interbedded with a lens of facies SST$_M$. Note the out-sized clasts in the middle-left part of the picture. **B)** Stacked beds of CGL$_{CS}$. There is a general fining upwards trend from coarse cobbles to fine pebbles in the top. **C)** CGL$_{CS}$ pebble dominated bed interbedded with a lens of CGL$_{MS}$. Also, notice the aligned cobbles below the CGL$_{MS}$ lens. **D)** CGL$_{CS}$ grading in the top to CGL$_{MS}$. **E)** CGL$_{CS}$ at the base shifting to cross-stratified CGL$_{MS}$ above the white line. SST$_M$ facies situated at the top. **F)** a(t)b(i) imbrication from logged section 1 (see section 3.3). The strata at this locality are tilted 90 degrees. Paleocurrent direction is towards the bottom of the figure.

Facies CGL$_{CS}$: Massive clast-supported conglomerate

Description:

This facies consists of clast-supported conglomerates. Clasts range from granules to coarse cobbles and are usually dominated by the coarse pebble fraction. Certain beds are dominated by either medium to fine pebbles or cobbles. Some outsized clasts are common (Fig. 4.1).

There are large variations in grain sizes and sorting of this facies. It is commonly moderately sorted and bimodal to polymodal although well-sorted, bimodal sections do occur (Fig. 3.4B, F, 4.2B). The fabric is commonly disorderly with scattered imbrication. Where imbrication occurs, it is localised and includes a limited number of clasts (Fig. 4.2F, 5.6D). Where observable in three dimensions, clast imbrication is of a(t)b(i) imbrication (Fig. 3.4D, 4.2F). On average, clasts are sub-rounded to well rounded (Fig. 3.4C). High sphericity clasts are abundant, but elongate clasts are also common.

For the most part, the facies appear as massive, but crudely defined bed boundaries are observed, commonly in the form of change in clast size. Normal grading occurs in a few localities (Fig. 4.2B), as does very crudely define cross-stratification.

The lower boundaries are commonly erosive. Upper boundaries are commonly sharp and flat (Fig. 4.2C), but at some localities it grades to facies CGL$_{MS}$ (Fig. 4.2D) or facies SST$_M$ (Fig. 5.6F). Thicker strata of this facies may consist of poorly defined scour and fill sets. Sets are commonly aligned at the base by clasts coarser than the surroundings, either concave up or bedding aligned clast horizon (Fig. 4.1, 4.2C). The facies may also be interbedded with other facies such as facies CGL$_{MS}$, CGL$_D$ and SST$_M$- At the top of some sets, the facies fine upwards to facies CGL$_{MS}$. Observed bed thicknesses vary from 10 centimetres to 1.6 metres.

Interpretation:

The coarse grain sizes of this facies indicate high competence flow. Grain sizes vary with competency so that well-sorted beds of pebble conglomerates were deposited by less competent flow than that of cobble conglomerates. The mainly disorderly fabric with scattered imbrication is evidence of high capacity flow in which clasts only have limited ability to move freely relative to each other (Harms et al., 1975; Hemelsdaël et

al., 2017). Imbrication type a(t)b(i) suggest rolling-clast imbrication (Collinson et al., 2006).

The well rounded and spheroid nature of clasts suggests constant abrasion, weathering and reworking (Collinson et al., 2006). This yields a high maturity of single clasts.

Normal grading suggests waning flow conditions (Nemec and Steel, 1984), whereas the appearance of concave up and bedding aligned cobble clast horizons suggest clast size segregation due to the winnowing of finer-grained clasts in the base of a fluvial channel. The concave-up units indicates erosional base of a channel as channel-floor lags (Gobo et al., 2014; Vincent, 2001). The very crude cross-stratification occurs only in a few localities, and indicate transport and deposition of gravel dunes or bars.

The facies is interpreted to have been deposited within a fluvial channel and bar system of high competency and capacity flow in which variations in flow velocity is evident due to the scour-and-fill pattern indicated by erosional bases of beds.

Facies CGL$_L$: Low-angle stratified clast-supported conglomerate
Description:
This facies consists of clast-supported conglomerate. The average clast size is medium pebbles, although clasts range from fine pebbles to cobbles. Cobble-sized clasts are scarce and out-sized. Sandy matrix fills pore spaces.

The sorting of this facies is in the range of moderately to well sorted (Fig. 3.4F). The fabric has a disorderly appearance with only scattered imbricated clasts (Fig. 3.4D). Clasts are sub-rounded to well rounded (Fig. 3.4C) and of high sphericity (Fig. 3.4C,E).

Crudely defined low-angle stratification is observed in the range of 10-20 degrees. The stratification is evident due to slight variations in grain size and is commonly enhanced by fracture patterns (fig 5.4E-F). Beds reach a thickness of up to 1.5 metres in area 3 (Fig. 5.4).

Interpretation:

The grain size and sorting indicate high competency flow conditions. The apparent disorderly fabric may be an effect of the abundance of spherical clasts. The observed imbrication is interpreted as rolling imbrication a(t)b(i) (Fig. 3.4D, 4.2F). High sphericity and well-rounded nature suggests high degree maturity of individual clasts.

Low-angle stratification is common in gravel deposits as migration of low-relief barforms in a braided river stream. The low angle suggests downstream deposition of longitudinal bars possibly transported and deposited from traction or gravel sheets (Gobo et al., 2014; Hemelsdaël et al., 2017; Santos et al., 2014; Vincent, 2001).

Facies CGL$_{MS}$: Matrix-supported conglomerate

Description:

This facies consists of matrix-supported conglomerate. The matrix is mostly medium to very coarse sandstone, and the clasts consist of granules and fine to medium sized pebbles. Dominant pebble size is between one and two centimetres. Visual measurements of clasts/matrix gives approximately 30 to 60 per cent clasts by volume. It is commonly polymodal to bimodal and moderately to poorly sorted (Fig. 3.4B, F). The fabric is disorderly (Fig. 3.4D) and clasts are rounded to well rounded.

Facies CGL$_{MS}$ occurs in association with other facies in different associations. In some localities, it occurs as a lens imbedded in facies CGL$_{CS}$ (Fig. 4.2C). At the top of the conglomerate bed at some localities, there is a grading relationship, where facies CGL$_{CS}$ grades vertically to facies CGL$_{MS}$ (Fig. 4.2D). Cross-stratification including facies CGL$_{MS}$ only occurs at one locality (Fig. 4.2E).

The thickness of CGL$_{MS}$ beds ranges from 10 to 30 centimetres. Lateral extent is difficult to determine when there is a gradational trend from CGL$_{CS}$, but a maximum length of 1 metre has been observed.

Interpretation:

The occurrence of lens-shaped bodies of facies CGL$_{MS}$ within or above beds of facies CGL$_{CS}$ indicates waning or pulsating flow conditions. High capacity flow is needed to be able to transport and deposit such a large variety of grain sizes. Lenses with sharp boundaries may reflect rapid deposition, whereas upwards gradational change from

facies CGL_{CS} to CGL_{MS} may simply reflect waning current condition of a sediment-laden flow (Nemec and Steel, 1984).

Cross-stratification of the facies indicates migration and deposition of dunes. The trough shape of the bed indicates scouring whereas the abundance of sandstone concentrated at the base of the trough indicates deposition from sand-rich flow. The upwards coarsening character may also be a result of dispersive forces in heavily sediment-laden flow pushing coarser particles towards the top of the flow (Nemec and Steel, 1984).

Facies CGL_{GL}: Gravel lag in sandstone

Description:

This facies consists of clast-supported medium to fine-grained pebbles conglomerate with clasts commonly <1 centimetre. The clasts are sub-rounded to rounded and commonly of high sphericity. They are well sorted.

The facies is commonly one pebble thick but reaches a thickness up to 10 centimetres. Conglomerate horizons of this facies are laterally extensive and commonly horizontal but may have a crudely defined convex up shape. The facies only occurs at the base or top of beds of facies SST_{CS} and facies SST_M (Fig. 4.8B, 5.2E, 5.6).

Interpretation:

Gravel lags are typically a result of winnowing by strong currents when the current transports and erode finer grain sizes. Gravel lags may represent erosional bases for new sets of planar cross-stratification (Collinson, 1996).

The convex up shape of gravel lags may indicate winnowing of finer sediments by Aeolian processes on top of dunes at low-flow stage, as deflation surfaces (Langford and Chan, 1988, 1989). However, the convex up shape is only evident in one layer of the facies, and more evidence is needed to conclude this.

Units thicker than a few pebbles are more likely to have been deposited on the channel floor when flow strength is high (Collinson, 1996). Rounding and sphericity of clasts together with well-sorted nature of the facies are characteristics of high maturity.

Facies CGL$_D$: Disorganized clasts- to matrix-supported conglomerate

Description:

This facies consists of disorganised clast- to matrix-supported conglomerate. The texture changes on decimetre scale vertically and laterally. It consists of clast sizes ranging from granules to cobbles. Outsized clasts are common (Fig. 4.2A). Coarse isolated clasts situated at the very top of the conglomerate facies occurs in some localities (Fig. 5.5E). It is poorly sorted and polymodal (Fig. 3.4B, F) and the fabric is disorderly. However, scattered imbrication does occur (Fig. 3.4D). Clasts are sub-rounded to well rounded and sub-spherical to spherical (Fig. 3.4C, E, 4.2A).

Vertical boundaries are generally poorly defined. However, there are some subtle vertical changes in average grain size giving the impression of bedding within the same facies. This facies also appears in well-defined interbedding with facies SST$_M$ (Fig. 3.4A, 5.3).

Interpretation:

This facies is associated with high competency and capacity flow, as indicated by the coarse MPS (Table 1) and the large variety of clast sizes. Oversized floating clasts indicate either rapid deposition or active dispersive pressure in the flow. The disorderly fabric indicates that clasts were not free to move relative to each other (Harms et al., 1975).

This facies is interpreted as a result of pulsating and rapidly shifting flow conditions in a sediment-laden stream. Bedding within this facies and between this facies and other facies is indicated by slight clast size differences. These differences reflect a rapid alteration in current strength.

The disorganised texture, a wide range in clast sizes and outsized clasts suggests deposition from sediment gravity flow (Nemec and Steel, 1984). However, the degree of maturity (sphericity and rounding) of individual clasts argues that the sediments were well reworked before final deposition. Thus it is possible that these deposits are resultant of flashy, pulsating flows. Alternately they may represent the deposition from a local source during high competency-capacity flooding in a stream resulting in bar or bank collapse.

Facies SST$_{CS}$: Sandstone with cross-stratification

Description:

This facies consists of sandstone with trough and planar cross-stratification. Both planar and trough cross-stratification have been observed in the logged sections and the virtual outcrops (Fig. 4.1, 4.3). Sets of cross-stratified sandstone are from 8 to 60 centimetres in thickness.

The average grain size is medium sand. At some localities, pebbles of facies CGL$_{GL}$ are aligned at the base of sets. Some beds also have pebbles scattered within (Fig. 4.1). These pebbles are generally ~1 centimetre, although elongated pebbles reach a length of four centimetres. The base bed boundaries are mostly, either with a trough shape or parallel to bedding. Organic debris is also very common, from small granule-sized fragments to elongate branch-like debris of more than 40 centimetres in length. This cross-stratified sandstone usually grades laterally and vertically to facies SST$_M$ within the same bed (e.g. Fig. 5.6C-D).
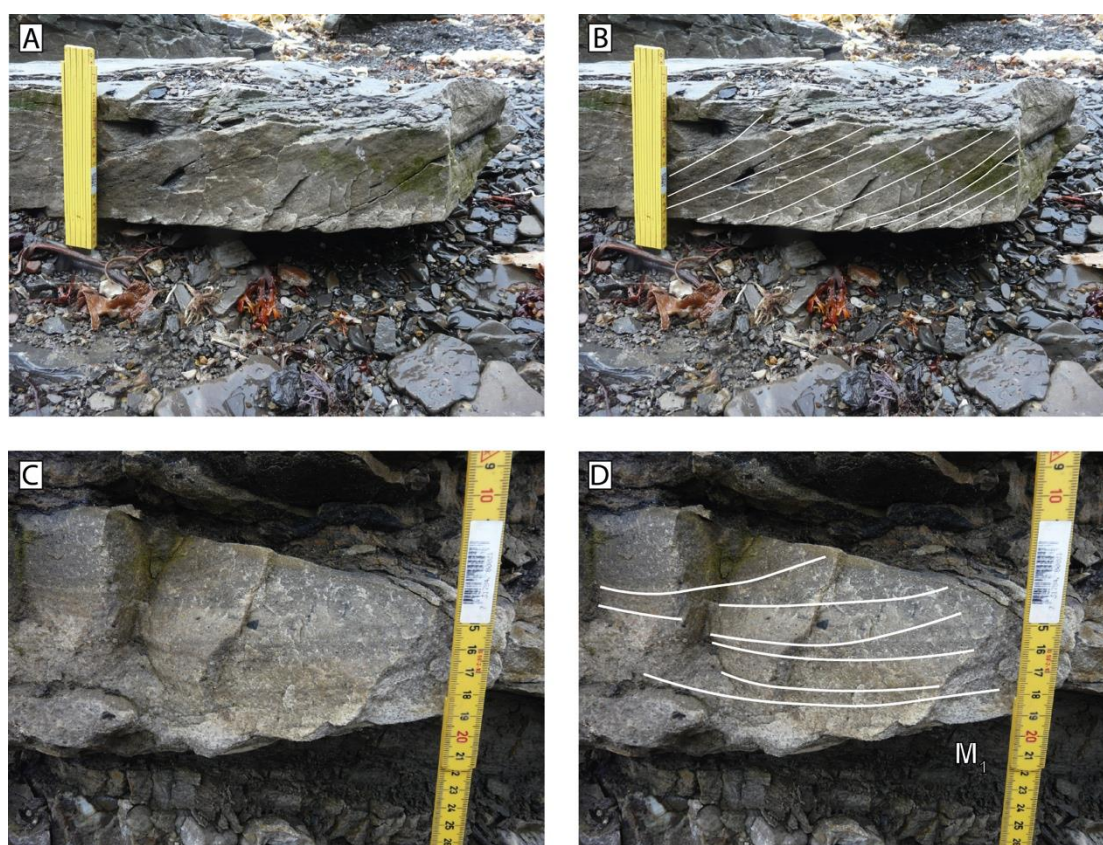

Figure 4.3: Sedimentary structures of facies SST$_{CS}$. **A-B)** Planar cross-stratification from a block situated on the beach below the exposure without and with interpretive lines. This block was chosen because it represents the facies well. **C-D)** Trough cross-stratification from above the conglomerate in logged section 2 (Fig. 4.1) without and with interpretive lines. Note how it cuts down into siltstone of facies M$_1$ situated directly above the conglomerate.

Interpretation:

The cross-stratified sandstones are interpreted to have been deposited as migrating dunes. Dunes are created by unidirectional currents in the upper part of the lower flow regime (Fig. 3.3). The tabular cross-stratification is a result of transport and deposition of straight- or long-crested dunes, whereas trough cross-stratification is a result of deposition of linguoid or lunate dunes (Collinson et al., 2006).

Pebbles aligned at the base of the sets indicate a period of stronger flow conditions with possible erosion and deposition of these pebbles. Organic material of a large size spectre is evidence of large amounts of accessible plants at the time of deposition.

There are several reasons for the faint appearance and lateral and vertical transition of the cross-stratification. One reason might be that the sand is extremely well sorted. Another might be the well-cemented and strong weathering of the rock.

Facies SST$_{RCL}$: Sandstone with ripple cross-lamination

Description:

This facies consists of mixed siltstone/very fine sandstone to medium sandstone with ripple cross-lamination (Fig. 4.4). Both 2D and 3D ripples appear as sets. On 3D ripple sets, darker laminations are observed. Some ripples appear as small undulations. Climbing ripples are also observed. Thickness varies from solitary ripple cross-laminated sets of ~1 centimetre to co-sets up to 50 centimetres thick. Upper and lower boundaries range from transitional to sharp. The facies is commonly associated with facies SST$_{CS}$, SST$_M$ and M$_1$.

Figure 4.4: Sedimentary structures of facies SST$_{RCL}$. **A-B)** Two-dimensional ripple cross-lamination. **C-D)** Three-dimensional ripple cross-lamination. **E-F)** Climbing ripple cross-lamination. Some lines have been added to more clearly distinguish the cross-lamination. In all three cases presented, there is a seemingly smooth transition to facies SST$_M$. This is marked with a black arrow in **A)**.

Interpretation:

This facies is interpreted to be a product of sand transport in the form of migrating 2D and 3D ripples. Ripples are a product of weak unidirectional currents of the lower part of the lower flow regime (Fig. 3.3). Ripples and cross-lamination are principal features of sand-grade sediment, but also occur in coarse silts (Collinson et al., 2006). Drapes of darker material are probably of fine-grained silt and organic material and indicate brief episodes of hydraulic slackening (Reineck and Singh, 1980). The climbing ripple cross-lamination observed is of class A, pattern II according to the classification from Allen (1973). Climbing ripple cross-lamination is also a product of

unidirectional currents. It is characteristic of sediment-laden flows in which the steeper the climb, the higher the sediment saturation/flow strength ratio is (Collinson et al., 2006).

Facies SST$_{PPS}$: Sandstone with plane-parallel stratification
Description:
This facies consists of sandstone with plane-parallel stratification (Fig. 4.5). Some beds are associated with small pebbles of ~1 centimetre in size. Grain sizes are from fine to coarse-grained sandstone. As with other sandstone facies, this also gradually changes laterally and vertically into sandstones of facies SST$_M$ (Fig. 4.2). Observed thickness is from 2 to 30 centimetres (Fig. 4.1, 4.5). The facies is mostly associated with facies SST$_{CS}$ as toe-sets and with facies SST$_M$.
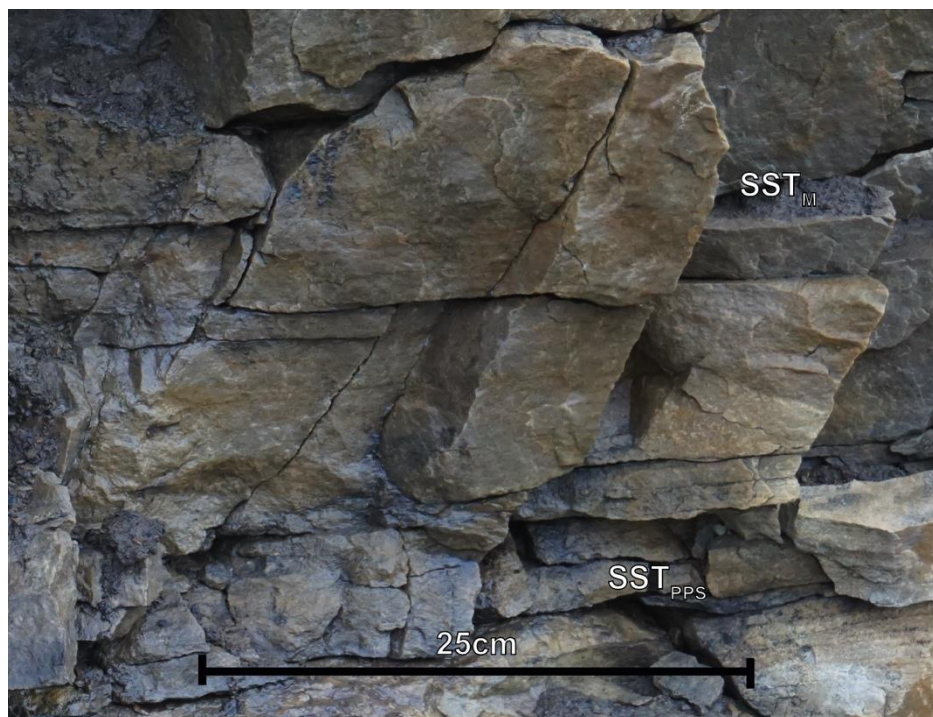

Figure 4.5: Faintly defined facies SST$_{PPS}$. There is a very smooth transition from facies SST$_{PPS}$ to SST$_M$.

Interpretation:
Due to the association with cross-stratified sandstone beds and the apparent grain sizes, facies SST$_{PPS}$ is interpreted to be deposited by unidirection tractional currents of the lower part of the upper flow regime (Fig. 3.3) (Collinson et al., 2006). The conditions that allow plane parallel stratification to occur flow velocity is too high for

ripples or dunes to establish and flow depth too great for standing wave to develop (Harms et al., 1975). At this point, this facies cannot assist in determining paleocurrent direction and is solely an indicator of upper flow regime current strength.

Facies SST$_M$: Sandstone with massive appearance
Description:

This facies consists of sandstone with a massive appearance (fig 4.6). Grain size ranges from fine to coarse sand. Bed appearance varies a lot throughout the exposure, from thin tabular beds interbedded with M_1 to thick strata of this facies together with other sandstone facies. Some of the beds are associated with facies CGL$_{GL}$ (Fig 4.6B). At a few localities along the profile where the facies is situated directly above the conglomerate facies, it occurs in shallow troughs or scours in the otherwise flat, sharp top of the conglomerate. There are also beds of apparently massive sandstone interbedded as lenses within the conglomerate facies at some localities (Fig 4.2A). This facies is the most abundant of the sandstone facies. This facies is associated with the other sandstone facies, which grade laterally and vertically into each other (e.g. Fig. 4.4, 4.5).
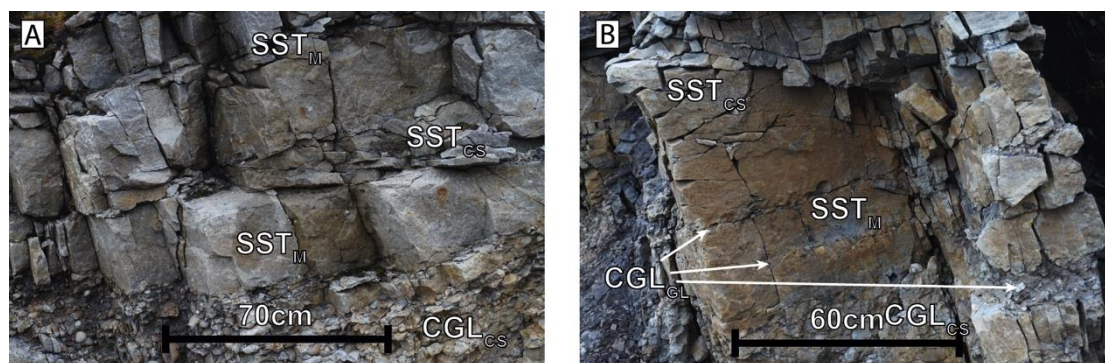

Figure 4.6: Characteristics of facies SST$_M$ and some associated facies. **A)** Facies SST$_M$ and SST$_{CS}$ above CGL$_{CS}$. **B)** Facies SST$_M$ alternating with horizons of facies CGL$_{GL}$ with a thickness of 1-2 pebbles.

Interpretation:

Facies SST$_M$ may have several different origins, either depositional or as a result of post-depositional destruction of any original lamination. According to Collinson et al. (2006), the most common cause of massive sandstone is rapid deposition of heavily sediment-laden currents. Destruction of sedimentary structures can also originate from intense reworking by organisms. However, no observations of bioturbation have

been observed. This facies may be associated with dune-front collapse and liquefaction of the sands during or after deposition (Allen, 1982; Hildebrandt and Egenhoff, 2007; Jones and Rust, 1983). At logging locality 2, a clean cut was made in sandstone of massive appearance, which on detailed inspection revealed weak trough cross-stratification (Fig. 4.3A-B). Observations may support that this facies is a result of heavy weathering and strong cementation of the rocks, due to exposure and deep burial (see section 2.3) and thus not a primary depositional feature.

Facies M_1: Thin silts and mud

Description

This facies consists of thin beds of fine-grained deposits of silt and mud grade (Fig. 4.1). The beds appear as tabular, capping coarser-grained deposits as sand and conglomerate. The beds range from very thin lamina up to a thickness of 20 centimetres. Some of the siltstone beds are abundant in organic material. Erosional truncation is evident in the top of some beds (Fig. 4.1, 4.3). There are also undulations and weak lamination in some of the siltstone beds (Fig. 4.7). The facies is mostly interbedded with thin beds of SST_{RCL} and SST_M in laterally tabular beds. Evident from this figure is a thin siltstone layer that lies directly on top of the conglomerate facies.

Figure 4.7: Facie M_1 sample with small-scale undulations and weak lamination.

Description:

Facies G represents fallout from suspension or at times when there is little tractional current at the bed resulting in weak lamination and undulations. Fine lamination could also be a result of short-term fluctuations in weak, sustained currents (Collinson et al., 2006). Although larger organic fragments are not present, fine-grained organic debris is found in abundance in some of the siltstone beds demonstrating an absence of organisms living in this environment. Lack of any bioturbation and the presence of lamination suggests low energy environment.

Facies M$_2$: Shale

Description:

The facies consists of shale deposits with few observed primary or secondary sedimentary structures (Fig. 4.8), although it has a fissile cleavage. No bioturbation is observed.

There is a clear change in colour of the shale, from grey to reddish and then a transition into grey again below the coal that marks the top of the succession (Fig. 4.8). These colour changes can be recognised at some places in the logged sections and the virtual outcrops (Fig. 5.1). Thin, reddish bedding parallel laminae are also present. The facies appears as one bed, ranging in thickness from 1.5 metres to 4.5 metres. Where exposed, the upper boundary is defined by a thin coal seam (facies C). The lower boundary differs laterally and is either on sandstone facies or conglomerate facies.
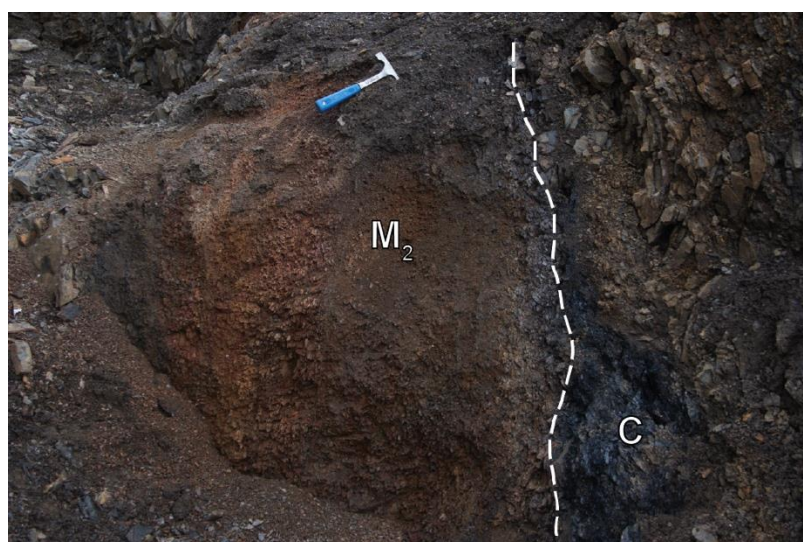

Figure 4.8: Facies M$_2$ below the dashed white line and facies C above. Note the colour changes in facies M$_2$ from grey to red and then transition from red to grey. The coal seam is distorted by a fault. Hammer for scale.

Interpretation

Shale deposits consist of fine-grained sediments settled from suspension in standstill waters. The general absence of sedimentary features if facies M_2 could be related to intense weathering and possibly also to shear within the shale caused by tectonic deformation. However, the fissility of the facies is probably caused by very thin parallel lamination (Collinson et al., 2006). Red colour, either thin or thick probably originates from oxidation of iron-rich minerals.

Facies C: Coal

Description:

The facies consists of black biogenic material (Fig. 4,8) May contain silt (reported by Lüthje (2008)). The thickness was measured at logging location 2 to ~30 centimetres (Fig. 4.1). Where facies C is observed it is situated above facies M_2. Only one coal seam is seen in the outcrop area. However, coal has been mined in the area, and the presence of coal seams higher in the stratigraphy is certain.

The thin coal seam seen in the outcrop section is difficult to follow laterally due to erosion, soil establishment, scree cover and tectonic elements.

Interpretation:

Schopf (1956) proposed the definition of coal "Coal is a readily combustible rock containing more than 50 per cent by weight and more than 70 per cent by volume of carbonaceous material, formed from compaction or induration of various altered plant remains similar to those of peaty deposits".

Coal is a sedimentary rock, and like any other sedimentary rock, it was deposited as layers, which may have lateral or vertical facies changes. Coal originally accumulates as peat in mires. Anoxic conditions, which leads to protection from biodegradation and oxidation, are favourable for peat accumulation and preservation (Serigstad, 2011). These conditions are commonly found in low-lying wetlands with high groundwater table (Nagy, 2005; Serigstad, 2011).

4.3 Facies associations

Introduction:

The different facies described above are in this study organised onto three facies associations to describe and interpret the depositional environment for the Grønfjorden Bed and associated sedimentary rocks. Some facies are constituents of two or three facies associations.

Facies association 1: Gravel-bed fluvial channel deposits

Description:

Facies association 1 (FA1) consists of facies CGL_{CS}, CGL_L, CGL_{MS}, CGL_D and SST_M, CGL_{CS} being the more abundant facies. The facies association is present throughout the exposure, however in varying thickness and characteristics. The base is always sharp and erosive and is always represented by any of the three conglomerate facies, most commonly facies CGL_{CS}. Facies SST_M appears as lenses of different size within conglomerate facies. The top of FA1 varies from sharp, commonly associated with the transition to FA3, to gradual, commonly associated with the transition to FA2.

The thickness of FA1 varies between 45 centimetres (Fig. 5.6) and 2 metres (Fig. 4.1). The vertical stacking pattern of the different facies vary laterally, although a crude fining upward trend is common (Fig. 4.2B). Very common is a thick succession of facies CGL_{CS} containing cobble horizons and imbricated pebbles. Facies also stack in CGL_D – SST_M – CGL_D – SST_M – CGL_D (Fig 5.3F) pattern, and a third occurring pattern is CGL_{CS} – CGL_{MS} (Fig. 4.2D-E).

Interpretation:

The fining upwards succession that FA1 constitutes reflects an overall decrease in flow strength. To transport and deposit the coarse-grained conglomeratic unit at the base, very high competence flow is needed. The largest clast in the conglomerate is 24 centimetres on its long axis, and to transport such a grain size as bedload requires flow strength tens of times stronger than to deposit any sand fragment. This explains why there is little matrix the in cobble-dominated beds (e.g. Fig. 4.3B, 5.3C-D).

The clast-supported texture is characteristic for gravel deposited by streams (Rust, 1972b, 1977). The observed imbrication type a(t)b(i) (Fig. 4.3E, 5.6C-D)

indicate tractional deposition in a stream (Collinson et al., 2006; Gobo et al., 2014), whereas the aligned cobbles in facies CGL$_{CS}$ indicate winnowing and deposition of higher competency flow as channel lags (Gobo et al., 2014; Vincent, 2001). The fining upwards trends indicate waning flow strength. The low angle stratification of facies CGL$_L$ (e.g. Fig 5.4B-D) provides evidence of unidirectional bedform transport and deposition (Hemelsdaël et al., 2017; Santos et al., 2014; Vincent, 2001). Longitudinal bars are elongated barforms with a long axis parallel to flow (Rust, 1972b).

The isolated lenses of facies CGL$_{MS}$ indicate a drop in stream velocity and sudden deposition from a heavily sediment-laden flow. Upwards fining from clast-supported to matrix-supported conglomerate (e.g. Fig. 4.3D) represents falling-stage to low-stage flow when the system changes from winnowing to infiltration of smaller grain-sizes (Nemec and Steel, 1984). The lenses of SST$_M$ interbedded with conglomerate facies represent deposition during waning flow conditions (Owen et al., 2017; Rust, 1972b). Their limited lateral shape indicates erosion as the flow strength increases.

Lenticular alterations between gravel and matrix dominated conglomerate described in facies CGL$_D$ represents slight fluctuations in flow velocity and is a common signature for gravelly braided river deposits (Harms et al., 1975). Parts with great variety in clast sizes may also suggest mass flow characteristics (Nemec and Steel, 1984). However, debris flows commonly inhibit the texture and maturity of originally weathered debris (Nemec and Steel, 1984). Individual clasts with a high degree of maturity positively reflect well-reworked sediment. Thus, mass flows may be locally sourced (e.g. gravel bar collapse) during major flooding.

Based on these characteristics, FA1 is interpreted as deposits in a gravel bed fluvial channel environment. Furthermore, the probable in-channel barforms, coarse grain size, evidence of shifting flow conditions and the sheet-like geometry suggests a braided river environment. Coarse grain sizes could imply that a proximal environment, although not necessarily. The maturity of individual clasts is high, and positively reflects a high degree of reworking (Nemec and Steel, 1984), which is further evidence of a fluvial environment. Furthermore, due to the presence of longitudinal bar deposits as well as the lack of riverbank deposits in this facies association, it is interpreted to have been deposited in a mid-river environment.

Facies association 2: Sand-bed fluvial channel deposits

Description:

Facies association 2 (FA2) consists of all sandstone facies, facies CGL_{GL} and M_1. Facies SST_{CS} and SST_M are the dominant facies. The facies association is of limited lateral extent and appears in three different areas (Fig. 5.1). The base varies from gradual to erosive over FA1. At logging locality 2 (Fig. 4.1) the base is erosive above a thin FA3. The top is either sharp or gradual into FA3. FA2 comprises both trough and cross-stratification of facies SST_{CS} and 2D and 3D ripple cross-lamination of facies SST_{RCL}. The colour of sand in this facies is generally yellowish-grey.

The thickness of FA2 varies between 50 centimetres and 1.3 metres. The overall facies stacking reflects a fining upwards trend. Common stacking pattern is presented in figure 4.1. However this varies greatly. In area 5 (Fig. 5.6) the facies stack like this: SST_{CS} - CGL_{GL} – SST_M – CGL_{GL} – SST_{CS}.

Interpretation:

Presence of facies SST_{CS} indicates flow strength in the lower flow regime whereas SST_{PPS} indicate periodic shifts to higher flow regime. This may coincide with facies SST_M possibly reflecting bar collapse at high flow state (Jones and Rust, 1983). Facies CGL_{GL} is also associated with these sandstone facies and may reflect winnowing of finer fractions at high-flow state (Collinson, 1996). Thicker units of facies CGL_{GL} represent deposition on the channel floor when flow strength is high (Collinson, 1996).

The grain size change from dominating conglomerate to domination sandstone demonstrates a change to a lower flow state. The presence of sand-bed barforms barforms suggests more constant flow conditions than that of the underlying FA1. Sediment load is probably also reduced (Owen et al., 2017).

Thin facies M_1 laminae on top of facies SST_{CS} sets possibly reflects abandonment at low-flow stage. These are usually abundant in organic material. They also inhibit some plane lamination and small-scale ripple undulations, which indicate sorting and tractional transport by very weak current.

Facies SST_{CS} is at one locality (Fig. 5.5C-D) present as a preserved barform, roughly 70 centimetres in thickness. Barform tops would normally get eroded (Collinson et al., 2006) but when they are preserved, they may indicate approximate channel depth. In area 1, large-scale cross-stratification of facies SST_{CS} may represent

a lateral accretion surface (Fig. 5.2B). However, more evidence is needed to conclude as the exposure is partly covered in scree.

The upward facies change from facies SST_{CS} and SST_{PPS} to facies SST_{RCL} positively reflects waning current conditions. Furthermore, vertical change from FA2 to FA3 reflects further slackening of flow conditions upwards.

Based on the above-described characteristics, FA2 is interpreted to represent depositions in a sand-bed fluvial channel environment. Furthermore, the presence of preserved in-channel barforms and the relatively thin succession may suggest rapid channel abandonment. The size of bedfroms as indicated by cross-stratified sets, low-angle shallow cut and fill features, and rapid lateral transitions suggest shallow water flow, probably a braided stream environment.

Facies association 3: Overbank and floodplain deposits
Description:
Facies association 3 (FA3) consists of facies SST_{CS}, SST_{RCL}, SST_{PPS} and SST_M, facies M_1 and M_2 and facies C. The facies association is present throughout the exposure in varying thickness and characteristics. The colour of the sandstone beds is darker than those of FA2, and range from orange-yellow to dark grey.

FA3 consists of three sub-units: 1) Interbedded sandstone facies and facies M_1 unit, 2) a thick facies M_2 unit and 3) a unit of facies C. The interbedded sandstone and facies M_1 unit has limited lateral extent. Single sandstone beds have a tabular geometry and reach a length of up to 40 metres. They contain a variety of structures based on discharge and sediment load. There are a few observed siderite concretions in the sandstones. Facies M_1 define sharp bed boundaries between the tabular sandstone beds. This unit laps on to FA1 in area 3 (Fig. 5.4). The facies M_2 unit is overlying the interbedded sandstone and facies M_1 unit and is present in the whole exposure in varying thickness. The facies C has limited exposure in the outcrop due to scree cover or erosional truncation (Fig. 5.1). Facies C defines the top of the whole succession.

The thickness of FA3 varies, but only over great distances. In logging locality 2 (Fig. 4.1) the thickness is 4.4 m, whereas in area 3 (Fig. 5.1, 5.4A-B) it reaches a thickness of ~6 metres.

The stacking pattern of FA3 is fining upwards from interbedded sandstone and M_1 unit to the uniform facies M_2 unit and capped by facies C (Fig. 4.1). Where the

interbedded sandstone and M_1 facies unit is not present, the facies M_2 lies directly on top of FA1.

Interpretation:

Overbank deposits have often been neglected in favour of channel deposits in descriptions of braided river depositional settings (Miall, 1977). However, researchers (Collinson, 1996; Friend, 1977) have documented that they are associated with all types of fluvial environments and that the overbank deposits can represent thick strata. They are divided into proximal and distal areas based on the proximity to the channel (Collinson, 1996).

The interbedded facies in the overbank setting are interpreted as crevasse splays deposits that are interbedded with fine-grained floodplain deposits (Farrell, 1987). Facies SST_{RCL} climbing ripple cross-lamination is evident from a few blocks of sandstone only but is believed to consist in greater abundance than initially observed, due to poor exposure quality. This facies is characteristic of high sedimentation rates, which is typical in crevasse splay deposits. The vertical facies change observed, in this setting fining up from interbedded sandstones and facies M_1 to thick shale strata possibly reflects the migration and avulsion of adjacent channels (Collinson, 1996). The crevasse splay deposits are related to FA2 and probably sourced from the same fluvial channel at high flow stage.

As bioturbation is fairly common in levee and overbank deposits, and thus the often massive appearance of facies SST_M may be due to intense bioturbation (Collinson, 1996). However, no evidence of trace fossils have been observed in the sandstones and mudstones of FA3, and the massive appearance could be related to severe weathering and cementation. The dark colour of the sandstone facies may be due to contamination of fine-grained sediment and organics, but may also simply be an effect of weathering and staining by the overlying shale and coal deposits.

Floodplains are flooded by a rise in the water table, which may lead to the formation of floodplain lakes in depressions (Collinson, 1996). The thick mudstone that is present in the whole study area is interpreted as deposits in a lacustrine floodplain environment. This interpretation is further supported by observations by Nagy (2005) from the Basilikaelva section located in Van Keulenfjorden (Fig. 2.1).

The thin coal seam that caps the whole succession represents a swampy terrain that eventually overgrew the area (Nagy, 2005; Nemec, 1992).

5 OUTCROP CHARACTERISTICS

5.1 Lateral and vertical facies changes

Introduction

The exposure of the Paleogene rocks in the study area is approximately 300 metres long and runs northwest to southeast along the waterfront of Grønfjorden (Fig. 1.1, 5.1). The exposure has been divided into five separate areas of interest (Fig. 5.1B). These areas have been chosen on the basis of good exposure and accessibility. They represent thick strata of exposed conglomerate, sandstone, shale and coal that have been examined in detail. The vertical character of the succession change laterally, both within areas and from one area to another, but shows an overall fining upwards trend. The conglomerate facies of FA1 are exposed throughout the whole study area (Fig. 5.1), whereas the other facies and facies associations have more restricted exposures.

Poor exposure due to a high degree of weathering, scree cover and poor accessibility have lead to less emphasis on the areas between those of special interest. Between area 1 and 2 the scree cover is very prominent and the outcrop represents a slope rather than a cliff like it does in most other localities. Between area 3 and 4 there is a clear thrust fault separating the two areas. The large section in between area 4 and 5 suffers from scree cover and poor accessibility. There is a large slump block together with scree that evidently covers the outcrop. What is also clear from this section is the difference in elevation of the outcropping conglomerate bed. The difference in elevation is a result of de eastwards dip of the strata. There is also evidence for one, possibly two thrust faults affecting the exposure (Fig. 5.1B).
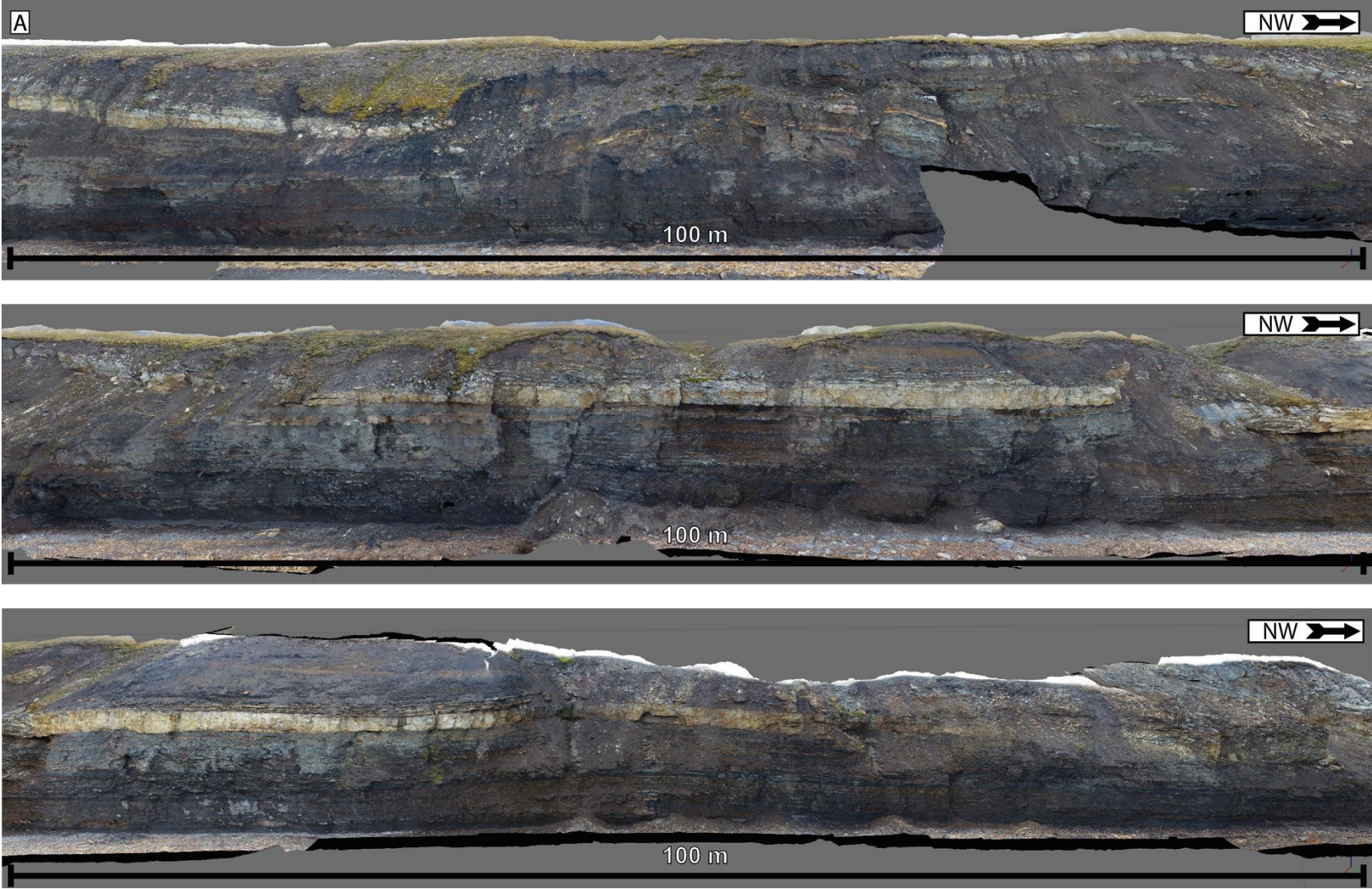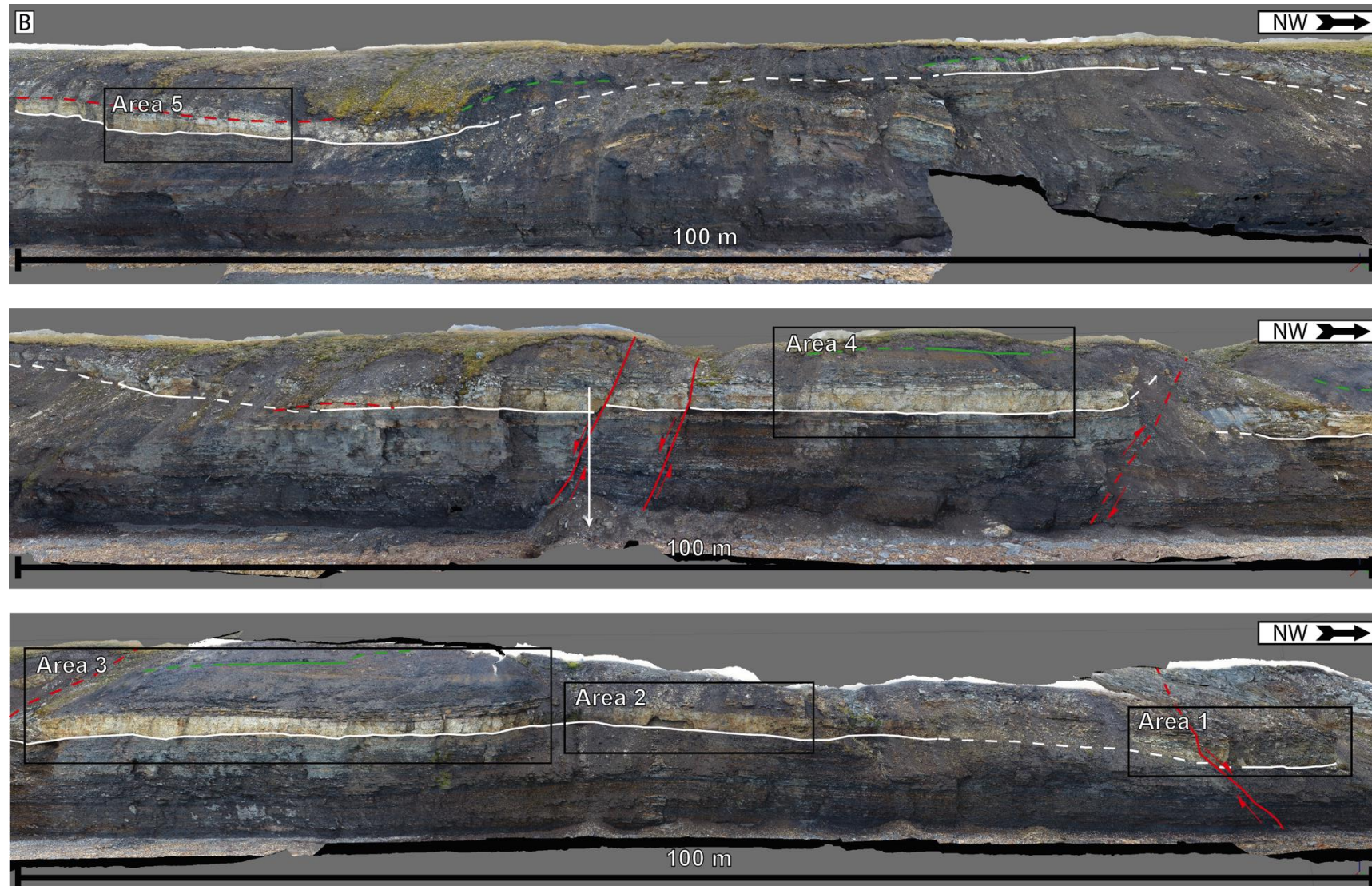
Figure 5.1: A-B) Virtual outcrop of the whole main outcrop area. **B)** Large-scale interpretations of the outcrop are indicated by the lines. Faults are indicated by the red lines. The erosional unconformity is marked by the white line. The presence of coal at the top of the succession is marked by green lines. The white arrow indicates logging locality 4 (Fig. 5.7).
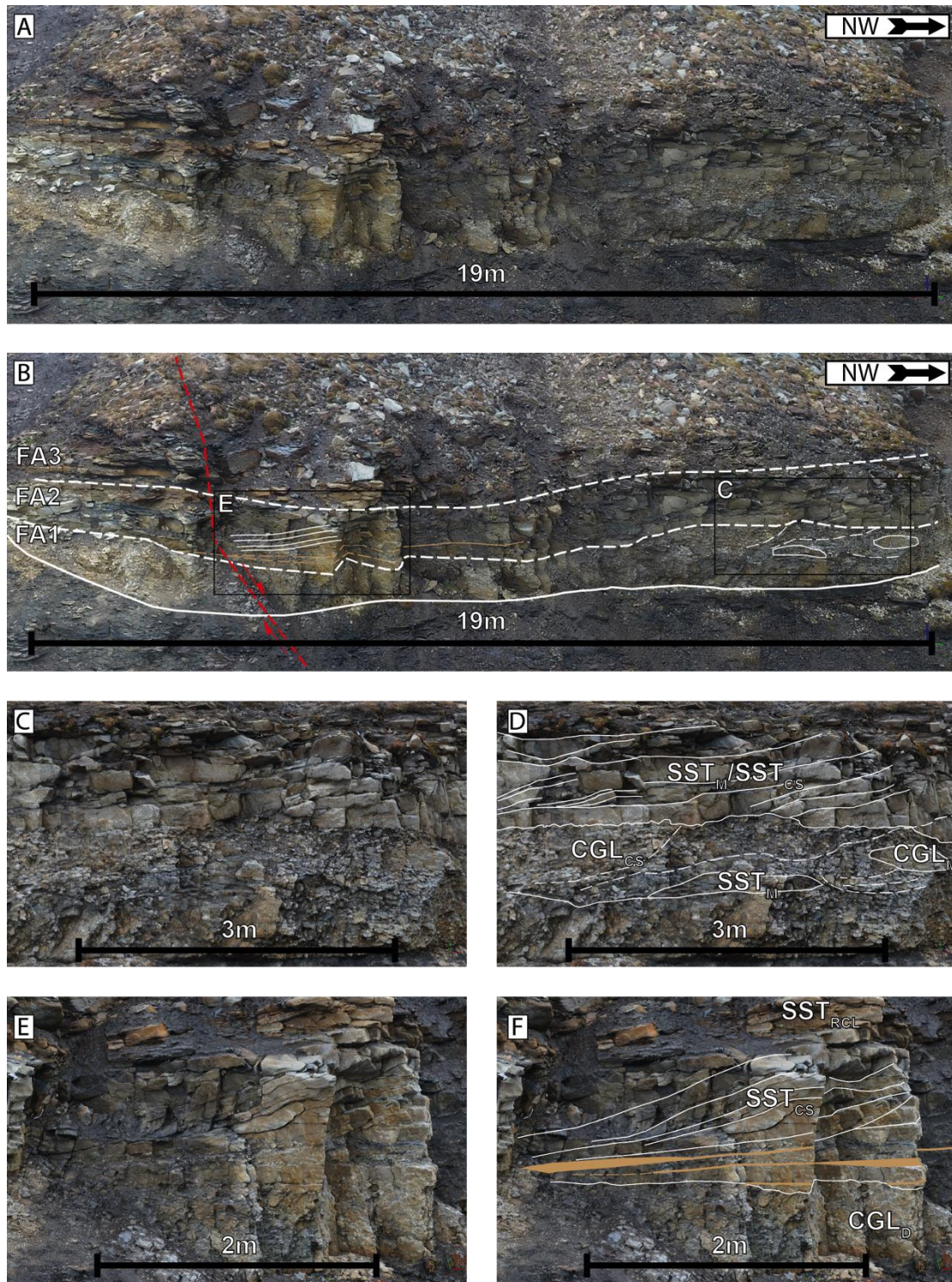
Area 1

Figure 5.2: Characteristics of area 1. **A-B)** Overview of the area without and with interpretation. The erosional unconformity and the transitions between the facies associations are marked with thick white lines. Facies CGL$_{GL}$ is marked by brown lines. The red line indicates the presence of a fault. There is a marked lateral thinning of FA1 from the right to the middle of the section. FA2 thickens in the same pattern. **C-D)** FA1 and FA2 in the right part of area 1. The conglomerate bed overlain by crudely cross-stratified sandstone is evident. Within the FA1 there are lenses of facies CGL$_{MS}$ and SST$_M$. The dotted lines represent possible crude cross-stratification as well as aligned cobbles of facies CGL$_{CS}$. **E-F)** FA1 and FA2 in the left part of area 1. Cross-stratified sandstone with incorporated beds of facies CGL$_{GL}$ overlain by ripple cross-laminated sandstone.

In area 1, FA1 and FA2 are prominently present, whereas FA3 is only vaguely present at the very top right (Fig. 5.2A-B), mainly covered by scree.

FA1 is dominated by facies CGL_{CS}. Facies CGL_{CL} and CGL_{MS} are also evident (Fig. 5.2C-D). Facies CGL_{CS} is dominated by medium to coarse pebbles and is moderately sorted throughout. Facies CGL_{CS} indicates scouring and winnowing by a strong current (Fig. 5.2C-D). Very crudely defined cross-stratification may indicate dune migration. FA1 forms a bar feature that is thickest at the section covered by figure 5.2 C-D, and thins to 50 centimetres over 5 metres. The base of FA1 is straight with a few local scours with relief on centimetre-scale.

FA2 is dominated by facies SST_M and SST_{CS}, but also contains SST_{PPS}, SST_{RCL}, CGL_{GL} and M_1. Thickness reaches a maximum of 1.5 metres in a compensational stacking pattern (Straub et al., 2009). Facies SST_{CS} comprises both planar and trough cross-stratification. In figure 5.2 E-F, however, facies SST_M does not have a fracture pattern imitating structures and is only massive. The boundary between FA1 and FA2 is gradational to sharp, with plenty of pebbles in the lower part of FA2. The presence of the scattered pebbles, as well as facies CGL_{GL} indicates that the depositional agent of FA2 was strong enough to erode and transport the top of FA1. Cross-stratification dip direction in FA2 is roughly in a north to south direction.

FA3 is only very vaguely outcropping in this area and is mostly covered in scree. However, where it is present, both 2D and 3D sets of facies SST_{RCL} are visible in tabular sandstone beds, along with facies SST_{CS}. These show a roughly western migration direction
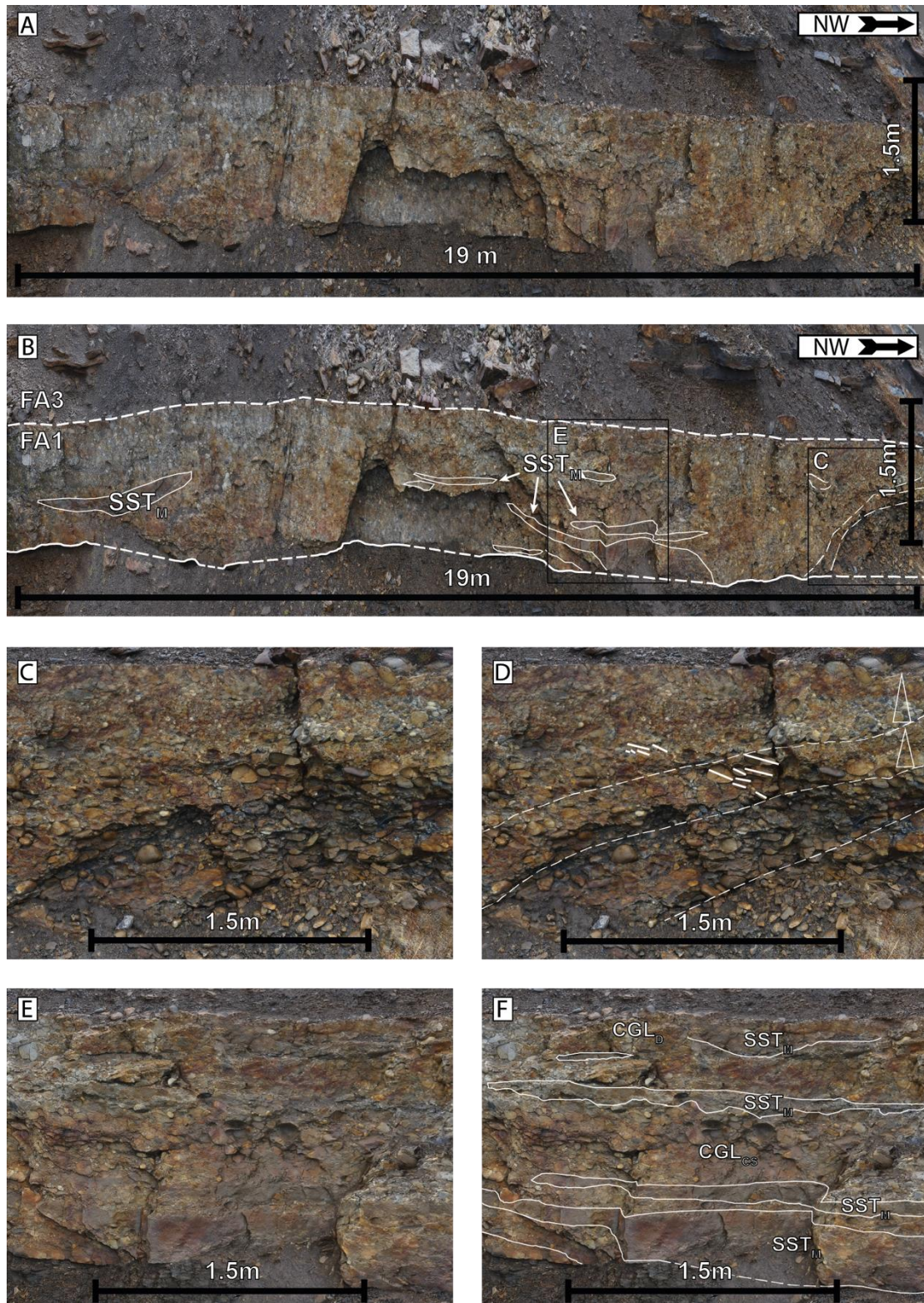
Area 2

Figure 5.3: Characteristics of area 2. **A-B)** Overview of the area without and with interpretation. The erosional unconformity and the transitions between the facies associations are marked with thick white lines. Lenticular beds of SST_M enveloped in the conglomerate are marked with white polygons. FA2 sandstone unit is not present above the FA1 conglomerate unit in this area. Vertical exaggeration x2. **C-D)** FA1 in the right part of area 2. There is a general fining upward trend and crude cross-stratification in the clast-supported conglomerate. Well-defined imbrication of clasts is marked by white lines. **E-F)** FA1 in the middle of area 2. Interbedding of facies CGL_D and lenses of facies SST_M.

Area 2 is represented by FA1 and FA3. FA1 is prominently outcropping at the base of the succession whereas FA3 is only vaguely outcropping, and is mostly covered in scree. FA2 that is present above FA1 in area 1 is absent in this area.

FA1 changes character laterally from facies CGL_{CS} dominated to facies CGL_D dominated. It also contains lenses facies SST_M and CGL_{MS}. Figure 5.3 C shows clear clast-supported texture, whereas figure 5.3E-F shows very disorderly conglomerate texture. The facies CGL_{CS} in Fig. 5.3C-D forms an overall fining upwards succession. The lower part is cobble dominated, whereas the upper part is dominated by fine to medium pebbles. The dominating clast size through the rest of the area is difficult to determine, but the average is in the pebble fraction. Crude cross-stratification and well-defined imbrication is evident. Interbedded facies CGL_D and SST_M indicate shifting flow conditions, more so than other localities. The shift from facies CGL_{CS} to CGL_D indicates different flow conditions. The clast-supported succession in figure 5.3C-D may indicate a braided river barform. The disorganised conglomerates in 5.3E-F are probably channel deposits from a stream of shifting flow strength (see section 4.2).

FA3 directly overlay FA1 in this area, and the boundary between the two is sharp. FA3 is poorly outcropping and mainly covered in scree. However, indications of the presence of tabular sandstone beds of the interbedded unit of FA3 are evident in the top right of figure 5.3A.
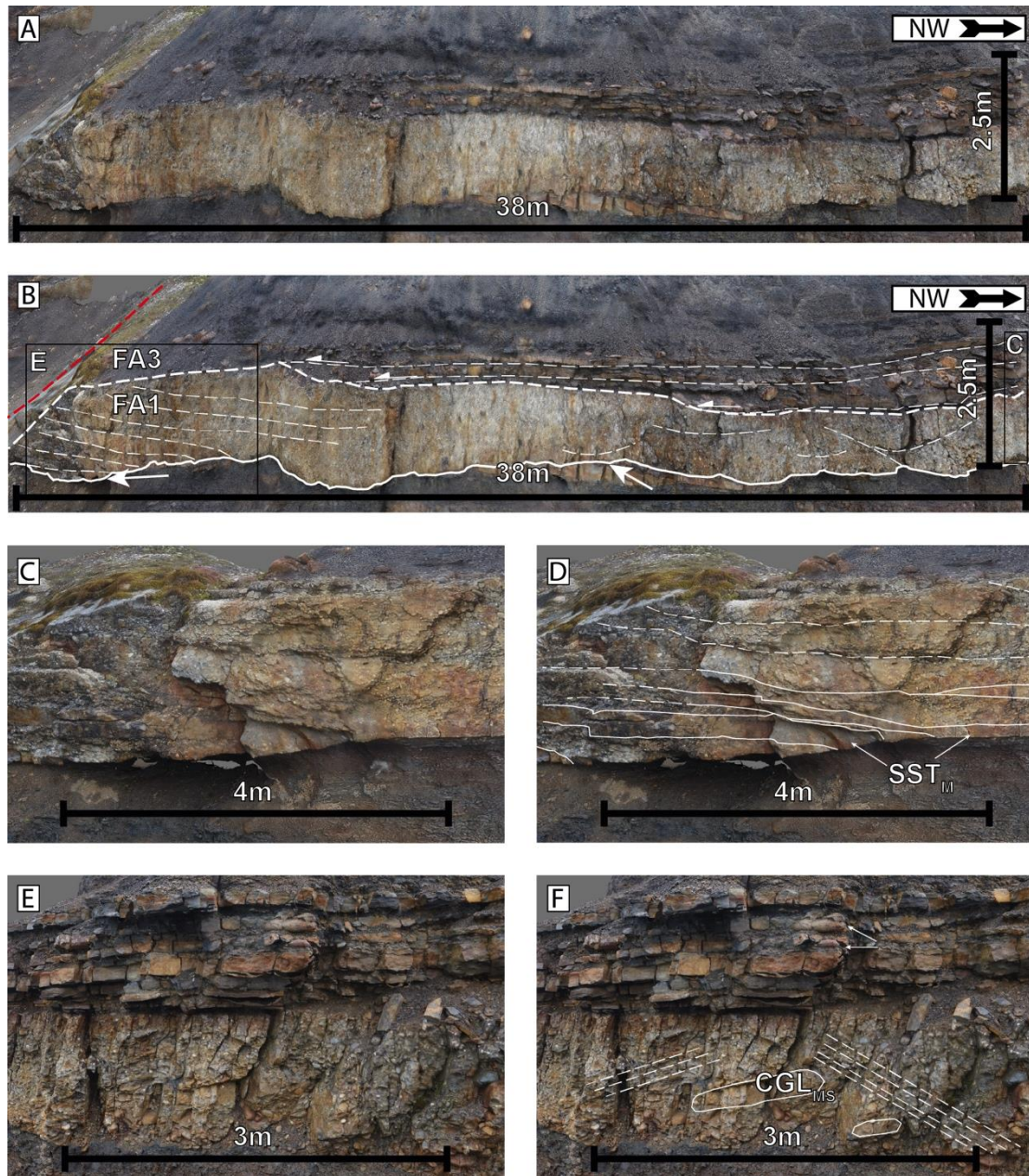
Area 3

Figure 5.4: Characteristics of area 3. **A-B)** Overview of the area without and with interpretation. The erosional unconformity and the transitions between the facies associations are marked with thick white lines. Low-angle stratification of facies CGL$_L$ is marked by dashed white lines in the left part of FA1, whereas aligned cobbles of facies CGL$_{CS}$ are marked by dashed white lines in the middle and right in FA1. Sandstone beds of FA3 are onlapping above FA1. FA2 sandstone unit is not present above the FA1 conglomerate unit in this area. Vertical exaggeration x2. **C-D)** FA1 in the right part of area 3. Low-angle cross-stratification of CGL$_L$ interbedded with beds of facies SST$_M$ is marked by dashed white lines. **E-F)** FA1 and FA3 in the left part of area 3, the photo is situated at 90 degrees to **A-B)**. The bulk of FA1 consists of facies CGL$_D$ with a few lenses of facies CGL$_{MS}$. Possible cross-stratification is indicated by dashed white lines. Siderite concretions in FA3 are indicated by the two white arrows.

Area 3 is a continuation of area 2. Both FA1 and FA3 are prominently outcropping in this area, which is delimited in the SW part by a fault (Fig. 5.1B).

FA1 changes character laterally as in area 2. In the right part (Fig. 5.4C-D), it is a continuation of facies CGL_D. Very disorderly fabric and disorganised texture, with lenses of SST_M and CGL_{MS} and large outsized clasts, dominates (Fig. 5.4E-F). However, there is evidence of possible cross-stratification within the otherwise disorganised conglomerate. This part indicates a channel in which shifting flow strength dominates.

The disorganised texture grades laterally to more orderly and dominated by facies CGL_{CS}. Channel floor lags of facies CGL_{CL} are evident in the otherwise coarse pebble dominated facies CGL_{CS}.

Facies CGL_L dominates FA1 in the very left of figure 5.4A-B. The evident low-angle stratification is interpreted as a longitudinal bar. Clast sizes are generally finer than the rest of the area. The barform is laterally poorly defined, as stratification fades towards the right (Fig. 5.4B).

FA3 includes all three units in this area. Interbedded tabular sandstone beds and facies M_1 beds reach a thickness of one metre in the right part (Fig. 5.4A-D). The sandstone beds consist of facies SST_{RCL}, SST_{CS} and SST_M, which thin laterally and laps onto FA1 (Fig. 5.4B). The one-metre thick unit pinches out over 25 metres. This indicates that the FA1 unit constituted a high during deposition of the overlying unit. Situated above the interbedded facies unit is an up to six metres thick unit of facies M_2, whereas the very top is defined by a facies C. FA3 reaches a thickness of 7.5 metres whereas the whole succession reaches a thickness of 8.7 metres. This is the thickest succession in the whole exposure.

The dip direction of facies SST_{RCL} in FA3 is roughly east to west.
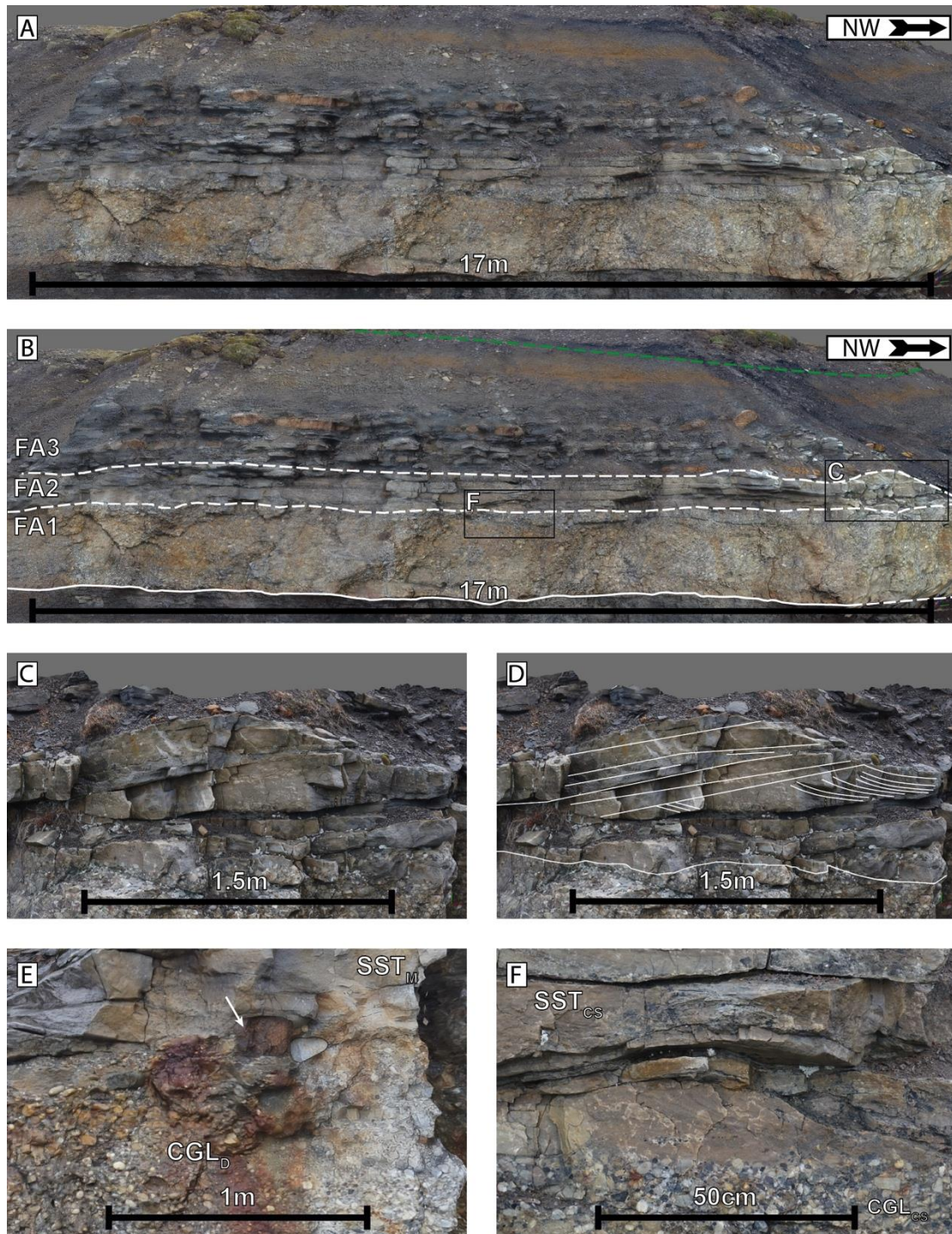
Area 4

Figure 5.5: Characteristics of area 4. **A-B)** Overview of the area without and with interpretation. The erosional unconformity and the transitions between the facies associations are marked with thick white lines. FA1 has almost uniform thickness throughout the area and is capped by a thin succession of FA2. FA2 is capped by a thick succession of FA3. This is the only area that has good exposure of all three facies associations. The coal bed at the top of the succession is marked by a green line. **C-D)** FA1 and FA2 in the right part of area 4 with an erosional nase separating the units. Above is a preserved barform with cross-stratification dipping in two directions. **E)** FA1 and FA2 from five metres left of area 4 boundary. Facies CGL_D with floating outsized clasts at the top of FA1. The arrow indicates a sideritic mudclast of intra-formational origin. **F)** FA1 and FA2 from the middle of the area. Trough cross-stratification of facies SST_{CS} directly overlie well-sorted pebble conglomerate of facies CGL_{CS}.

In area 4, all three facies associations are present. FA1 is prominently outcropping throughout, and its character changes less than in the previous areas. FA2 is only very thinly present, whereas FA3 has a strong presence. Area 4 represents a distinct fining upwards succession of the Grønfjorden Bed system, much like that in the main logged section of figure 4.1.

FA1 is dominated by facies CGL_{CS} in the right part of the area, whereas the left part of the area is dominated by facies CGL_L (Fig. 5.5A-B). Further SW than the area 4 outline (Fig. 5.5A-B) CGL_D dominates (Fig. 5.5E). This locality is very disorganised with elevated clasts at the top of the conglomerate bed with a general coarsening upwards trend. This indicates debris flow deposition of the CGL_D facies (Nemec and Steel, 1984) The large reddish clasts (Fig. 5.5E) is interpreted to be an intraformational sideritic mudclast (also noted by Nagy (2005)).

Facies CGL_{CL} is also evident (Fig. 5.5B) and represents winnowing in a fluvial channel. The top of FA1 is sharp to the overlying FA2 (Fig. 5.5F). The transition to FA2 is at some localities marked by a thin bed of facies M_1. FA1 has a thickness of approximately 1.2 metres with little variation throughout the area (Fig. 5.5B).

FA2 is represented by facies SST_{CS}, SST_M, SST_{PPS} and M_1. Facies SST_M is dominant. Facies SST_{CS} comprises trough (Fig. 5.5F) and planar (Fig. 5.5C-D) cross-stratification. In figure 5.5C-D the cross-stratification constitutes a barform with two main dip directions. FA2 has quite uniform thickness except from a few places where there are undulations at the top and scours at the base (Fig. 5.5B-D). The cross-stratification dips towards the west and southeast.

FA3 shares characteristics with that of area 3. Interbedded facies SST_M and facies M_1 reaches a thickness of 1 metre at the base, whereas the overlying facies M_2 reaches a thickness of 4 metres. As in the previous area (Fig. 5.4A), as well as in logging location 2 (Fig. 4.1) there is a 1 metre thick reddish horizon in the thick facies M_2 unit. The whole succession is capped by facies C.
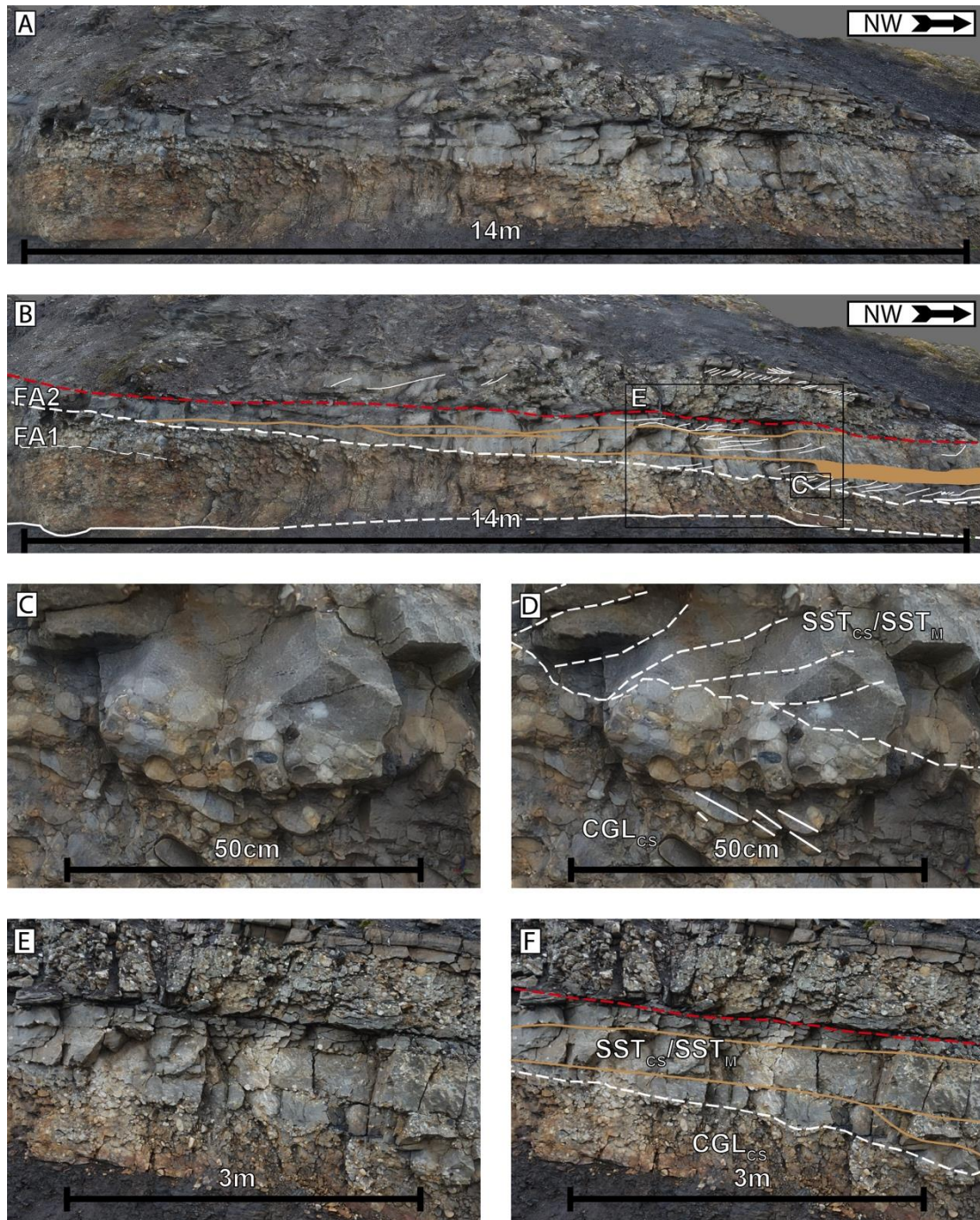
Area 5

Figure 5.6: Characteristics of area 5. **A-B)** Overview of the area without and with interpretation. The erosional unconformity and the transition between the facies associations are marked with thick white lines. The thickness of FA1 changes from 1.4 metres to 40 centimetres over a lateral distance of 14 metres from left to right. FA2 thickens in the same pattern. The red line marks a thrust fault that cuts through the strata sub-horizontally, causing repetition of FA1 and FA2. Facies CGL_{GL} is marked by brown lines, whereas cross-stratification of facies SST_{CS} is marked by white lines. **C-D)** Transition between FA1 and FA2 from the right in the area. FA2 contains well-developed imbrication in facies CGL_{CS} whereas the overlying sandstone contains faint cross-stratification of facies SST_{CS}. **E-F)** FA1 and FA2 from the right in the area. Facies CGL_{GL} laps on to FA1, and defines the base of overlying sets of facies SST_{CS}. Sandstone facies define centimetre to decimetre scale erosional troughs into the underlying FA1.

Area 5 is more than 100 metres SW of area 4, separated by a large, poorly outcropping and accessible area (Fig. 5.1). There is a thrust fault dividing the area causing overlapping of FA1 and FA2 (Fig. 5.6B). The deposits overlying the fault are poorly outcropping. Thus the lower section has been emphasised. Nevertheless, there is evident cross-stratification in the upper FA2 which is important to note.

FA1 is solely represented by facies SST_{CS}. The average clast size of the facies is medium to coarse pebbles. Imbrication of clasts is common (Fig. 5.6D). The transition to FA2 is sharp, although grading over a few centimetres occurs (Fig. 5.8C-D). FA1 reaches a thickness of 1.4 metres in the SW part, and thins to 40 centimetres over 13 metres in the northwestern part (Fig. 5.8A-B).

FA2 stacks with FA1 in a compensational stacking pattern (Straub et al., 2009). It is represented by facies SST_M, SST_{CS} and CGL_{GL} (Figs. 5.6C-F). Furthermore, sets of facies SST_M and SST_{CS} are separated by facies CGL_{GL}. Sandstone sets with cross-stratification all lap onto the top of FA1 towards the southeast. Facies CGL_{GL} beds are horizontal to crudely convex up. They probably define the base on which new sets of cross-stratification develops.

The cross-stratification observed in FA2 both above and below the fault dip in the same direction, towards the southeast (Fig. 5.6B).

From the different areas, it is evident that the different facies associations vary greatly both laterally and vertically. The conglomerates of FA1 change from facies CGL_{CS} to CGL_D over short distances in areas 2 and 3. The facies CGL_{CS} is the most abundant of the conglomerate facies of FA1, and dominates in most areas.

The lateral occurrence of FA1 is more restricted than that of the other facies associations. This goes for the interbedded sandstone-siltstone unit of FA3 as well. It has poor occurrence in area 2 and unknown occurrence in area 5.

Logged section 4 (Fig. 5.7) is, as indicated in figure 5.1, located approximately 20 metres southeast of area 4. In this logged section there has been observed an approximately 20 centimetres thick bed of facies M_1 directly above the conglomerates of FA1 and directly below the sandstones of FA2. This indicates that the fluvial channels transporting and depositing the fluvial channel sandstones may have been subject to channel avulsion and caused erosion of associated overbank deposits.
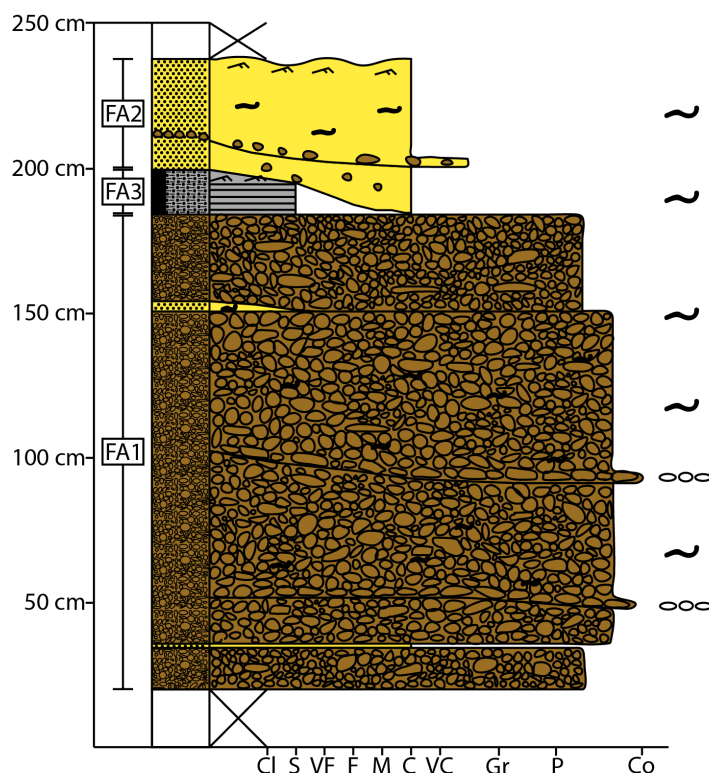
Figure 5.7: Logging locality 4. In this locality it is evident that the facies CGL$_{CS}$ bed is made up of sets of amalgamated character distinguishable by aligned cobbles. There is also a 20 cm thick unit of facies M$_1$ between FA1 and FA2. This logged section is from a large block situated at the beach below the outcrop.

5.2 Unconformity characteristics

The erosional unconformity between the Lower Cretaceous and Paleogene is seemingly flat (Fig. 5.1-5.6). However, local scours and outcrop scale scouring do occur.

Local scours are defined as erosional depressions in the otherwise flat lying erosional contact, on which deposits of the Grønfjorden Bed has settled and truncate layers of the underlying Carolinefjellet Formation. These scours are on centimetre to decimetre scale, and present at a few localities. The deepest scour is located at logging locality 1 and reaches a depth of 50 centimetres over 1.5 metres (Fig. 5.8A). At the SW boundary of area 3, there is a wide scour (Fig. 5.4B). Dimensions are difficult to determine due to the fault that delimits the area, but a relief of ~30 centimetres and width of ~3 metres is definite. At the base of the overlying conglomerate in this trough-shaped scour, there are ridges of decimetre scale (Fig. 5.8B). These ridges may represent scour marks or tool marks, and they show a direction of 69/249 degrees. There is also evidence of differential erosion of the

sandstone and shale of the underlying Carolinefjellet Formation. The erosional agent has reworked and eroded the shale more than the sandstone due to sandstone being more persistent to erosion.

Outcrop-scale scouring is defined as the character of the whole unconformity in the study area. Angular discordance of the unconformity is not obvious within the study area. Detailed inspection of the virtual outcrops does, however, indicate a slight discordance. Measurements between area 1 and 3 yield a slope of 2 per cent towards the southeast. Lüthje (2008) also reported this. This slope coincides with slope measurements of tributary fan systems from Rust (1972b).

Figure 5.8: A) The northernmost outcropping of Grønfjorden bed. It has been deposited in a trough-shaped scouring feature with a relief of ~50 centimetres over 1.5 metres, such that the layers of the underlying strata are truncated. Photo direction is towards the south. The strata are tilted ~90 degrees. The yellow measuring stick is 20 centimetres. **B)** Ridges at the base of Grønfjorden Bed in the southeastern corner of area 3. Photo direction is towards the west.

5.3 Paleocurrent direction indicators

The dip directions of cross-stratification, cross-lamination and elongate clasts are all used as paleocurrent direction indicators.

Cross-stratification is largely observed in FA2. Trough cross-stratification is the most accurate indicator of paleocurrent direction (DeCelles et al., 1983). Only a handful of beds with trough cross-stratification are exposed well enough for paleocurrent direction measurements. More well-exposed are sets of planar cross-stratification. In areas 1 and 5, the cross-stratification show a general dip direction towards the southeast along the outcrop. In area 4 the exposed cross-stratification dips in different directions, towards the west, south (Fig. 5.5B-C) and northeast (Fig. 5.5F).

Cross-stratification and cross-lamination have also been observed in the lower unit of FA3 (Fig. 5.4E-F). It is only well enough exposed to measure dip at two localities in areas 1 and 3. At these localities, the dip of climbing ripples cross-lamination and faint cross-stratification is towards the west.

Table 2: Measurement of dip direction of elongate clasts from nine localities used as indicators for paleocurrent direction.

Measurement number	Area	Facies	Number of readings	NW	SE	Horizontal	Vertical	Trend
1	2	CGL_{CS}	59	30	9	20	0	NW
2	2	CGL_D	51	39	7	5	0	NW
3	3	CGL_D	131	75	24	30	2	NW
4	3	CGL_D	195	100	30	61	4	NW
5	3	CGL_L	113	28	39	44	2	Horizontal to SE
6	3	CGL_{CS}	213	105	40	64	4	NW
7	4	CGL_{CS}	88	32	39	15	2	SE - NW
8	4	CGL_{CS}	168	45	84	36	3	SE
9	4	CGL_D	162	87	27	44	4	NW

Imbricated clasts deposited both by streams and cohesive flows show a general trend of upstream dip-direction (Collinson et al., 2006; Rust, 1972a; SenGupta, 1966).

The dip of elongate clasts has been measured in nine different localities from areas 2, 3 and 4. The localities in which measurements have been conducted were chosen by abundance of elongate clasts, but also due to the absence of large volumes of matrix. This is to minimise the incorporation of possible pseudo-imbrication, which

can develop on slip-faces of sand dunes and matrix-supported gravel dunes (SenGupta, 1966). Thus, no measurements were conducted in facies CGL$_{MS}$.

Evident from these measurements is a general dip trend of northwest along the outcrop face. Area 4 shows the greatest difference, with a preferred dip direction towards the southeast.

Although measurements of the different paleocurrent indicators show faint scatter in dip direction, the dominating trend indicates a flow direction towards the east and southeast. These measurements are consistent with observations by Kalgraff (1978), who reported paleocurrent direction measurements towards the southeast for the basal conglomerates and northeast for the overlying sandstones. Furthermore, the southwest dipping character of the unconformity reported by Kostro (2005) and the northwest to southeast trending depressions in the unconformity reported by Marshall (2013) coincide fairly well with the general northwest to southeast slope of the unconformity in the study area.

5.4 Faults

A number of faults have been observed both in the field and on the virtual outcrops. There are at least three thrust faults, possibly more, with an approximate dip direction towards the east. In addition, there are three clearly visible normal faults with displacement of approximately one metre (Fig. 5.1, 5.2). All the faults with observable fault planes have clear slickensides, indicating post-depositional formation.

Some of these thrust faults are not very well-exposed, but are evident due to deformation of the outcrop in some sections. One of these causes doubling of the conglomerates and sandstones in area 5 (Fig. 5.6). The displacement of these thrust faults is very uncertain, but can be estimated to between 20 and 150 metres (pers. comm. Alvar Braathen).

6 DISCUSSION

6.1 Introduction

In this chapter, the results from this study are discussed in context with previous work concerning the Grønfjorden Bed and its associated sedimentary rocks. The basal unconformity of the Paleocene succession and its characteristics play an important role in the evolution of these deposits, and is also discussed.

6.2 Sedimentary development of the Grønfjorden Bed and associated strata

The sedimentary rocks of the Grønfjorden Bed represent the first deposits of Paleogene age in the Central Tertiary Basin. The succession defines a fining upwards sequence that is interpreted to be caused by the initial transgression of the basin, leading to a rise in relative sea level. In turn, the this lead to an elevation of the groundwater table, which gradually caused a reduction in the flow competency of the depositional agent (Nagy, 2005; Serigstad, 2011).

The unconformity on which the Grønfjorden Bed rests is a subaerial unconformity, and defines a major regressive surface of fluvial erosion (Catuneanu et al., 2009; Serigstad, 2011). It marks a hiatus of between 43 and 50 Myr (see section 2.2) and is commonly used as a sequence boundary in sequence stratigraphic models (Catuneanu, 2006; Catuneanu et al., 2009).

The Lower Cretaceous Carolinefjellet Formation has been interpreted as already lithified at the time of deposition of the Grønfjorden Bed. This is implied by the long time span of the hiatus between the Lower Cretaceous and the early Paleogene strata (see section 2.2) It has been suggested, but not concluded, that there are Upper Cretaceous strata on Sørkapp Land (Smelror and Larssen, 2016) (Figure 2.1). If that is the case, and these were to extend north in the basin at the time of deposition, it could provide further evidence for lithification of the Lower Cretaceous strata prior to deposition of the Paleogene strata in the Central Tertiary Basin. Another reason to assume this is the occurrence of mudstone flake conglomerate derived from the Carolinefjellet Formation in parts of the Grønfjorden Bed (Kostro, 2005; Lüthje, 2008). This type of clasts is not found in the study area of this thesis, arguably due to the high energy level of the fluvial flows depositing the conglomerate

beds in this area. However, a few mudclasts have been observed that does not at all resemble the former. These are more rounded and spherical, constrained to the upper part of the conglomerate facies and are sideritized (Nagy, 2005) (Fig 5.6E). These mudclasts, in contrary to the former, are interpreted as intraformational, possibly derived from upstream overbank areas.

The Conglomerates in the study area are interpreted as gravel bed fluvial deposits, favouring a braided river depositional environment (Fig. 6.1A). Different conglomerate facies are linked to different depositional processes resulting in deposits such as barforms and channel fill deposits within a braided river setting. The geometry of the conglomerate facies indicates a depositional environment closer to that of a braid plain than sinuous, meandering channel. This is backed up by the coarse grain sizes, evidence of mid-channel bars and the lack of lateral accretion surfaces. The coarse grain sizes of the clasts as well as the facies assemblages, which shows evidence of very sediment-laden flows or in some parts even debris flows in, suggest deposition in a proximal part of a larger system. The deposits from the study area have further been interpreted as deposits in a mid-river context due to the interpretations of longitudinal bars of facies CGL_L together with a lack of riverbank deposits. However, this appearance of the conglomerates may also be a result of continuous reworking due to a low base level (Hoey and Ferguson, 1997).

The fluvial channel sandstones (Fig. 6.1B) have have a more restricted lateral distribution than that of the conglomerates. Based on the observed facies assemblages and lateral distribution of the fluvial sandstones, they are interpreted to represent a more channelised fluvial environment. Furthermore, based on preserved barforms and possible lateral accretion surface in area 1, it can possibly be attributed to a mixed, shallow water fluvial environment. Preserved barforms (Fig. 5.4C-D) indicate approximate water depth at the time of deposition of less than one metre. Crevasse splay deposits are associated with the fluvial sandstones, and indicate that the fluvial environment they are deposited from experienced periods of flooding, which may have led to channel avulsion (Fig. 5.7).

As a response to the onset of transgression, the overlying shale (Fig. 6.1C) and coal (Fig. 6.1D) were deposited in what has been interpreted as lacustrine and vegetated deltaic coastal plain environments by Nagy (2005). The succession in the study area in Grønfjorden closely resembles this, and has been interpreted as a lacustrine environment in an overbank context, such as a floodplain lake (see section

4.3). This was later overgrown by swamps or marshes as indicated by the presence of coal at the top of the succession. This vertical stratigraphic transition from fluvial through lacustrine to vegetated swam environment is interpreted to be a response to an elevated groundwater level associated with an overall transgression (Nemec, 1992).
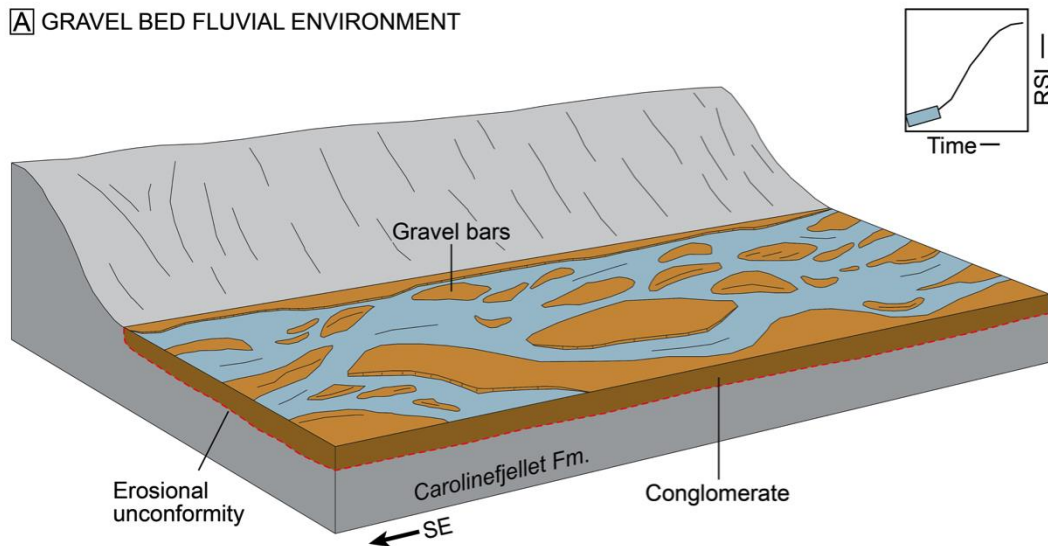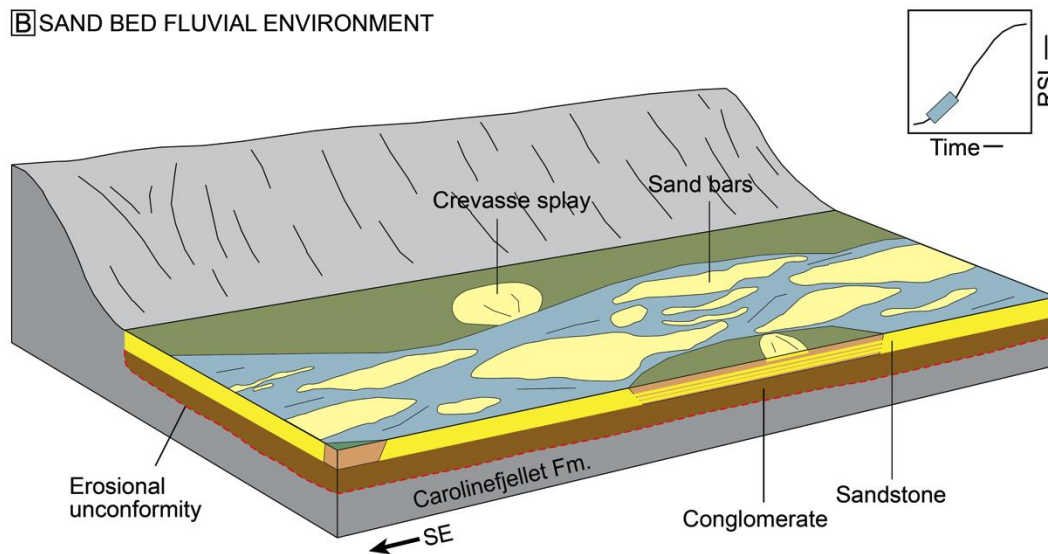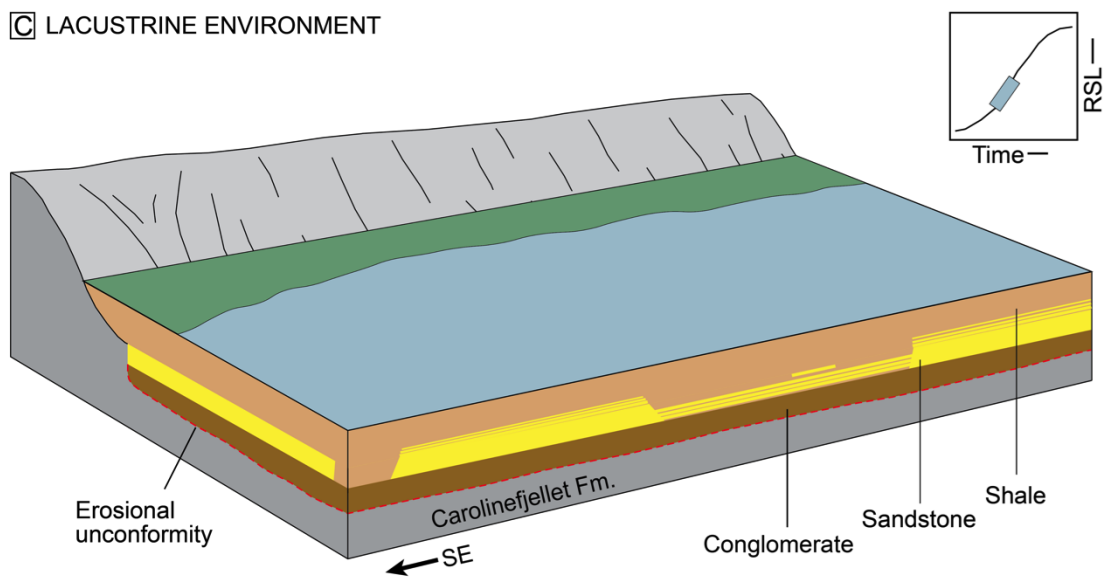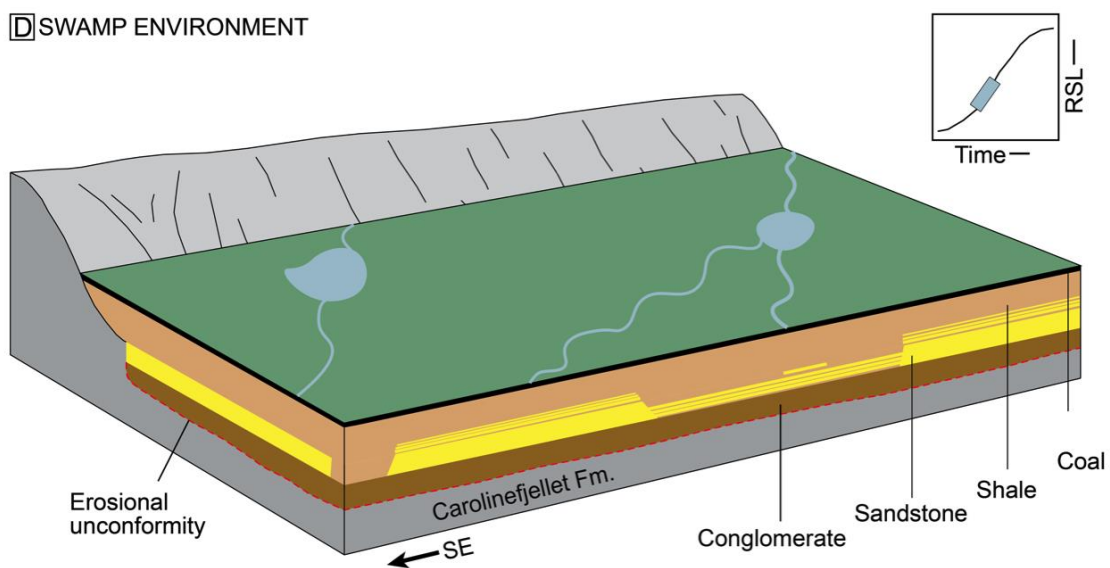
Figure 6.1: Evolution of the sedimentary environment of the lowermost Todalen Member. Previous to deposition there was a prolonged period of sediment bypass and erosion. **A)** Transport and deposition of gravel in a gravel-bed braided river environment. **B)** Transport and deposition in a sand-bed braided river environment. At this stage, there was already a noticeable influence of the initial transgression, which led to an elevated water table. This caused floodplain environments to develop. **C)** At this stage, the transgression had influenced further, which would lead to flooding of depressions in the topography due to the elevated groundwater level. **D)** The system would eventually overgrow, possibly due to a halt in further elevation and stabilisation of the groundwater level, leading to a favourable environment for swamps and marshes to grow in.

6.3 The Grønfjorden Bed in a regional context

The Grønfjorden Bed exposure in the study area of northwestern Grønfjorden is interpreted to be part of a larger incised valley system. This is evident from nearby outcrops that show the same vertical succession of the basal conglomerates and sandstones. The basal conglomerates are present at Heerodden (pers. comm. Malte Jochmann) and Heerstupet (Kalgraff, 1978) (Fig. 2.1). The Heerodden exposure is located 4.5 kilometres east of the study area, whereas the Heerstupet profile is located 12.5 kilometres southeast. There is no published work on the Heerodden exposure, but the analysis by Kalgraff (1978) from Heerstupet describes a vertical succession that resembles that of the study area.

Paleocurrent measurements from the Heerstupet profile conducted by Kalgraff (1978) show a paleocurrent direction towards the southeast in the basal conglomerates, shifting towards the east in the overlying sandstones. This coincides with the general southeasterly paleocurrent direction measured in the study area in northwestern Grønfjorden. The MPS of clast-supported conglomerates in the Heerstupet exposure is reported to be from 9 – 10 centimetres, significantly finer than measurements from those described in this thesis (Table 1), suggesting a more distal location. Thus, the Heerstupet succession is interpreted as a downstream part of the same fluvial system interpreted in the study area.

These observations lead to the interpretation that there was a fluvial system of significant size in the Grønfjorden area at the time of deposition. Assuming that the basal conglomerates from all three outcrop areas in Grønfjorden are synchronous, the braided river at the time of deposition can be estimated to a minimum width of 4.5 kilometres. Furthermore, the thrust faults that have been observed in the study area may have led to significant shortening in an east-west direction post depositionally (see section 5.4). Correction of this shortening could add additional width to the estimate of 4.5 kilometres.

Lüthje (2008) argued for a western and northwestern source area for the conglomerates of the Grønfjorden Bed and suggested that the uplift of the West Spitsbergen Fold and Thrust Belt was as early as the Paleocene. The paleogeographic model proposed by Lüthje is in line with the paleocurrent measurements from the study area of northwestern Grønfjorden and supports that of a northwestern and western source area for the Grønfjorden Bed. This model also explains the coarseness

of the conglomeratic clasts in context with alluvial fans prograding towards the east and southeast from the uplifted rocks to the west (Fig 6.2). A western provenance area for the conglomerates is also considered likely as the most probable sources for the conglomeratic clasts are outcropping towards the west and northwest (Fig. 2.1).
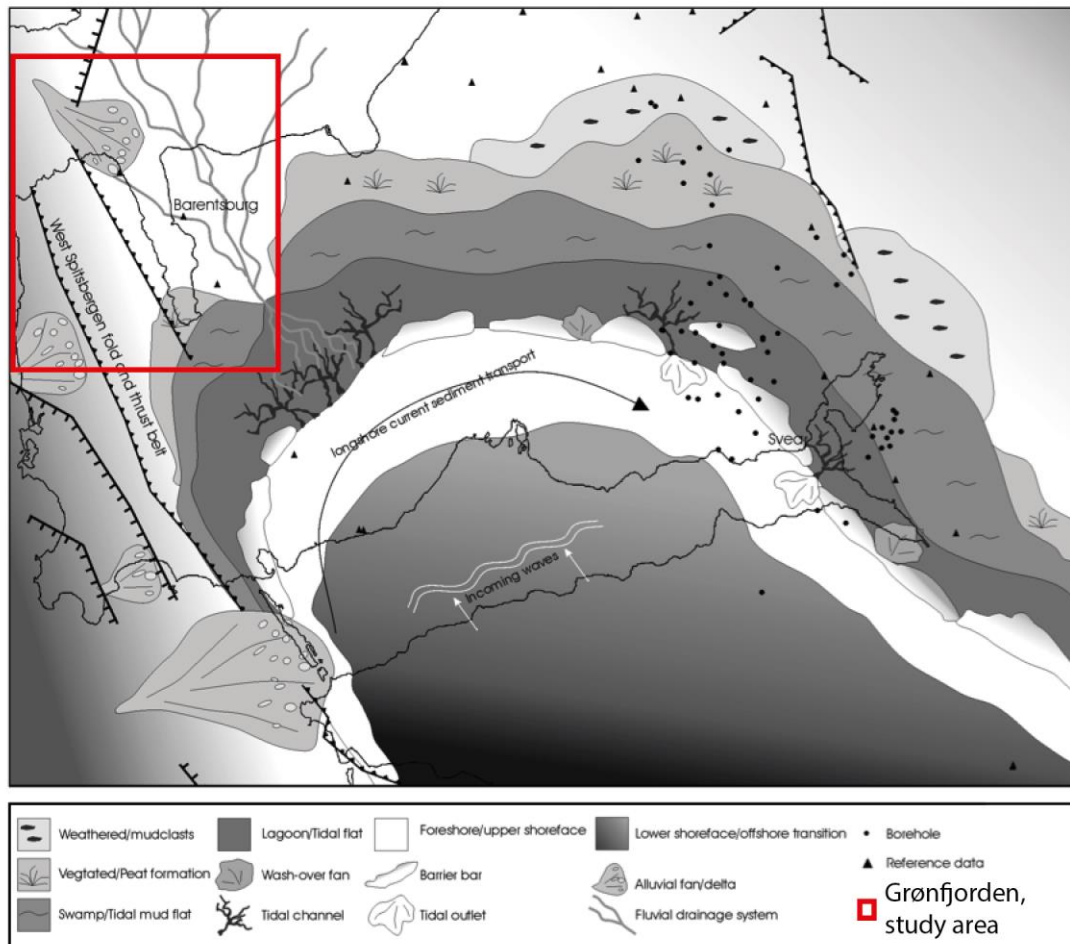

Figure 6.2: Paleogeographic reconstruction of the Central Tertiary Basin from Lüthje (2008). It shows the sedimentary transport pattern, fluvial drainage and the interpretation of the environmental setting during the deposition of the Todalen Member. The red square outlines the study area, interpreted as an alluvial fan to fluvial setting fed with sediments from the northwest. Slightly modified from Lüthje (2008).

Both Kostro (2005) and Marshall (2013) recognised a series of depressions and swells in the basal unconformity (fig 6.3A). These are reported by Marshall (2013) as a series of northwest to southeast trending depressions and swells controlled by underlying tectonic structures. These are contributing to the overall topography of the unconformity surface on which the Grønfjorden Bed has been deposited (Fig. 6.3B).

The study by Marshall (2013) did not recognise any swells and depressions in the westernmost part of the Central Tertiary Basin, where the study area of this thesis

is located. This may be due to the fact that there is a strong influence of tectonism in this area, which may obscure these subtle geometries. However, as shown in figure 6.3A, and also discussed by Marshall, is the apparently equal distance between these swells and depressions. Extrapolating the same distance and direction of these swells and depressions westwards from the Irrdalen depression (Fig. 6.3A) would position a depression approximately through the middle of modern-day Grønfjorden (Fig 6.4). With this contribution, it would mean that the Grønfjorden Bed valley would act as a tributary to the main fluvial valley system flowing from east to west. This suggests that the fluvial system discussed in section 6.1 could have been a tributary valley within the overall Grønfjorden Bed valley system proposed by Marshall (2013) (Fig. 6.3B, 6.4).

The interpretation of the Grønfjorden Bed being a tributary in a larger system situated roughly northwest to southeast as shown in figure 6.4 coincides well with the observations from the study area. The unconformity has a slope which coincides with measured slopes of tributary systems from Rust (1972b), and is dipping in the favourable direction, towards the southeast. Furthermore, the thickness of Grønfjorden bed in the study area is similar to what is found in the depressions in the eastern parts of the Central Tertiary Basin (Kostro, 2005; Lüthje, 2008; Marshall, 2013). Marshall argued that the basal conglomerates were deposited in these depressions whereas thicker coals were associated with the swells. The transgression leading to an elevated water table would cause flooding of the remaining topographic depressions in which lacustrine environments would establish such as in figure 6.1C, further supporting this interpretation.
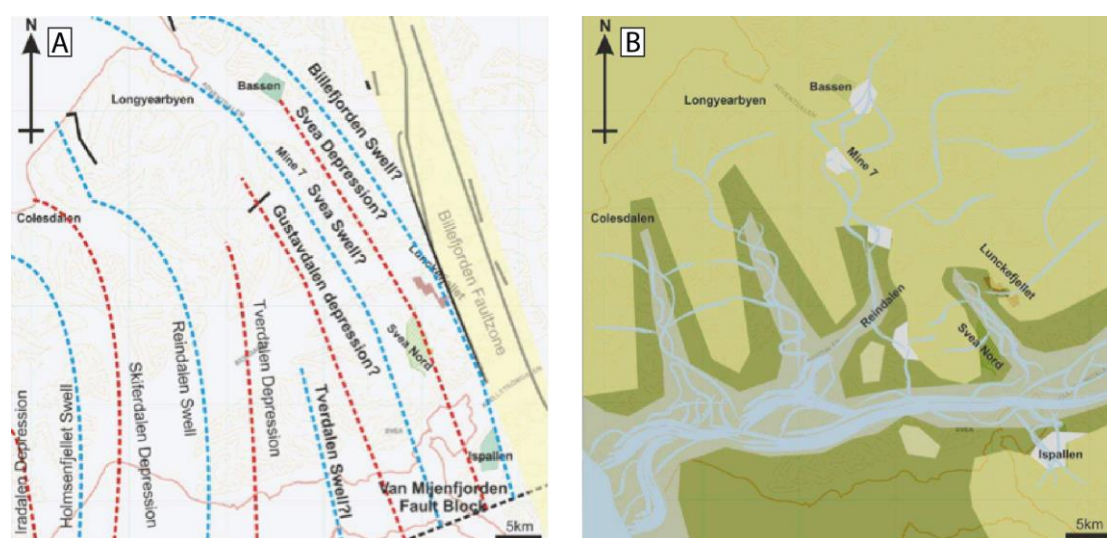
Figure 6.3: Controls of the deposition of the Grønfjorden Bed and interpretation of the earlies Paleogene depositional environment. The study area of this thesis is located approximately 17 kilometres west of the area covered by these figures **A)** Tectonically controlled swells and depressions of the Upper Cretaceous unconformity in the Central Tertiary Basin. Swells are marked by blue dashed lines whereas depressions are marked by red dashed lines.. **B)** The Grønfjorden Bed valley system as interpreted from the swells and depressions of the Upper Cretaceous unconformity and the presence and thickness of the Grønfjorden Bed predominantly in the eastern Central Tertiary Basin. From Marshall (2013).

This depression and swell controlled paleotopography also contributes to the understanding of the coal deposits that are capping the succession in the Grønfjorden area. Thicker coal seams reflect thicker peat deposits, which further reflect longer periods of hydrological stability. Thus thick peats are expected to accumulate adjacent to topographic highs, where the groundwater table is more stable, and there is less clastic influence (Marshall, 2013). This may be the reason for the relatively thin coal seam in the study area compared to other Todalen Member coal seams. For example, the Longyear coal seam, which has commercial potential in Lunckefjellet, near Svea (Fig. 1.2), reaches a thickness of more than 2 metres (Aspøy, 2011).

Coal mining has been conducted in the Festningen area. This coal mine is located approximately 400 metres northwest of the main exposure covered in this study, where the Grønfjorden Bed is tilted 90 degrees, and it is impossible to correlate between these areas. However, the extracted volumes of more than 400 tons of coal during one winter (Brekke and Kjærnet, 2005), suggests that it is unlikely that the mined coal seam is the same as observed at the top of the described succession.
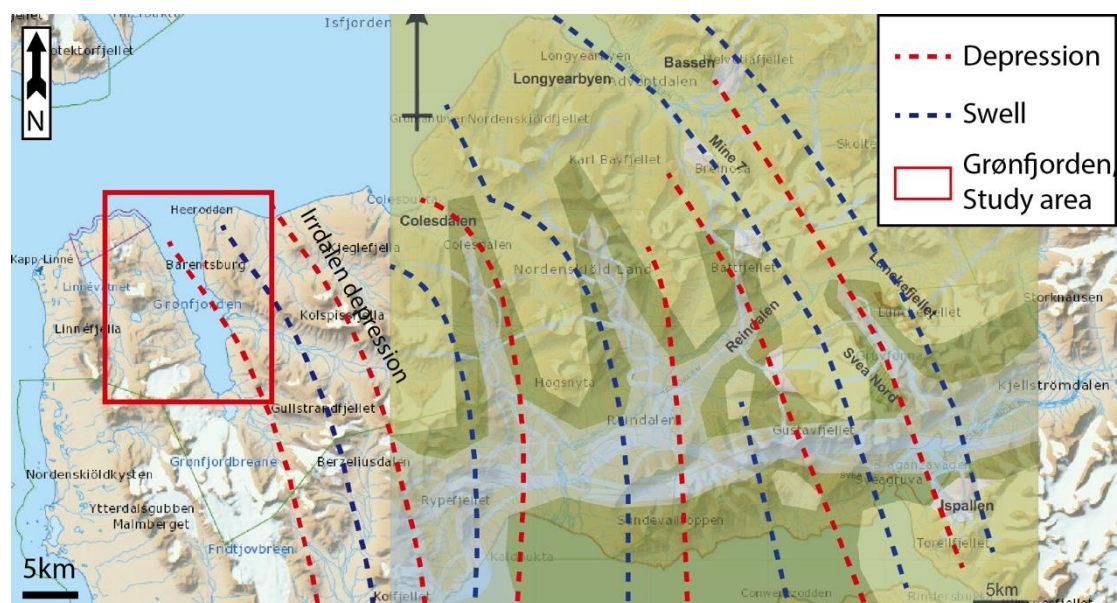

Figure 6.4: The swells and depressions from Marshall (2013), with added swells and depressions in the western Central Tertiary Basin.

Through this detailed sedimentological study, many aspects of the Grønfjorden Bed deposits of northwestern Grønfjorden, as well as in a regional context have been clarified. However, there is still work that can be performed to further improve the understanding of the sedimentary rocks analysed in this study. Some recommendations for further work are:

- Further investigation of core data from the coal mining settlements of Barentsburg (Fig. 1.2) and Coles Bay (Fig. 6.3) to try to determine the presence of depressions and swells in the Upper Cretaceous topography.

- Compare the coal seams in the study area with the coal in Barentsburg to determine if the coals are related.

- Create thin sections of the matrix in the conglomerates and of the overlying sandstones to investigate maturity and petrology of the sand fractions.

- Do a chemical analysis of conglomerate clasts in the study area and compare them to the potential source rocks to expand the knowledge of the sources for the conglomeratic clasts.

- Collect sediment samples of the facies M_2 shale to investigate possible foraminifera occurrences to closer determine the sedimentary environment. This could also possibly help with dating of the sedimentary rocks as a tool to relate occurrences of these sedimentary rocks in different localities in the Central Tertiary Basin.

7 CONCLUSIONS

This is the first detailed sedimentological analysis performed on the steeply situated outcrops of the Grønfjorden Bed in the northwestern Grønfjorden area. The outcrop has been studied on the basis of sedimentary logs and virtual outcrops with an aim to improve the understanding the general understanding of the sedimentary environment in which these rocks were initially deposited. By incorporation of more regional work, this study leads to the following main conclusions:

- The Lower Cretaceous Carolinefjellet Formation is, based on observations in this study as well as others, interpreted to have been already lithified prior to the deposition of the Grønfjorden Bed conglomerates and sandstones.

- The unconformity between the Lower Cretaceous and the Paleogene strata is close to horizontal, but shows a slight dip towards the southeast. This dip coincides with previous studies of unconformity character, and substantiates the interpretations of a general paleocurrent towards the southeast.

- The conglomeratic clasts show great level of maturity in terms of rounding and sphericity, which reflects reworking and considerable abrasion of individual clasts.

- The conglomerates and associated sandstones of the Grønfjorden Bed were deposited in a fluvial depositional environment and are capped by lacustrine and swamp deposits. Furthermore, the general fining upwards succession represented by the sedimentary rocks is interpreted to be associated with the initial transgression of the Central Tertiary Basin. The transgression lead to an elevated groundwater table, which gradually reduced the flow competence in the fluvial environment.

- The Grønfjorden Bed in the study area in northwestern Grønfjorden shows a general trend of a northwest towards the southeast paleocurrent direction. This direction of paleocurrent coincides with other measurements in the Grønfjorden area, leading to the conclusion that Grønfjorden Bed was a fluvial environment transporting and depositing sediment from the northwest towards the southeast.

- The conglomerate and sandstone facies are clean in the sense that they do not contain mudstone as matrix, and mudstone clasts have only been observed at

one locality. This demonstrates a high-energy environment in which the preservation potential for mud was unfavourable.

- Based on observations from nearby exposures, the Grønfjorden Bed has been interpreted to be part of a wide fluvial valley system flowing from the northwest towards the southeast. This fluvial system has been interpreted to be a tributary to the regional fluvial valley system named the Grønfjorden Bed valley system that covered large parts of the Central Tertiary Basin. The basal conglomerates and sandstones of the Grønfjorden Bed represent the deposition at maximum regression, prior to the initial transgression that flooded the basin.

REFERENCES

Allen, J. R. L., 1973, A classification of climbing-ripple cross-lamination: Journal of the Geological Society, 129, no. 5, p. 537-541.

Allen, J. R. L., 1982, Sedimentary Structures: Their Character and Physical Basis, Developments in Sedimentology, Elsevier, Amsterdam, 30A, 593 p.

Aspøy, I., 2011, Sediemntological Deveopment of the Askeladden Sequence of the Todalen Member (Paleocene) at Lucnkefjellet, Svalbard [Master thesis]: University of Bergen, 93 p.

Bergh, S. G., Braathen, A., and Andresen, A., 1997, Interaction of basement-involved and thin-skinned tectonism in the Tertiary fold-thrust belt of central Spitsbergen, Svalbard: AAPG bulletin, v. 81, no. 4, p. 637-661.

Blatt, H., Middleton, G. V., and Murray, R. C., 1980, Origin of Sedimentary Rocks: Englewood Cliffs, New Jersey, Prentice-Hall Inc., 782 p.

Brekke, P., and Kjærnet, T., 2005, Befaringsrapport - Kullgruve syd for Festningen, Grønfjorden, Bergvesenet, p. 1-6.

Bruhn, R., and Steel, R., 2003, High-resolution sequence stratigraphy of a clastic foredeep succession (Paleocene, Spitsbergen): An example of peripheral-bulge-controlled depositional architecture: J. Sed. Res., 73, no. 5, p. 745-755.

Braathen, A., Bergh, S., and Maher, H., 1995, Structural outline of a Tertiary Basement‐cored uplift/inversion structure in western Spitsbergen, Svalbard: Kinematics and controlling factors: Tectonics, 4, no. 1, p. 95-119.

Braathen, A., Bergh, S. G., and Maher, H. D., 1999, Application of a critical wedge taper model to the Tertiary transpressional fold-thrust belt on Spitsbergen, Svalbard: Geological Society of America Bulletin, 111, no. 10, p. 1468-1485.

Catuneanu, O., 2006, Principles of sequence stratigraphy, Elsevier, Amsterdam, 386 pp.

Catuneanu, O., Abreu, V., Bhattacharya, J., Blum, M., Dalrymple, R., Eriksson, P., Fielding, C. R., Fisher, W., Galloway, W., and Gibling, M., 2009, Towards the standardization of sequence stratigraphy: Earth-Science Reviews, 92, no. 1, p. 1-33.

Collinson, J. D., 1996, Alluvial Sediments, in Reading, H. G., ed., Sedimentary Environments: Processes, Facies and Stratigraphy, Blackwell Science, Oxford, p. 37 - 82.

Collinson, J. D., Thompson, D. B., and Mountney, N., 2006, Sedimentary Structures, 3rd edn.: Edinburgh, Scotland, Terra Publishing, 292 p.

Compton, R. R., 1985, Geology in the Field, New York, Wiley, 416 p.

Dallmann, W. K., 1999, Lithostratigraphic Lexicon of Svalbard: Review and Recommendations for Nomenclature Use: Upper Palaeozoic to Quaternary Bedrock, Norwegian Polar Institute, 318 p.

Dallmann, W. K., 2015, Geoscience Atlas of Svalbard, Tromsø, Norwegian Polar Institute, 148, 292 p.

DeCelles, P. G., Langford, R. P., and Schwartz, R. K., 1983, Two new methods of paleocurrent determination from trough cross-stratification: Journal of Sedimentary Research, 53, no. 2, p. 629-642.

Dypvik, H., Riber, L., Burca, F., Rüther, D., Jargvoll, D., Nagy, J., and Jochmann, M., 2011, The Paleocene–Eocene thermal maximum (PETM) in Svalbard—clay

mineral and geochemical signals: Palaeogeography, Palaeoclimatology, Palaeoecology, 302, no. 3, p. 156-169.

Eiken, O., 1985, Seismic mapping of the post-Caledonian Svalbard: Polar research, 3, no. 2, p. 167-176.

Farrell, K. M., 1987, Sedimentology and facies architecture of overbank deposits of the Mississippi River, False River region, Louisiana, *in* Ethridge, F. G., Flores, R. M., and Harvey, M. D., eds., Recent Developments in Fluvial Sedimentology, Soc. Econ. Paleoontol. Mineral. Spec. Publ., p. 111-121.

Friend, P., 1977, Distinctive features of some ancient river systems, *in* Miall, A. D., ed., Fluvial Sedimentology, Canadian Society of Petroleum Geologists, Calgary, p. 531-542.

Gobo, K., Ghinassi, M., Nemec, W., and Sjursen, E., 2014, Development of an incised valley-fill at an evolving rift margin: Pleistocene eustasy and tectonics on the southern side of the Gulf of Corinth, Greece: Sedimentology, 61, no. 4, p. 1086-1119.

Grundvåg, S.-A., and Olaussen, S., 2017, Sedimentology of the Lower Cretaceous at Kikutodden and Keilhaufjellet, southern Spitsbergen: implications for an onshore–offshore link: Polar Research, 36, no. 1, 1302124. http://dx.doi.org/10.1080/17518369.2017.1302124.

Harding, I. C., Charles, A. J., Marshall, J. E., Pälike, H., Roberts, A. P., Wilson, P. A., Jarvis, E., Thorne, R., Morris, E., and Moremon, R., 2011, Sea-level and salinity fluctuations during the Paleocene–Eocene thermal maximum in Arctic Spitsbergen: Earth and Planetary Science Letters, 303, no. 1, p. 97-107.

Harland, W. B., 1969, Contribution of Spitsbergen to Understanding of Tectonic Evolution of North Atlantic Region, *in* Kay, M., ed.., North Atlantic Geology and Continental Drift, Mem. Am. Assoc. Petrol Geol., p. 827-851.

Harland, W. B., Anderson, L. M., Manasrah, D., Butterfield, N. J., Challinor, A., Doubleday, P. A., Dowdeswell, E. K., Dowdeswell, J. A., Geddes, I., and Kelly, S. R., 1997, The Geology of Svalbard, Geological Society of London, 521 p.

Harms, J. C., Southard, J. B., Spearing, D. R., and Walker, R. G., 1975, Depositional environments as interpreted from primary sedimentary structures and stratification sequences: Society of Economic Paleontologists and Mineralogists, Short Course, no. 2, p. 161.

Harms, J. C., Southard, J. B., and Walker, R. G., 1982, Structures and sequences in clastic rocks: Society of Economic Paleontologists and Mineralogists, Short Course, no. 9.

Helland-Hansen, W., 1990, Sedimentation in Paleogene Foreland Basin, Spitsbergen: AAPG Bulletin, 74, no. 3, p. 260-272.

Helland-Hansen, W., 2010, Facies and stacking patterns of shelf‐deltas within the Palaeogene Battfjellet Formation, Nordenskiöld Land, Svalbard: implications for subsurface reservoir prediction: Sedimentology, 57, no. 1, p. 190-208.

Hemelsdaël, R., Ford, M., Malartre, F., and Gawthorpe, R., 2017, Interaction of an antecedent fluvial system with early normal fault growth: Implications for syn-rift stratigraphy, western Corinth rift (Greece): Sedimentology, 64, no. 7, p. 1957-1997.

Hoey, T. B., and Ferguson, R. I, 1997, Controls of strength and rate of downstream fining above a rise in base level: Water Resources Research, 33, no. 11, p. 2601-2608.

Hildebrandt, C., and Egenhoff, S., 2007, Shallow-marine massive sandstone sheets as indicators of palaeoseismic liquefaction-An example from the Ordovician shelf of Central Bolivia: Sedimentary Geology, 202, no. 4, p. 581-595.

Hurum, J. H., Roberts, A. J., Dyke, G. J., Grundvåg, S.-A., Nakrem, H. A., Midtkanal, I., Ślivinska, K. K., and Olaussen, S., 2016, Bird or maniraptoran dinosaur? A femur from the Albian strata of Spitsbergen: Arctic Norway. Acta Palaeontologica Polonica, 67, p. 137-147.

Jones, B. G., and Rust, B. R., 1983, Massive sandstone facies in the Hawkesbury Sandstone, a Triassic fluvial deposit near Sydney, Australia: Journal of Sedimentary Research, 53, no. 4., p. 1249-1259.

Jones, M. T., Augland, L. E., Shephard, G. E., Burgess, S. D., Eliassen, G. T., Jochmann, M. M., Friis, B., Jerram, D. A., Planke, S., and Svensen, H. H., 2017, Constraining shifts in North Atlantic plate motions during the Palaeocene by U-Pb dating of Svalbard tephra layers: Scientific Reports, 7, no. 1., doi:10.1038/s41598-017-06170-7.

Jones, M. T., Eliassen, G. T., Shephard, G. E., Svensen, H. H., Jochmann, M., Friis, B., Augland, L. E., Jerram, D. A., and Planke, S., 2016, Provenance of bentonite layers in the Palaeocene strata of the Central Basin, Svalbard: implications for magmatism and rifting events around the onset of the North Atlantic Igneous Province: Journal of Volcanology and Geothermal Research, 327, p. 571-584.

Kalgraff, K. L., 1978, Aspects of sedimentation in Firkanten Formation, Tertiary, Svalbard, [Master thesis]: University of Bergen, 178 p.

Kellogg, H. E., 1975, Tertiary stratigraphy and tectonism in Svalbard and continental drift: AAPG Bulletin, 59, no. 3, p. 465-485.

Kostro, F., 2005, Character of the basal unconformity of the Paleocene succession in the Central Basin, Svalbard, [Master thesis]: University of Freiburg, 64 p.

Krumbein, W. C., and Sloss, L. L., 1951, Stratigraphy and Sedimentation, LWW, v. 5.

Langford, R., and Chan, M. A., 1988, Flood surfaces and deflation surfaces within the Cutler Formation and Cedar Mesa Sandstone (Permian), southeastern Utah: Geological Society of America Bulletin, 100, no. 10, p. 1541-1549.

Langford, R., and Chan, M. A., 1989, Fluvial‐aeolian interactions: Part II, ancient systems: Sedimentology, 36, no. 6, p. 1037-1051.

Leever, K. A., Gabrielsen, R. H., Faleide, J. I., and Braathen, A., 2011, A transpressional origin for the West Spitsbergen Fold-and-Thrust Belt: Insight from analog modeling: Tectonics, 30, no. 2., http://dx. doi.org/10.1029/2010TC002753.

Livsic, J. J., 1965, Paleogene deposits of Nordenskiold Land, Vestspitsbergen, in Sokolov, V.N., ed., Materialy po geologii Shpitsbergena, English transation: Bosten Spa, Yorkshire, England, National Lending Library Science and Technology, 1970, p. 193-215.

Livsic, J. J., 1974, Palaeogene deposits and the platform structure of Svalbard: Norwegian Polar Institute, no. 138, p. 1-58.

Lüthje, C. J., 2008, Transgressive development of coal-bearing coastal plain to shallow marine setting in a flexural compressional basin, Paleocene, Svalbard, Arctic Norway: [Doctoral Thesis]: University Centre in Svalbard, 181 p.

Maher, J., Harmon D, 2001, Manifestations of the Cretaceous High Arctic large igneous province in Svalbard: The Journal of Geology, 109, no. 1, p. 91-104.

Major, H., and Nagy, J., 1964, Geological Map of Svalbard C9G, Adventdalen, 1: 100,000: Norsk Polarinstitutt.

Major, H., and Nagy, J., 1972, Geology of the Adventdalen map area: with a geological map: Norwegian Polar Institute, 138, 58 p.

Manum, S. B., and Throndsen, T., 1978, Rank of coal and dispersed organic matter and its geological bearing in the Spitsbergen Tertiary: Norwegian Polar Institute, Årbok 1977, p. 159-177.

Marshall, C., Uguna, J., Large, D. J., Meredith, W., Jochmann, M., Friis, B., Vane, C., Spiro, B. F., Snape, C. E., and Orheim, A., 2015, Geochemistry and petrology of palaeocene coals from Spitzbergen-Part 2: Maturity variations and implications for local and regional burial models: International Journal of Coal Geology, 143, p. 1-10.

Marshall, C. J., 2013, Palaeogeographic development and economic potential of the coal-bearing Palaeocene Todalen Member, Spitsbergen [Doctoral Thesis]: University of Nottingham, 339 p.

Miall, A. D., 1977, A review of the braided-river depositional environment: Earth-Science Reviews, 3, no. 1, p. 1-62.

Müller, R. D., and Spielhagen, R. F., 1990, Evolution of the Central Tertiary Basin of Spitsbergen: towards a synthesis of sediment and plate tectonic history: Palaeogeography, Palaeoclimatology, Palaeoecology, 80, no. 2, p. 153-172.

Nagy, J., 2005, Delta-influenced foraminiferal facies and sequence stratigraphy of Paleocene deposits in Spitsbergen: Palaeogeography, Palaeoclimatology, Palaeoecology, 222, no. 1, p. 161-179.

Nagy, J., Jargvoll, D., Dypvik, H., Jochmann, M., and Riber, L., 2013, Environmental changes during the Paleocene—Eocene Thermal Maximum in Spitsbergen as reflected by benthic foraminifera: Polar Research, v. 32., 19737.

Nagy, J., Kaminski, M. A., Kuhnt, W., and Bremer, M. A., 2001, Agglutinated foraminifera from neritic to bathyal facies in the Palaeogene of Spitsbergen and the Barents Sea, in Hart, M. B., Kaninski, M. A., Smart, C. W., eds., Proceedings of the Fifth International Workshop on Agglutinated Foraminifera, Grzybowski Foundation, 7, p. 333-361.

Nagy, J., Tovar, F. J. R., and Reolid, M., 2016, Environmental significance of Ophiomorpha in a transgressive–regressive sequence of the Spitsbergen Paleocene: Polar Research, 35, no. 1, 24192. https://doi.org/10.3402/polar.v35.24192

Nemec, W., 1992, Depositional controls on plant growth and peat accumulation in a braidplain delta environment: Helvetiafjellet Formation (Barremian-Aptian), Svalbard: Geological Society of America Special Papers, 267, p. 209-226.

Nemec, W., and Steel, R. J., 1984, Alluvial and coastal conglomerates: their significant features and some comments on gravelly mass-flow deposits, in Koster, E. H., and Steel, E. J., eds., Sedimentology of Gravels and Conglomerates, Canadian Society of Petroleum Geologists, Calgary, 10, p. 1-31.

Nøttvedt, A., Berglund, L., Rasmussen, E., and Steel, R., 1988, Some aspects of Tertiary tectonics and sedimentation along the western Barents Shelf: Geological Society, London, 39, no. 1, p. 421-425.

Nøttvedt, A., Livbjerg, F., Midbøe, P., and Rasmussen, E., 1993, Hydrocarbon potential of the Central Spitsbergen Basin: Arctic Geology and Petroleum Potential. Norwegian Petroleum Society (NPF), 2, p. 333-362.

Ohta, Y., Andresen, A., Dallmann, W. K., and Salvigsen, O., 1992, Geological map of Svalbard, Temakart 16: Oslo, Norsk Polarinstitutt, sheet B9G, Isfjorden, Scale 1:100 000.

Orheim, A., Bieg, G., Brekke, T., Horseide, V., and Stenvold, J., 2007, Petrography and geochemical affinities of Spitsbergen Paleocene coals, Norway: International Journal of Coal Geology, 70, no. 1, p. 116-136.

Orvin, A. K., 1940, Outline of the geological history of Spitsbergen: Skr. on Svalbard og Ishavet, 78, p. 57.

Owen, A., Ebinghaus, A., Hartley, A. J., Santos, M. G. M., and Weissmann, G. S., 2017, Multi-scale classification of fluvial architecture: An example from the Palaeocene–Eocene Bighorn Basin, Wyoming: Sedimentology, 64, no. 6, p. 1572-1596.

Petersen, T. G., Thomsen, T., Olaussen, S., and Stemmerik, L., 2016, Provenance shifts in an evolving Eurekan foreland basin: the Tertiary Central Basin, Spitsbergen: Journal of the Geological Society, 173, no. 4, p. 634-648.

Piepjohn, K., von Gosen, W., and Tessensohn, F., 2016, The Eurekan deformation in the Arctic: an outline: Journal of the Geological Society, 173, no. 6, p. 1007-1024.

Powers, M. C., 1953, A new roundness scale for sedimentary particles: Journal of Sedimentary Research, 23, no. 2., 117-119.

Ravn, J. P. J., 1922, On the Mollusca of the Tertiary of Spitsbergen: Skr. om Svalbard og Ishavet, 1, p. 1-28.

Reading, H., and Levell, B., 1996, Controls on the sedimentary rock record, in Reading, H. G., ed., Sedimentary Environments: Processes, Facies and Stratigraphy, Blackwell Science, Oxford, p. 5-36.

Reineck, H. E., and Singh, I. B., 1980, Depositional Sedimentary Environments, with Reference to Terrigenous Clastics, Berlin, Springer-Verlag, 549p.

Rust, B. R., 1972a, Pebble orientation in fluvial sediments: Journal of Sedimentary Research, 42, no. 2, p. 384-388.

Rust, B. R., 1972b, Structure and process in a braided river: Sedimentology, 18, no. 3-4, p. 221-245.

Rust, B. R., 1977, Depositional models for braided alluvium, in Miall, A. D., ed., Fluvial Sedimentology, Canadian Society of Petroleum Geologists, Calgary, p. 605-625.

Santos, M. G. M., Almeida, R. P., Godinho, L. P. S., Marconato, A., and Mountney, N. P., 2014, Distinct styles of fluvial deposition in a Cambrian rift basin: Sedimentology, 61, no. 4, p. 881-914.

Schopf, J. M., 1956, A definition of coal: Economic Geology, 51, no. 6, p. 521-527.

SenGupta, S., 1966, Studies on orientation and imbrication of pebbles with respect to cross-stratification: Journal of Sedimentary Research, 36, no. 2, p. 362-369.

Serigstad, E., 2011, Paleoenvironment and its influence on the distribution of coal deposits in the Todalen Member, Firkanten Formation (lower Paleocene), Svalbard, [Master Thesis]: University of Bergen, 95 p.

Smelror, M., and Larssen, G. B., 2016, Are there Upper Cretaceous sedimentary rocks preserved on Sørkapp Land, Svalbard?: Norwegian Journal of Geology, 96, no. 2, http://dx.doi.org/10.17850/njg96- 2-05.

Sokolov, V., Krasiltchikov, A., and Livshitz, J. J., 1968, The main features of the tectonic structure of Spitsbergen: Geological Magazine, 105, no. 2, p. 95-115.

Steel, R. J., Dalland, A., Kalgraff, K., and Larsen, V., 1981, The Central Tertiary Basin of Spitsbergen: sedimentary development of a sheared-margin basin: Canadian Society of Petroleum Geologists, 7, p. 647-664.

Steel, R., Gjelberg, J., Helland-Hansen, W., Kleinspehn, K., Nøttvedt, A., and Rye-Larsen, M., 1985, The Teritary strike-slip basins and orogenic belt of Spitsbergen: Strike-slip Deformation, Basin Formation, and Sedimentation, 37, p. 339-359.

Steel, R. J., and Worsley, D., 1984, Svalbard's post-Caledonian strata-an atlas of sedimentational patterns and palaeogeographic evolution, Spencer, in, A. M., ed., Petroleum Geology of the North European Margin, Graham and Trotman, London, p. 109-136.

Straub, K. M., Paola, C., Mohrig, D., Wolinsky, M. A., and George, T., 2009, Compensational Stacking of Channelized Sedimentary Deposits: Journal of Sedimentary Research, 79, no. 9, p. 673-688.

Vincent, S. J., 2001, The Sis palaeovalley: a record of proximal fluvial sedimentation and drainage basin development in response to Pyrenean mountain building: Sedimentology, 48, no. 6, p. 1235-1276.

Vonderbank, K., 1970, Geologie und Fauna der Tertiären Ablagerungen Zentral-Spitsbergens, Norwegian Polar Institute, Skrifter, no. 151, 119p.

Walker, R. G., 1975, Generalized facies models for resedimented conglomerates of turbidite association: Geological Society of America Bulletin, 86, no. 6, p. 737-748.

Ytreland, G., 1980, Sedimentation along the western margin of the Central Tertiary basin, (Firkanten Formation), Spitsbergen, [Master Thesis]: University of Bergen, 183 p.

Online resources

Norsk Polarinstitutt (NPI)., 2017, Svalbardkartet:
http://svalbardkartet.npolar.no/html5/index.html?viewer=svalbardkartet.html5
(accessed 15.03.2017)

APPENDIX:

Sedimentary logs from outcrops

Legend

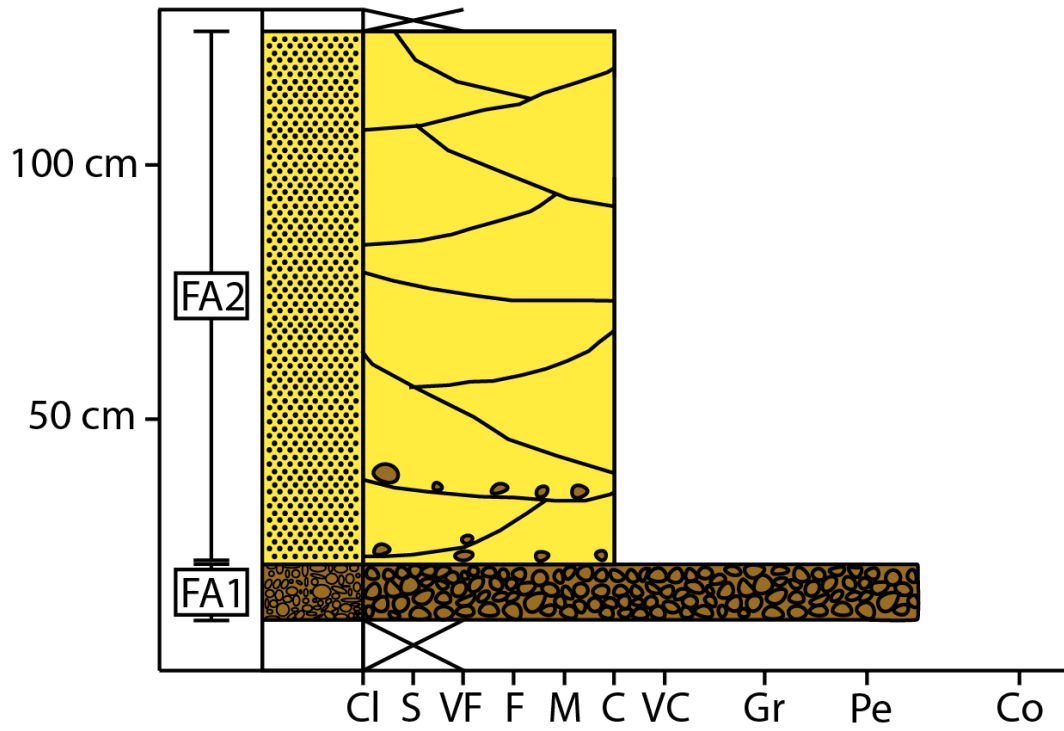|			
Shale		Aligned clasts	
Sandstone		Imbricated clasts	
Coal		Organic fragment	
Conglomerate		Trough cross-stratification	
Siltstone		Planar cross-stratification	
		Plane parallell lamination	
		Current ripple cross lamination	
		Ripple cross-lamination, indeterminable	
		Unconformity	
		Scour and fill features	
		Not present due to scree cover or other reasons	

Logging locality 1
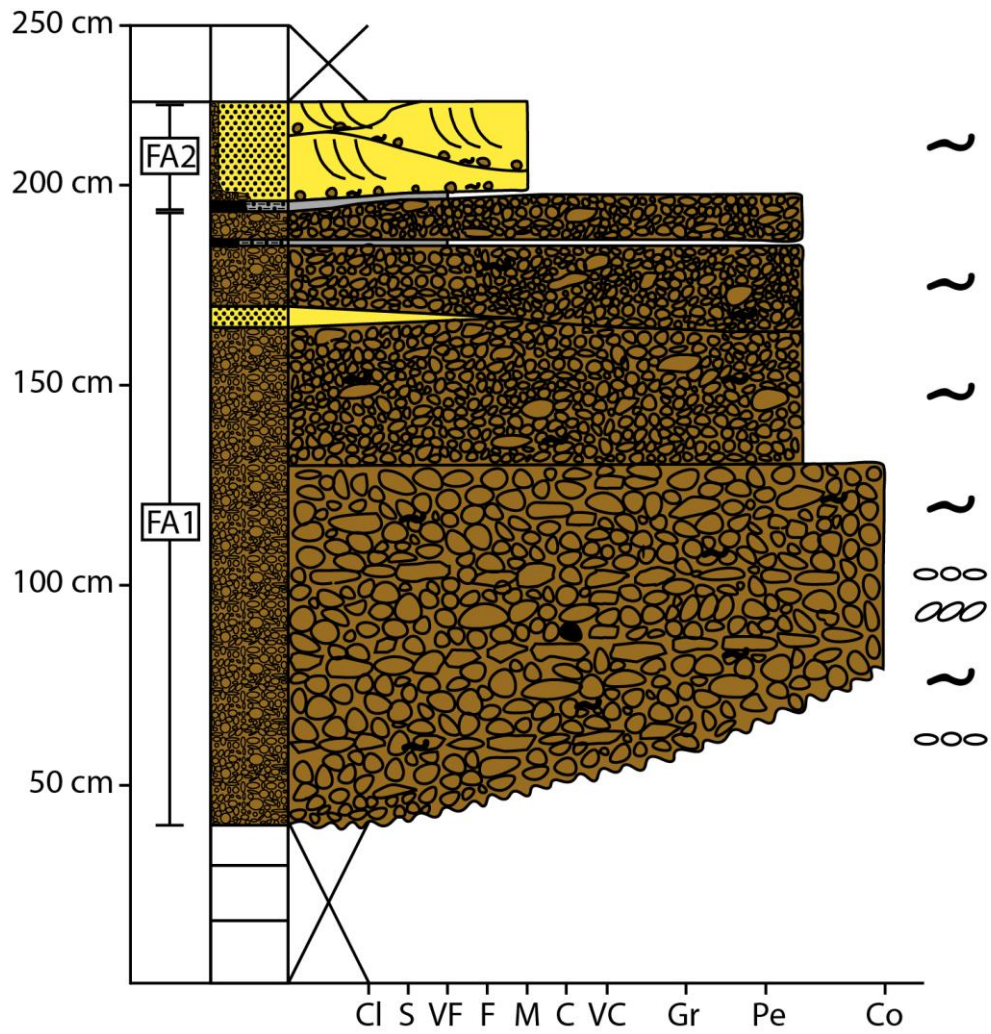
Logging locality 2
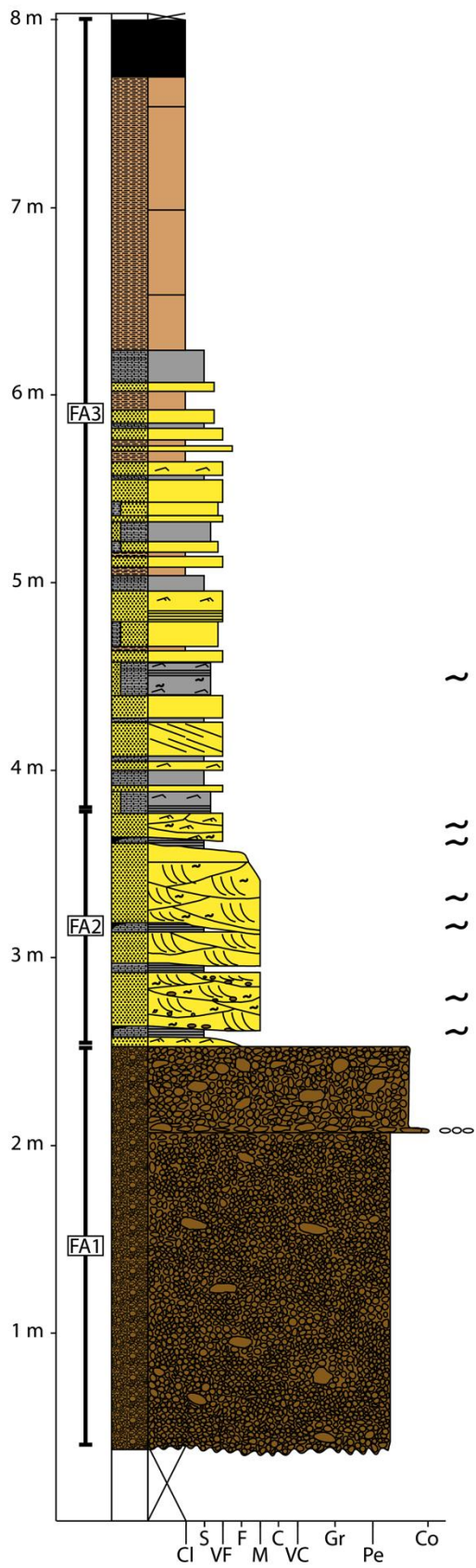
Logging locality 3

Logging locality 4